3-22-2018

Defender-assisted Evasion and Pursuit Maneuvers

Roger S. Anderson

Recommended Citation

DEFENDER-ASSISTED EVASION AND PURSUIT MANEUVERS

THESIS

Roger S Anderson, Captain, USAF

AFIT-ENG-MS-18-M-007

DEPARTMENT OF THE AIR FORCE
AIR UNIVERSITY

AIR FORCE INSTITUTE OF TECHNOLOGY

Wright-Patterson Air Force Base, Ohio

AFIT-ENG-MS-18-M-007

DEFENDER-ASSISTED EVASION AND PURSUIT MANEUVERS

THESIS

Presented to the Faculty

Department of Electrical and Computer Engineering

Graduate School of Engineering and Management

Air Force Institute of Technology

Air University

Air Education and Training Command

in Partial Fulfillment of the Requirements for the

Degree of Master of Science in Electrical Engineering

Roger S Anderson, B.S.E.E.

Captain, USAF

March 2018

AFIT-ENG-MS-18-M-007

DEFENDER-ASSISTED EVASION AND PURSUIT MANEUVERS

THESIS

Roger S Anderson, B.S.E.E.
Captain, USAF

Committee Membership:

Meir Pachter, Ph.D
Chair

John F. Raquet, Ph.D
Member

Capt. Joshuah A. Hess, Ph.D
Member

Abstract

Motivated by the possibilities afforded by active target defense, a 3-agent pursuit-evasion differential game involving an Attacker (Pursuer), a Target (Evader), and a Defender is considered. The Defender strives to assist the Target by intercepting the Attacker before the latter reaches the Target. A barrier surface in a reduced state space separates the winning regions of the Attacker and Target-Defender team. In this thesis, attention focuses primarily on the Attacker's region of win where, under optimal Attacker play, the Defender cannot preclude the Attacker from capturing the Target. Both optimal and suboptimal strategies are investigated. This thesis uses several methods to breakdown and analyze the 3-player differential game.

First, a heuristic analysis of the game is performed. This not only illustrates the game play, but provides insight into what optimal strategies might look like. The heuristic analysis selects points of interest for each of the players to chase, and then compares the results to find a global minimum or maximum of the points considered. The resulting strategies produce very effective chase points for each player to use against opposing player(s), however these points are not optimal when considering all possible strategies.

Next, a barrier analysis is performed. Considering the region where the Attacker is guaranteed to win if he plays optimal, and the region where the Target & Defender team is guaranteed to in if they play optimally, the barrier surface is the dividing membrane that separates the two independent regions. The barrier analysis constructs strategies for each player using the barrier surface. The strategies are then tested to see how they perform as the state representing game play moves away from the barrier. The results of the analysis are used to find a Game of Kind solution that

allows the Attacker to win, so long as the game begins in his region of win.

Finally, the game is considered when using time as the performance functional. This not only satisfies the Game of Kind differential game, but does so in minimum time for the Attacker, and maximum time for the Target & Defender team. Although a complete solution when using time as the performance functional is not obtained, a partial solution is presented with an analysis on pursuit curves. The Attacker's region of win is also split into two subregions that determine the strategies each player should employ. One region guarantees capture of the Target in minimum time by employing Pure Pursuit, and the other region opens a possibility for the Target to escape should the Attacker persist with Pure Pursuit.

This research compliments on-going research being performed by the Air Force Research Laboratory (AFRL) in conjunction with the Air Force Institute of Technology (AFIT). The game has been coined by this team as the Active Target Defense Differential Game (ATDDG) and seeks understanding of optimal strategies for a specific air-to-air engagement scenario described in Chapter I. Originally, the research being performed by AFRL focused primarily on the region where the Target & Defender team will win if they play optimally, however, recently their focused has changed to the region where the Attacker is guaranteed to win if he plays optimally. Where the work done by AFRL has used terminal distances between the players as the performance functional, this work expands upon the ATDDG by considering heuristics, the barrier surface, and temporal based strategies. Doing so strengthens the findings of AFRL, lends insight into how the barrier surface affects the players, and produces results that not only lead to a Game of Kind win, but do so while simultaneously minimizing/maximizing time.

Acknowledgements

    This work represents the culmination of 18 months of study at the Air Force Institute of Technology. It would not have been possible without the support and guidance of other's more intelligent and patient than myself. I would like to thank my research advisor Dr. Meir Pachter for the countless hours he put into mentoring and working with me on my research goals. His vision and direction were indispensable throughout this work. I would also like to thank my other thesis committee members, Dr. John Raquet and Capt. Joshuah Hess, for the time they sacrificed reviewing my thesis documents and the valuable feedback they provided. Finally, I would like to thank my wife and my daughter for putting up with the late nights and the time I've spent away completing this research.

Roger S Anderson

Table of Contents

List of Figures

List of Tables

DEFENDER-ASSISTED EVASION AND PURSUIT MANEUVERS

I. Introduction

1.1 Game Theory and Differential Games

In [13], Nobel Prize winner Roger Myerson defines Game Theory as "the study of mathematical models of conflict and cooperation between intelligent rational decision-makers." This simple expression sums up what mathematicians, engineers, and scientists are striving for within this field of research. Common applications of game theory are found in economics and military applications. Although military conflicts may produce scenarios where all intelligent actors are working for a common goal, the nature of war itself lends the military towards games of conflict, also known as zero sum games. The study of differential games focuses on these games of conflict.

The idea of differential games grew from the field of control theory and was introduced by Rufus Isaacs in 1951. The compilation of Isaac's work [10] was published in 1965 and built the foundation of which countless journal articles and hours of research have been dedicated. This book introduced strategies to analyze dynamic games of conflict using differential equations typically in the form of state dynamics. The strategies presented in Isaac's work culminated in the development and solution to the Homicidal Chauffeur Differential Game.

The Homicidal Chauffeur models the scenario of a pedestrian fleeing a car which is trying to run the pedestrian over. The pedestrian is more mobile and can turn on a dime, whereas the car is a Dubins car [8]. In other words, the Homicidal Chauffeur is a simple pursuit-evasion differential game where the car is faster, but is limited

in its turn radius. This simple game introduced concepts such as Game of Kind, Game of Degree, Barrier Surfaces, and a plethora of similar surfaces. Isaac's work was furthered by J. V. Breakwell [6], T. Merz [12], P. Bernhard [5], and countless others. [10] is still used today as the baseline reference to Differential Games.

Although Isaacs introduced the Homicidal Chauffeur differential game, he did not solve it for the entire state space. This was later completed by T. Merz in his Ph.D. dissertation – see [12], but the dissertation document itself is not readily available to the academic community at large. Seeing the lack of availability of this important work, Lt. S. Coates took it upon himself to rework the complete solution to the Homicidal Chauffeur for the classical parameters under the direction of his research adviser Meir Pachter. This solution is contained in his M.S. thesis paper [7]. Albeit the works of Coates and Merz provide a great in-depth analysis of the Homicidal Chauffeur, Isaac's work was the predominant reference in the strategies used to obtain optimal solutions.

The study of optimal controls is closely related and often used within differential games. Supporting optimal controls documentation used in this research include [11], [18], and [17].

1.2   The Active Target Defense Differential Game (ATDDG)

The ATDDG is a newer differential game with similarities to the Homicidal Chauffeur differential game. The ATDDG is a pursuit-evasion differential game which introduces a third player and removes the turn radius restrictions on the pursuer. This game was developed by the Air Force Research Laboratory (AFRL) in collaboration with AFIT, and is used to describe a 3-player engagement. In this game a hostile missile seeks to intercept a fleeing target aircraft. At the same time a defending missile, with a goal of protecting the target aircraft, is launched to intercept the hostile missile.

Recent conference papers from AFRL and AFIT on the subject include [9], [14], [15], and [16]. The conference articles contained in this paper compliment the previous work done at AFRL and AFIT.

The work in this thesis revolves around the ATDDG. As this is a current area of research for AFRL, the worked performed within this thesis compliments the work being performed without repeating or overlapping with their work. Originally, the research being performed by AFRL focused primarily on the region where the Target & Defender team will win if they play optimally, however, recently their focused has changed to the region where the Attacker is guaranteed to win if he plays optimally. The work done by AFRL primarily uses terminal distances between the players as the performance functional. Instead, this work expands upon the ATDDG by considering heuristics, the barrier surface, and temporal based strategies. Doing so not only strengthens the findings of AFRL, but also lends insight into how the barrier surface affects the players. Furthermore, considering such strategies produces results that not only lead to a Game of Kind win, but do so while simultaneously minimizing/maximizing time. The research presented herein seeks to add to what AFRL has already learned, and dives into state-space regions of the ATDDG yet to be considered by them.

1.3   Methodology

The research extensively used the methods presented in Isaacs in [10]. Strategies were worked out on paper, and then simulated on a computer. MATLAB was the primary software used to model the behaviors of the three actors, to build figures that accurately portray outcomes, and to compare results in search of optimality. MATLAB simulations also verified the predicted players' behaviors from the developed theory. Using MATLAB while developing the theory helped prevent false assump-

tions and interpret complex state behaviors.

1.4 Overview

This thesis contains 3 separate, but related works studying different aspects of the ATDDG.

Chapter II entails a heuristic analysis of the ATDDG in the region where the attacking missile is guaranteed to win if he plays optimally – see [1]. This is done by having players employ sets of strategies against each other in the MATLAB environment. For each strategy, performance is gauged by how close the target aircraft comes to escaping. Of the strategies considered, the optimal strategies are discovered and presented in the chapter. This represents an initial look into this region of play where the attacking missile wins. When this work was undertaken, AFRL was focused on the region of play where the target aircraft is guaranteed to escape given the target and defending missile play optimally.

Chapter III analyzes the barrier surface separating the winning regions of the attacking missile and the target aircraft and defending missile team – see [2]. The barrier surface was introduced by Isaacs in [10] and was used to analyze the Homicidal Chauffeur. This article uses the same idea presented by Isaacs and looks for optimal strategies based on the barrier surface. In this chapter, both the Game of Kind and the Game of Degree solutions are considered.

Chapter IV again analyzes the region where the attacking missile will win as long as he plays optimally – see [3]. Like in the Homicidal Chauffeur differential game, time is used as the performance functional. When research began on this aspect of the ATDDG, AFRL and AFIT had just obtained a guaranteed capture strategy for the attacking missile [16], but teh strategy did not use time as the performance functional. By instead using time as the performance functional, not only is capture

4

of the target aircraft by the attacking missile guaranteed, but it occurs in minimum time. Therefore, using time as the performance functional satisfies the Game of Kind win, but with the benefit of capture the target sooner. This paper also analyzes the pursuit curve of the attacking missile.

This work is the culmination of 18 months spent at the Air Force Institute of Technology (AFIT) researching differential games within the Autonomy and Navigation Center. During this time, three papers on the subject of differential games were composed and submitted the three separate conferences. This thesis represents the culmination of this work and the material includes three conference paper articles preceded by an introduction and concluded with an overall summary.

II. Heuristic Analysis]

2.1 Abstract

In this paper a zero-sum pursuit-evasion differential game involving three players is considered. How game play changes when a third defending player assists the evader by intercepting the pursuer is analyzed. Specifically, the game in the state-space region where capture of the evader by the faster pursuer is nevertheless preordained is addressed by evaluating the performance of heuristic strategies.

Nomenclature

A	Attacker
D	Defender
T	Target
χ	Attacker's heading
ψ	Defender's heading
ϕ	Target's heading
x_A	Attacker's x-position in reduced state space
x_T	Target's x-position in reduced state space
y_T	Target's y-position in reduced state space
α	Speed ratio $\triangleq \dfrac{\text{Target's Speed}}{\text{Attacker's Speed}}$
x_O	Apollonius circle center x-coordinate
y_O	Apollonius circle center y-coordinate

2.2 Introduction

The Homicidal Chauffeur is a classical differential game laid out in [10]. This game, invented by Rufus Isaacs, entails a pursuer—modeled as a Dubins Car—who is trying to minimize the time required to capture an evader—a pedestrian à la Isaacs—while the evader is trying to maximize said time. It is a zero-sum differential game because both players have the same performance functional with the only difference being one seeks to minimize the performance functional while the other seeks to maximize it.

In the case of the Homicidal Chauffeur, the objective (performance functional) is time. In Isaac's example this is logical for the evader because he wants to avoid being captured by the pursuer and if he can cause the performance functional to go to infinity then he has succeeded. Another rational for maximizing this time may be that help is on the way, and if he can hold out long enough, then he will survive. This line of thinking can be extended to assume a nearby building being already present, and the evader can escape the pursuer by entering the building before the pursuer reaches him. In other words a third entity, or the concept of a sanctuary/building, is introduced into the pursuit-evasion game. In this case of a pursuit/evasion game with three entities, it is likely better for the evader to run to the building instead of directly away from the pursuer. The evader's objective here may change to minimize his final distance from the building, with the hope that this distance will be zero upon game termination. The pursuer would likewise seek to maximize this distance to ensure capture. The game is now no longer about the time of capture, but instead the maximization/minimization of the distance from the sanctuary when capture of the evader occurs. Figure 1 illustrates the addition of a Safe Haven and the resulting capture and escape scenarios.

This paper considers such a scenario, albeit instead of a pursuer, an evader, and a building/static target, it deals with an Attacking missile, a dynamic Target aircraft,
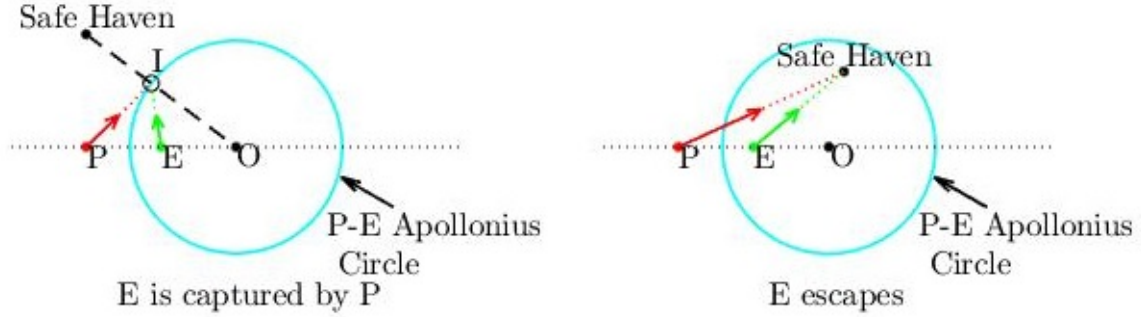
Figure 1. Pursuit/Evasion with Safe Haven

and a Defending missile, where the three players have simple motion à la Isaacs. This work expands upon [15], where the Defender is tasked with intercepting the Attacker before the latter intercepts the Target. Attention here however is given to the state-space region where under optimal Attacker play the Target's capture by the Attacker is guaranteed. Thus, in this region of the state-space the performance functional entails maximizing the distance between the Attacking and Defending missiles at termination for the Attacking missile, and minimizing the same for the Target-Defender team.

2.3   Problem Statement

A hostile missile designated as the "Attacker" seeks to capture a fleeing "Target" which can be thought of as an aircraft. A third player is introduced as a friendly missile, or "Defender", who seeks to intercept the Attacker before the Attacker intercepts its Target. Therefore this is as an active target defense differential game (ATDDG). This paper expands upon previous research [15] which investigated the R_e region of the state space where $\mathbf{T}$ will escape given the $\mathbf{T}$ & $\mathbf{D}$ team plays optimally. Here the situation is considered where the game evolves in the state-space region R_c where, under optimal play of the Attacker, the capture of the Target is preordained, irrespective of the Target-Defender team's actions.

8

Assumptions.

1. The Attacker, Target, and Defender have simple motion/are holonomic, à la Isaacs – think of a Beyond Visual Range (BVR) engagement.

2. The Target's speed is less than the Attacker's. If this were not the case then there would be no need for the Defender in the first place. Thus, the speed ratio $\alpha \triangleq \frac{v_T}{v_A} < 1$ where v_A and v_T are the Attacker's and Target's velocities respectively.

3. The Defender's speed is the same as the Attacker's: $v_D = v_A$; the **A** and **D** missiles have similar capabilities.

4. Point capture is considered.

5. It is assumed that all players are aware of each other's positions; this is a differential game with complete information in which state feedback strategies are sought.

Dynamics.

The state-space of the ATDDG can be represented by each of the players x and y-coordinates in the realistic plane, creating a 6-state system. However the 6-state system can be reduced to 3 states using a non-inertial, rotating reference frame by pegging the x-axis to **A** and **D**'s instantaneous positions. The y-axis is the orthogonal bisector of the $\overline{\textbf{AD}}$ segment. In this rotating reference frame the states are **T**'s x and y-positions (x_T, y_T) and **A**'s x-position x_A. In this state space **A**'s y-coordinate will always be 0 and **D**'s position will be $(-x_A, 0)$. This rotating reference frame is shown overlaid on the realistic plane in Figure 2 where the **A**, **T**, and **D** players' respective headings χ, ϕ, and ψ are also indicated. Initially the rotating frame (x, y) is aligned with the inertial frame (X, Y).
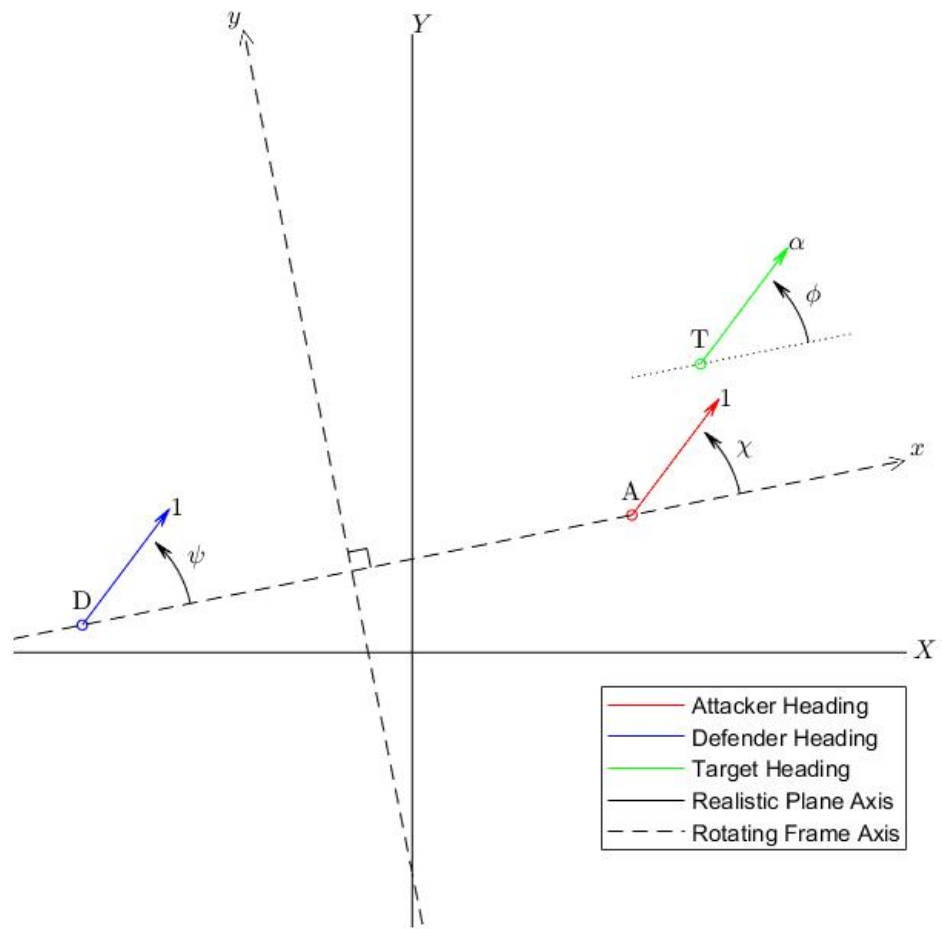
Figure 2. Rotating Reference Frame

Using this rotating reference frame the state space is reduced to $\{(x_A, x_T, y_T) | x_A \geq 0, \; y_T \geq 0\} \subset \mathbb{R}^3$ and the system dynamics in the reduced 3-D state space are

$$\dot{x}_A = \frac{1}{2}\left(\cos\chi - \cos\psi\right), \; x_A(0) = x_{A_0} \tag{1}$$

$$\dot{x}_T = \alpha\cos\phi - \frac{1}{2}\left(\cos\psi + \cos\chi\right) - \frac{1}{2}\frac{y_T}{x_A}\left(\sin\psi - \sin\chi\right), \; x_T(0) = x_{T_0} \tag{2}$$

$$\dot{y}_T = \alpha\sin\phi - \frac{1}{2}\left(\sin\psi + \sin\chi\right) + \frac{1}{2}\frac{x_T}{x_A}\left(\sin\psi - \sin\chi\right), \; y_T(0) = y_{T_0}, \; 0 \leq t \leq t_f \tag{3}$$

Performance Functional.

The performance functional codifies the goals of **A** and the **T** & **D** team. Ultimately it is what they seek to minimize or maximize as the game evolves in the state-space region R_c where, under optimal play by **A**, **T**'s capture is preordained.

Indeed, if **A** is solely concerned about minimizing the time to capture of **T** and uses Pure Pursuit (PP) strategies, he may end up neglecting **D**'s impact on the 3-player game and forfeit his opportunity to intercept **T**. **A** should therefore also be concerned with avoiding **D** while still guaranteeing **T**'s capture. This can be accomplished by having **A** strive to intercept **T** as far away from **D** as possible, that is, inhibit **T**'s possibility of escape.

Like **A**, the **T** & **D** team's objective is also a function of the final distance of **A** and **D**. Should **T** seek to instead maximize the time to capture without taking **D**'s presence into account, he may very well be captured further away from **D** than otherwise possible as shown in Figure 3. More importantly, by blindly running away from **A** and not approaching **D**, he might forfeit the opportunity to escape should **A** err. In order to produce an outcome that gives **T** a better chance of escape should **A**

err, both **D** and **T** will strive to minimize the **A** to **D** distance, or distance from **T** to the orthogonal bisector of $\overline{\mathbf{AD}}$, at termination/capture time.

For the example shown in Figure 3, **A** employed PP of **T** and **T** ran directly away from **A**. This illustrates the outcome when **T** and **A** are myopically only concerned with time to capture without regards to **D**'s presence in the region R_c.
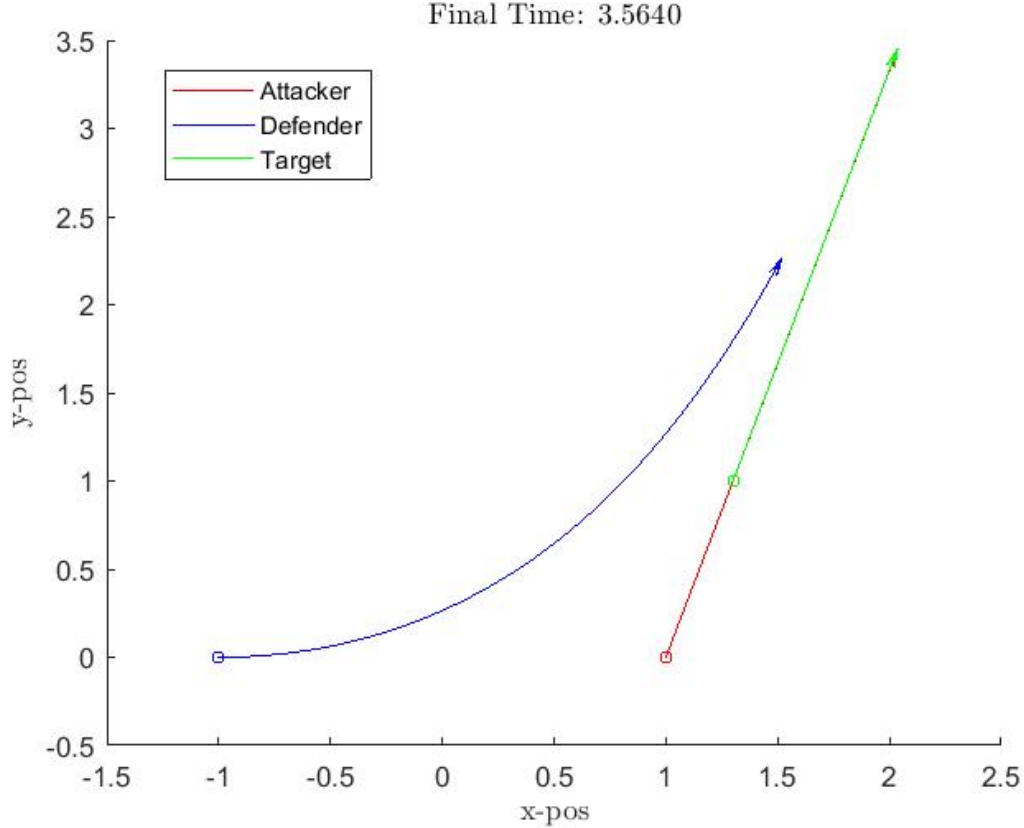
Figure 3. Maximizing the Time to Capture Without Regards to D's Presence

In view of these objectives we define the performance functional in Mayer form [11] as

$$\min_{\phi\psi} \max_{\chi} \quad J \tag{4}$$

where $J = x_a(t_f)$ and termination at t_f is determined by the state satisfying the condition

$$[x_A(t_f) - x_T(t_f)]^2 + y_T^2(t_f) = 0$$

Geometry.

The Apollonius circle is the locus of all points whose ratio of distances from two fixed points, in this case **A** and **T**, is constant. The ratio of the line segments from **T** and **A** to a point on the circumference of the Apollonius circle is the **A**-**T** speed ratio α. The Apollonius circle is critical to understanding the two regions of play of which the state space is partitioned: (1) R_c, where **T** is captured by **A** under optimal play by **A**; (2) R_e, where **D** intercepts **A** allowing **T** to escape. Should one of the player's err, the dynamic Apollonius circle also helps with understanding when the state, and consequently play, shifts from **A**'s winning region R_c to the **T** & **D** team's winning region R_e and vice versa.

Given the state of the game, that is the instantaneous positions of players **A** and **T**, and the speed ratio parameter α, the center of the dynamic Apollonius circle (x_O, y_O) is

$$x_O = \frac{1}{1 - \alpha^2}(x_T - \alpha^2 x_A), \quad y_O = \frac{1}{1 - \alpha^2} y_T$$

with a radius of

$$\rho = \frac{\alpha}{1 - \alpha^2} d$$

where $d = \sqrt{(x_T - x_A)^2 + y_T^2}$ is the current distance from **A** to **T**.

State-Space Partition.

The state-space region where under optimal play **A** wins, in which **T** is captured, is denoted by R_c and the state-space region where under optimal play the **T** & **D** team wins, in which **T** escapes, is denoted by R_e. As shown in [15], when $x_T > 0$, there is a minimum speed ratio $\bar{\alpha}$ which guarantees escape for **T** assuming **T** and **D** play optimally. This is attended by the Apollonius circle intersecting the y-axis.

13

Given x_A, x_T, and y_T, this critical speed ratio is

$$\bar{\alpha} = \frac{\sqrt{(x_A + x_T)^2 + y_T^2} - \sqrt{(x_A - x_T)^2 + y_T^2}}{2x_A} \qquad (5)$$

whereupon the Apollonius circle is tangent to the y-axis $\equiv$ the orthogonal bisector of the $\overline{\mathbf{AD}}$ segment.

Thus, when x_T is positive, the speed ratio parameter α defines the state-space region R_c, which is $\mathbf{A}$'s region of win in the reduced state-space,

$$R_c = \{(x_A, x_T, y_T) | x_A > 0, \ x_T > 0, \ y_T \geq 0,$$

$$x_A^2 + \frac{y_T^2}{1 - \alpha^2} - \frac{x_T^2}{\alpha^2} < 0\}$$

where under optimal play of $\mathbf{A}$, the capture of $\mathbf{T}$ is guaranteed.

The $\mathbf{T}$ & $\mathbf{D}$ team region of win complements the state space and thus is

$$R_e = \{(x_A, x_T, y_T) | x_A \geq 0, \ x_T > 0, \ y_T \geq 0,$$

$$x_A^2 + \frac{y_T^2}{1 - \alpha^2} - \frac{x_T^2}{\alpha^2} \geq 0\}$$

$$\cup \{(x_A, x_T, y_T) | x_A \geq 0, \ x_T \leq 0, \ y_T \geq 0\}$$

$$\cup \{(x_A, x_T, y_T) | x_A = 0, \ x_T \geq 0, \ y_T \geq 0\}$$

where under optimal play of $\mathbf{T}$ and $\mathbf{D}$, $\mathbf{T}$'s escape is guaranteed.

2.4   Analysis

The objective is to synthesize the players' optimal state feedback strategies, that is χ^*, ψ^*, and ϕ^*. Geometrically significant points, or *rabbits*, will be selected for each player to chase in the rotating reference frame. Initially all players will pursue selected rabbits followed by modifying a single player's rabbit to see if it helps or

hurts his objective. This process will be repeated until any deviation by any player results in worse performance in terms of his objective. Rabbits are obviously dynamic and will be updated at each time step.

The rabbit points considered herein which give rise to different heuristic strategies of the **A**, **T**, and **D** players are

1. The Attacker's instantaneous location **A**.

2. The Defender's instantaneous location **D**.

3. The Target's instantaneous location **T**.

4. The point on the circumference of the instantaneous Apollonius circle furthest from **A**.

5. The instantaneous point of intersection of the line segment $\overline{\mathbf{DO}}$ and the Apollonius circle (where **O** is the center of the Apollonius circle).

6. The point on the instantaneous Apollonius circle closest to the y-axis (orthogonal bisector of $\overline{\mathbf{AD}}$).

7. The point described in 6, but mirrored across the y-axis: If **D** chases this rabbit while **A** chases 6 then the (x, y) reference frame does not rotate.

8. The center of the instantaneous Apollonius circle.

The non-dimensional time step used to propagate the states forward in the numerical integration of the closed-loop dynamics (1) - (3) is a fixed $dt = 0.001$. Integration will cease when **T** enters **A**'s capture region of radius $l = 1dt$—this is considered point capture—or when the state-space leaves the region R_c due to **A** deviating from his optimal capture strategy.

15
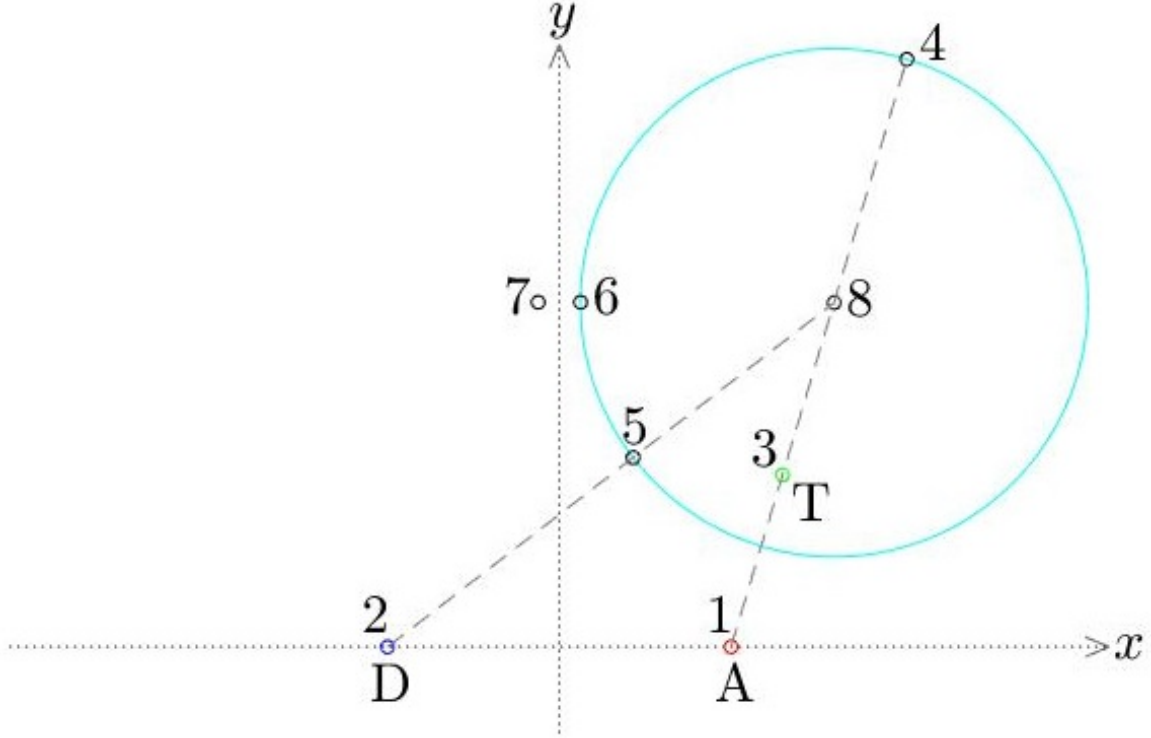
Figure 4. Dynamic Location of Rabbits

2.5 Experimentation

Two different kind of graphics will be used to illustrate the game play. The first entails the state's trajectory in the rotating reference frame according to the dynamics in equations (1) - (3). The most important part of this figure is the movement of the Apollonius circle. If at any time this circle contacts or intersects the y-axis during the game, then at this time **T** has a guaranteed escape path should the **T** & **D** team play optimally and thus the state exits the region R_c. **T** and **D** want to push this circle as close to the y-axis as they can, in the hope that should **A** err at some time during the game, then the Apollonius circle will intersect the y-axis and **T** will have a path to escape; obviously **T** forgoes the maximization of his time to capture hoping to escape altogether. At the same time **A** seeks to pull this circle away from the y-axis to relentlessly make his likelihood of a successful pursuit more favorable.

16

The additional figures shown in this paper are the players' trajectories in the realistic plane. This uses the control inputs of each player in the linear dynamics which evolve in $\mathbb{R}^6$. This is more intuitive than the reduced state space model as one can see the interactions in a fixed reference frame. These figures will be comprised of several subplots showing the development of the players' trajectories over time, from start to finish. Each figure will use the legend
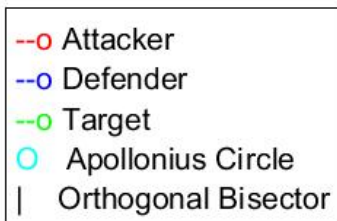
In all scenarios, without loss of generality, **A**'s initial position is $(1, 0)$ and consequently **D**'s initial position is $(-1, 0)$. **T**'s initial position is chosen to be $(1.3, 1)$. So the initial state is well within R_c, but close enough to R_e that **T** can escape should **A** employ a poor strategy.

Benchmark Scenario.

First we will look at the PP strategy where **A** chases **T**, **T** runs towards **D**, and **D** pursues **A**. In terms of the aim points, **A** chases rabbit 3, **T** chases rabbit 2, and **D** chases rabbit 1. Although one does not expect these to be the players' optimal strategies, this play is still significant as it is how players endowed with Artificial Intelligence might behave.

As shown in Figure 5 the left hand side of the Apollonius circle is pulled further into **A**'s side of the (x, y) plane, showing the possibility of **T**'s escape diminishing over time. It is not intuitive what is actually happening from this Figure and therefore,
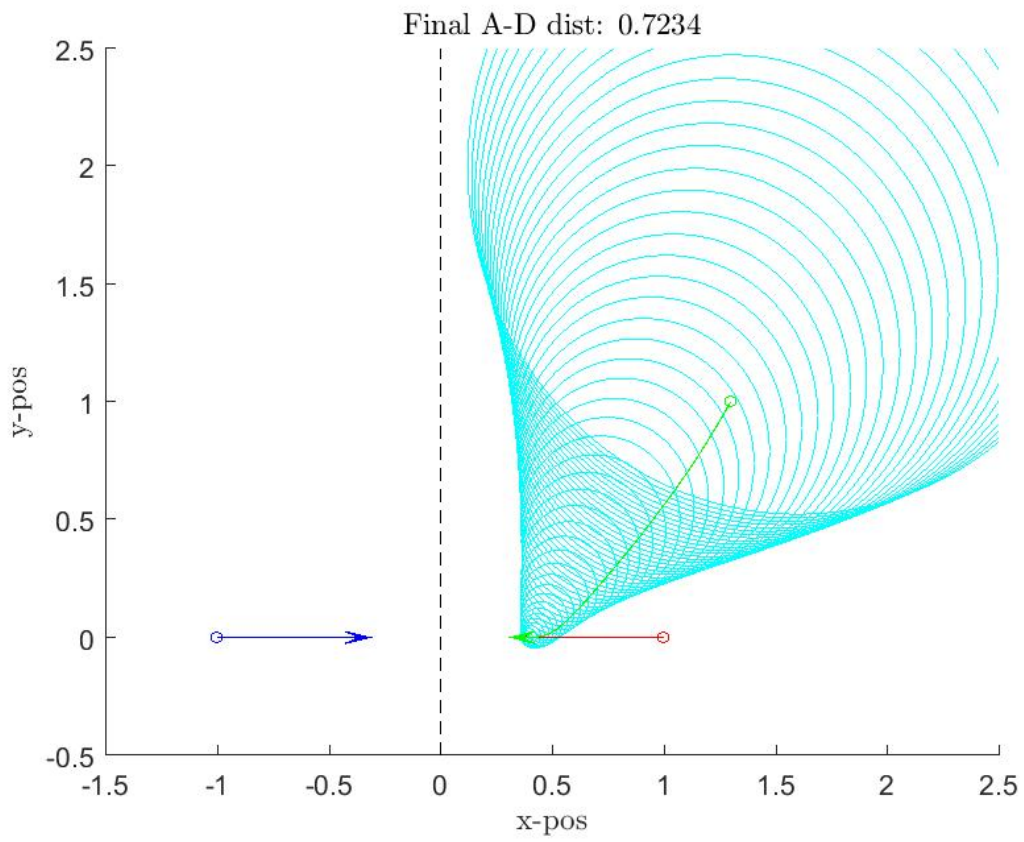
Figure 5. PP: Trajectories in the Rotating Reference Frame
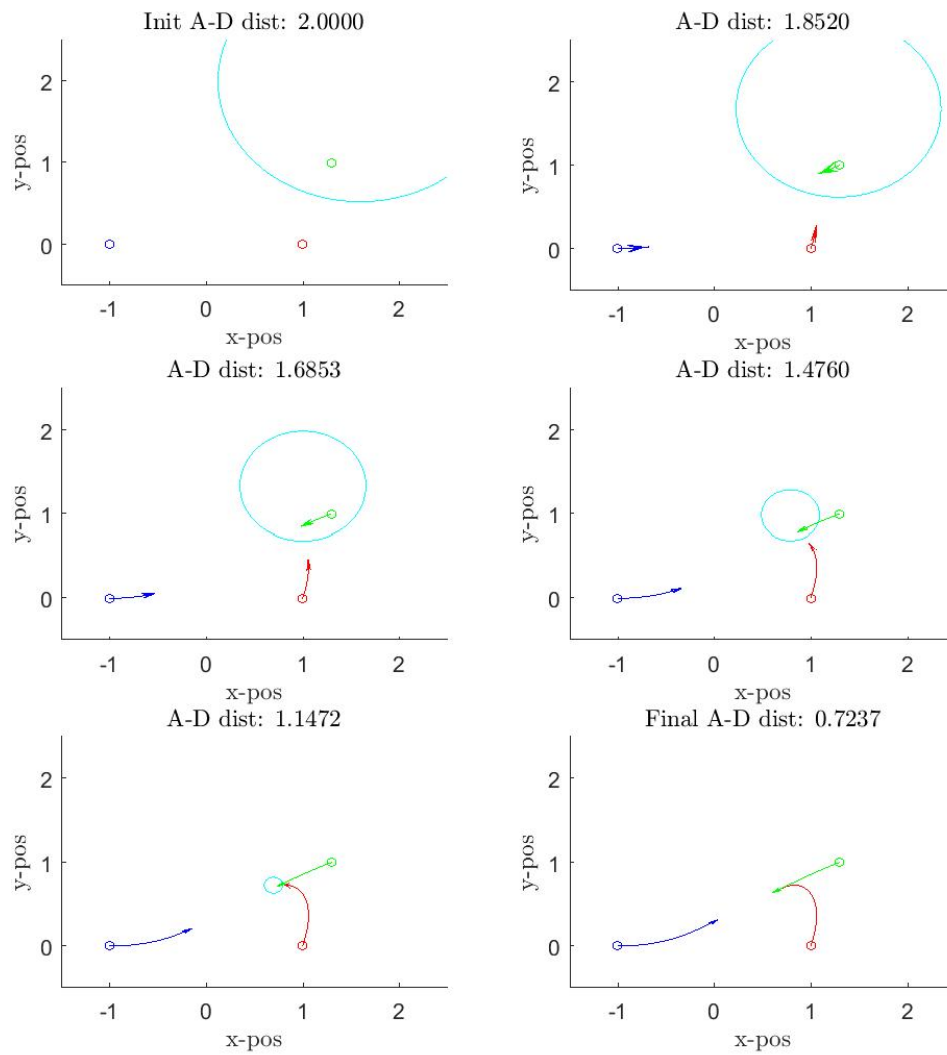
Figure 6. PP: Trajectories in Realistic State Space

as previously stated, the results are also shown in the realistic plane. Figure 6 clearly shows the game played out in this PP scenario. We see **A** has to curve around as **T** moves by him following line of sight/PP; this is in fact endemic to PP. One would expect **A** to perform better if he cut **T** off by predicting the interception point from **T**'s trajectory, which can be referred to as Collision Course (CC) guidance. Likewise, if **T** had a north component to his trajectory he may have been able to make it further west than he did here. The results of applying these strategies illustrate the dynamic nature of the game.

T & D Chase Same Rabbit.

In the pure pursuit scenario **T** and **D** chased different rabbits. Here **T** and **D** will chase the same rabbit. Comparisons of the performance of different strategies are presented in Table 1. This table will help narrow down the search for optimal strategies. Dashes in the table represent the state exited the region R_c — **T** can escape capture.

Table 1. Final Attacker-Defender Distance

A \ **T & D**	4	5	6	7	8
3	0.997	-	-	-	1.025
5	1.175	0.566	0.146	0.435	1.169
6	1.101	0.560	0.153	0.409	1.098
8	0.997	-	-	-	1.025

As is evident in Table 1, **A** performed poorly when chasing rabbits 3 and 8, which often resulted in **T** having an escape chance. Only when **T** and **D** also chose bad rabbits does an escape option fail to develop.

Attention therefore shifts to strategies based on chasing rabbits 5, 6, and 7. The set of strategies is sought where any deviation to **A**'s strategy decreases the terminal **A**-**D** distance and where any deviation to **T**'s and **D**'s strategies increases the **A**-**D** terminal separation. In other words any deviation by any player degrades their outcome in terms of their performance functional, displaying a saddle point in strategic behavior. We find this to be when all three players chase rabbit 6. Therefore this is the players' optimal strategies from the pool of strategies considered in Table 1.

Rabbit 6.

As chasing rabbit 6 has been identified as the "optimal" strategy for each player, the following provides insight on what is occurring when this strategy is adopted by **A**, **T**, and **D**.

Figure 7 presents the state's trajectory in the rotating reference frame and shows the left hand side of the Apollonius circle coming nearly straight down, illustrating neither side is improving their strategic position over time. Careful analysis of Figure 7, however, shows that the **T** & **D** team is able to push this edge a little closer to the y-axis (orthogonal bisector of $\overline{\textbf{AD}}$) in the final moments before capture. Since the rabbit lies to the right of the $\overline{\textbf{AD}}$ orthogonal bisector, **D** must take a less northing trajectory than **A**. This causes a slight rotation in the rotating reference frame, which rotation increases in angular velocity as the **A**-**D** separation decreases. As the rotation becomes noticeable in the final moments of play, rabbit 6 shifts slightly down the Apollonius circle when viewed in the realistic state space. Thus, in the final moments of play, **D** and **T** turn towards each other (as seen in Figure 8) and move the leftmost point of the Apollonius circle slightly in their favor.

Although not shown in Figure 7, it is noteworthy that as the initial state approaches R_e, but still is in R_c, this rotation in the endgame diminishes and all 3
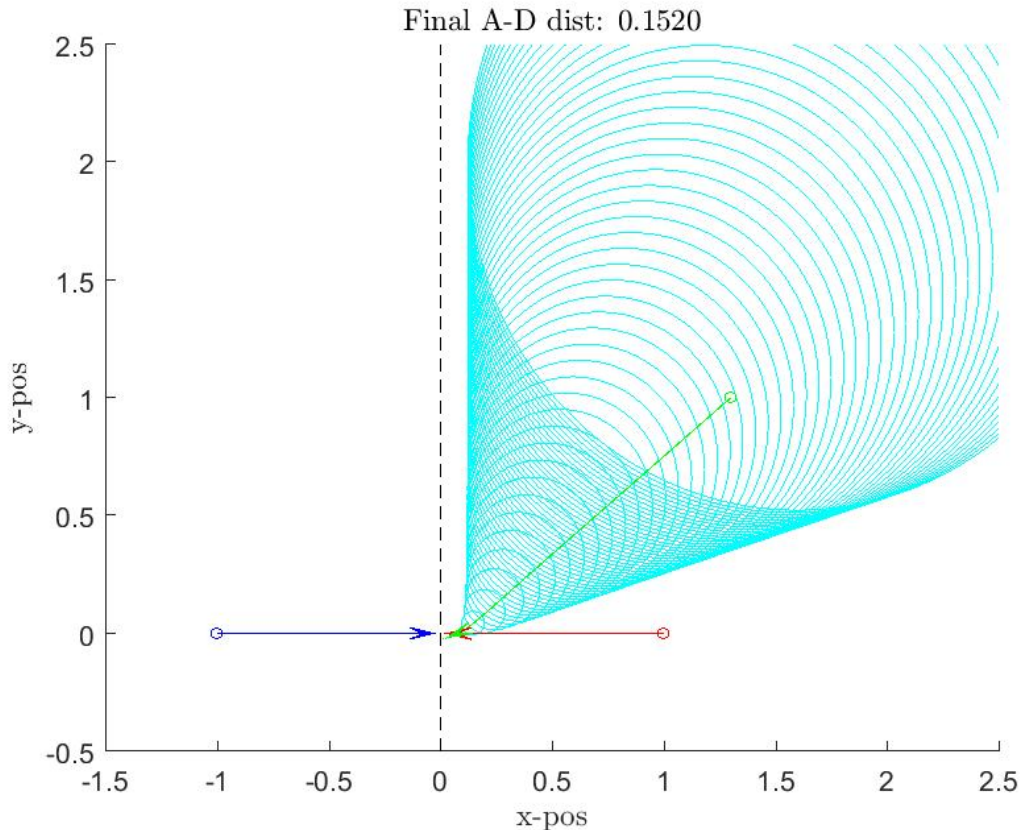
Figure 7. Rabbit 6: Dynamics in the Rotating Reference Frame

players' trajectories become straight lines in the realistic state space. Should the left-hand side of the Apollonius circle initially start right on the y-axis (when the state is on the barrier surface separating R_e and R_c), there would be no horizontal movement for this point on the Apollonius circle and the (x, y) frame will cease to rotate.

Figure 8 shows the players traveling in straight lines until the final moments of play when the heading of $\mathbf{D}$ compared to $\mathbf{A}$ begins to noticeably rotate the frame; so, at long range the dynamics are simple. We see that these results closely resemble the behaviors predicted in the Benchmark Scenario, that is, $\mathbf{A}$ attempts to cut off $\mathbf{T}$ while $\mathbf{T}$ takes a northward trajectory in an attempt to avoid a path towards $\mathbf{A}$.
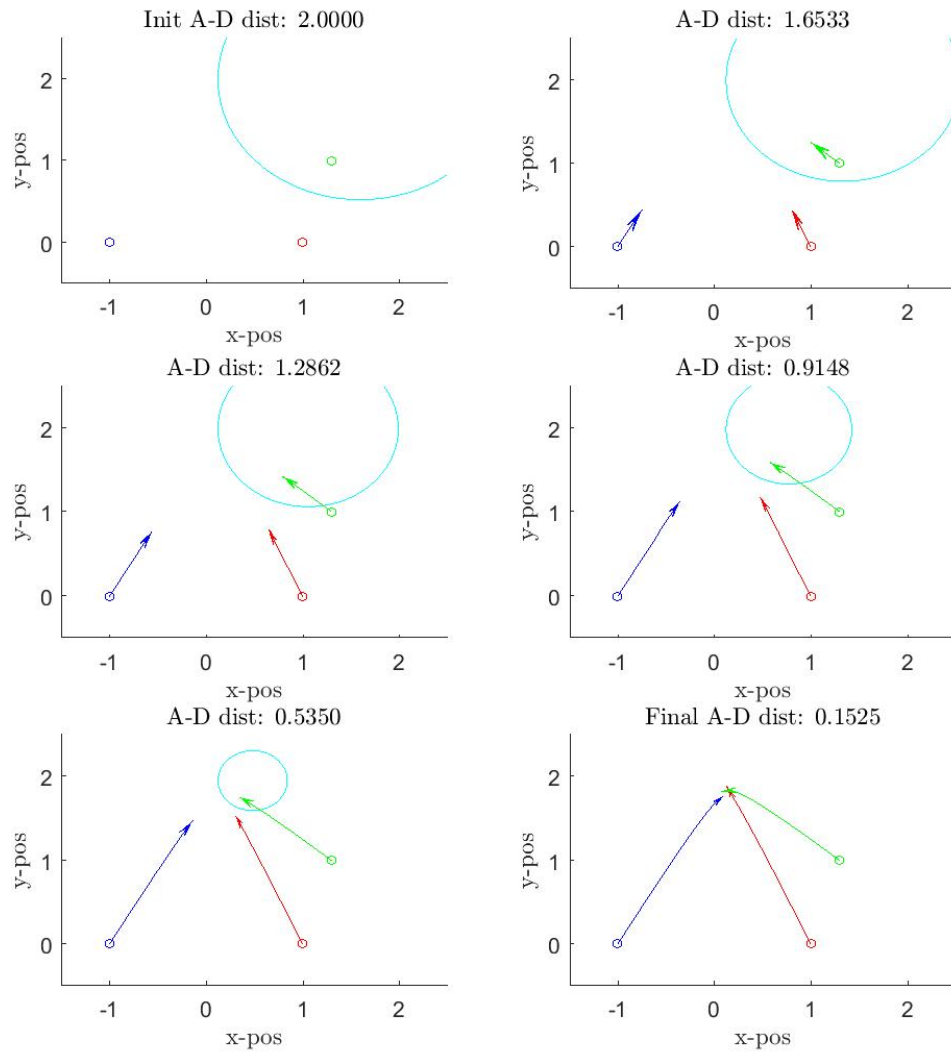
Figure 8. Rabbit 6: Dynamics in Realistic State Space

Defender and Target Deviations.

To arrive at the Rabbit 6 strategies, the assumption was made that both **T** and **D** chase the same rabbit. It has not been shown that **T** and **D** should both chase rabbit 6 if allowed to chase separate rabbits. This can now be done by experimenting with varying **D**'s rabbit while **T** follows rabbit 6 and then vice versa. If any rabbit decreases the terminal $\overline{\mathbf{AD}}$ distance when compared to rabbit 6, then rabbit 6 is not the optimal strategy.

Table 2. Varying the Defender's Strategy: Final Attacker-Defender Distance

A-T \ D	4	5	6	7	8
6	0.236	0.349	0.153	0.249	0.342

Table 3. Varying the Target's Strategy: Final Attacker-Defender Distance

A-D \ T	4	5	6	7	8
6	1.144	0.484	0.153	0.344	1.144

Both experiments show that the preferred "optimal" solution is the strategy that chases rabbit 6, which is the leftmost point of the Apollonius circle.

2.6 Conclusion

This paper investigated "optimal" strategies in a 3-player pursuit-evasion differential game. It was shown that by using a set of plausible rabbits as stipulated in the Analysis, the optimal strategy for each player is to pursue the leftmost point of

the Apollonius circle, that is, strategy #6. This does make sense as it is the closet point to the y-axis that **T** can reach given **A** is pursuing the same point. Should **A** deviate from optimality then his payoff will decrease and therefore **A** shares the same optimal aim point. **D** also pursues this aim point in a near straight line. In the final moments **D** cuts in towards **A** rotating the frame and causing **T** to move more towards **D**. This terminal maneuver allows **T** and **D** to end slightly closer than if the two continued in a straight line. By comparing this work with [15] we see that the choice of "optimal" strategies change when the Apollonius circle crosses the y-axis in the rotating reference frame.

Future Work.

The analysis presented considers heuristic strategies. Finding a global optimal solution cannot be accomplished using heuristics alone and therefore future work includes, but is not limited, to the following:

1. Solve for the global optimal strategies using time as the performance functional of the ATDDG in the R_c region.

2. Merging the optimal strategies in the R_c region with those in the R_e region as presented in [15].

3. Treating the ATDDG as a "Game-of-Kind" by more closely investigating the barrier surface that separates the R_c and R_e regions.

III. Barrier Surface Analysis

3.1 Abstract

In this paper a zero-sum pursuit-evasion differential game involving three players, an Attacker/Pursuer, a Target/Evader, and a Defender, is considered. The Defender strives to assist the Target/Evader by intercepting the Attacker/Pursuer before the latter reaches the Target. A barrier surface separates the winning regions of the Attacker and Target-Defender team when employing optimal strategies. The game in the Attacker's region of win, where the Attacker captures the Target despite the Defender's best efforts, is investigated in this paper. Nested surfaces, one being the barrier surface boundary, are constructed and behaviors are studied when barrier surface strategies are employed to develop capture and evasion strategies.

3.2 Introduction

Consider the archetypal pursuit-evasion differential game in the Euclidean plane where the players have simple motion à la Isaacs [10] and the pursuer is faster than the evader. The pursuer's optimal strategy entails pure pursuit (PP) while the evader runs for his life. However, what if there was a safe haven region close by and the slower evader could avoid being captured by the faster pursuer upon reaching the safe haven before the pursuer reaches him? In other words, a third entity, or the concept of a static sanctuary, is introduced into the pursuit-evasion game. In this case, rather than striving to maximize the time-to-capture, it might be better for the evader to run to the sanctuary instead of away from the pursuer. Consequently the evader's objective may change from striving to maximize the time-to-capture to minimizing the final distance from the evader to the sanctuary at the time of capture, so that should the pursuer err, this distance will be zero upon game termination and the evader will

26

escape. The pursuer would likewise seek to maximize this distance to ensure capture. Now the game of degree is no longer about the time of capture, but instead the maximization/minimization of the distance from the sanctuary when capture of the evader occurs. Such a game would be termed a "game of degree" because the goals are the minimization and maximization of a performance functional. In the end, the true objective of the pursuer and evader is to solve the "game of kind" in which case there are only 3 discrete outcomes: (1) the evader is captured; (2) the evader safely enters the sanctuary; (3) these two occur simultaneously and the outcome is a draw. The state-space is therefore partitioned in accordance with these outcomes. Figure 9 illustrates outcomes 1 and 2, which are determined by whether the safe haven is outside or inside the Pursuer(P)-Evader(E) Apollonius circle with center $\mathbf{O}$. The third outcome would have the safe haven on the Apollonius circle.
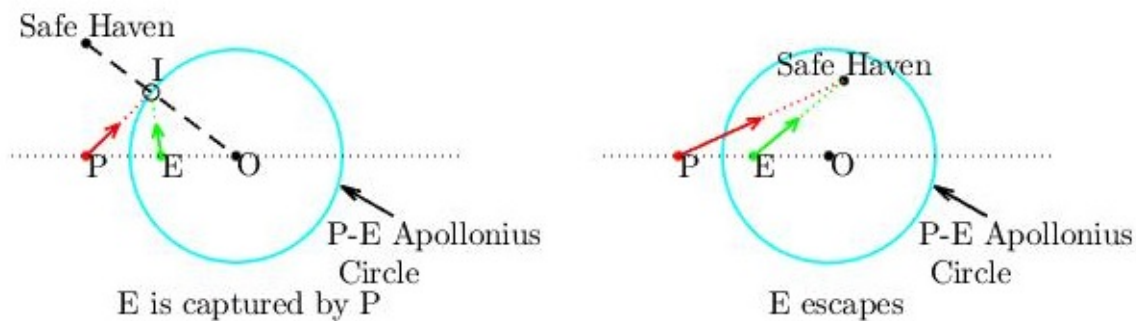
Figure 9. Safe Haven Example

This paper considers such a scenario, albeit instead of an evader, a pursuer, and a static sanctuary set, it deals with an Attacking missile ($\mathbf{A}$), a dynamic Target aircraft ($\mathbf{T}$), and a Defending missile ($\mathbf{D}$). Therefore, this is an Active Target Defense Differential Game (ATDDG) where the sanctuary is the Target and the roles of the Attacker and Defender are assigned to the Evader and Pursuer respectively, which in this paper are assumed to have equal speeds. This paper compliments the work in [15], where the game is played in the $\mathbf{T}$ & $\mathbf{D}$ team's region of win in which $\mathbf{D}$ intercepts $\mathbf{A}$

27

before the latter captures **T** under optimal play - see also [16]. In contrast, within this work attention is given to the state-space region where under optimal Attacker play, **T**'s capture by **A** is guaranteed despite the best efforts of the **T** & **D** team. Should all parties employ their respective optimal strategies and the game terminate with all three players co-located, it is a draw. A barrier surface B is thereby generated where the state trajectories which end in a draw reside. The surface B therefore separates the winning regions of **A** and of the **T** & **D** team. Since the focus in this paper is on **A**'s winning region, this requires us to develop a strategy which guarantees that **A** captures **T**, given the game is initiated within **A**'s capture region delimited by the barrier surface B. This solves the game of kind in **A**'s region of win.

3.3 Problem Statement

The following 3-player pursuit-evasion differential game is considered.

A hostile missile designated as the "Attacker" seeks to capture a fleeing "Target" which can be thought of as an aircraft. A third player is introduced, a "Defender" missile, who seeks to intercept the Attacker before the latter intercepts the Target.

Assumptions.

1. The Attacker, Target, and Defender have simple motion/are holonomic, à la Isaacs – think of a Beyond Visual Range (BVR) engagement.

2. The Target's speed is less than the Attacker's. If this were not the case then there would be no need for the Defender. Thus, the speed ratio $\alpha \triangleq \frac{v_T}{v_A} < 1$ where v_A and v_T are the Attacker's and Target's velocities respectively.

3. The Defender's speed is the same as the Attacker's: $v_D = v_A$; the **A** and **D** missiles have similar capabilities.

28

4. Point capture is considered.

5. It is assumed that all players are aware of each other's positions; this is a differential game with complete information in which state feedback strategies are sought.

Dynamics.

The state-space of the ATDDG can be represented by each of the players x and y-coordinates in the realistic plane, creating a 6-state system. However the 6-state system can be reduced to 3 states using a non-inertial, rotating reference frame by pegging the x-axis to **A** and **D**'s instantaneous positions. The y-axis is the orthogonal bisector of the $\overline{\mathbf{AD}}$ segment. In this rotating reference frame the states are **T**'s x and y-positions (x_T, y_T) and **A**'s x-position x_A. In this state space **A**'s y-coordinate will always be 0 and **D**'s position will be $(-x_A, 0)$. This rotating reference frame is shown overlaid on the realistic plane in Figure 10 where the **A**, **T**, and **D** players' respective headings χ, ϕ, and ψ are also indicated. Initially the rotating frame (x, y) is aligned with the inertial frame (X, Y).

Using this rotating reference frame the state space is reduced to $\{(x_A, x_T, y_T)|x_A \geq 0, \ y_T \geq 0\} \subset \mathbb{R}^3$ and the 3-state system dynamics are

$$\dot{x}_A = \frac{1}{2}\left(\cos \chi - \cos \psi\right), \ x_A(0) = x_{A_0} \tag{6}$$

$$\dot{x}_T = \alpha \cos \phi - \frac{1}{2}\left(\cos \psi + \cos \chi\right) - \frac{1}{2}\frac{y_T}{x_A}\left(\sin \psi - \sin \chi\right), \ x_T(0) = x_{T_0} \tag{7}$$

$$\dot{y}_T = \alpha \sin \phi - \frac{1}{2}\left(\sin \psi + \sin \chi\right) + \frac{1}{2}\frac{x_T}{x_A}\left(\sin \psi - \sin \chi\right), \ y_T(0) = y_{T_0}, \ 0 \leq t \leq t_f \tag{8}$$
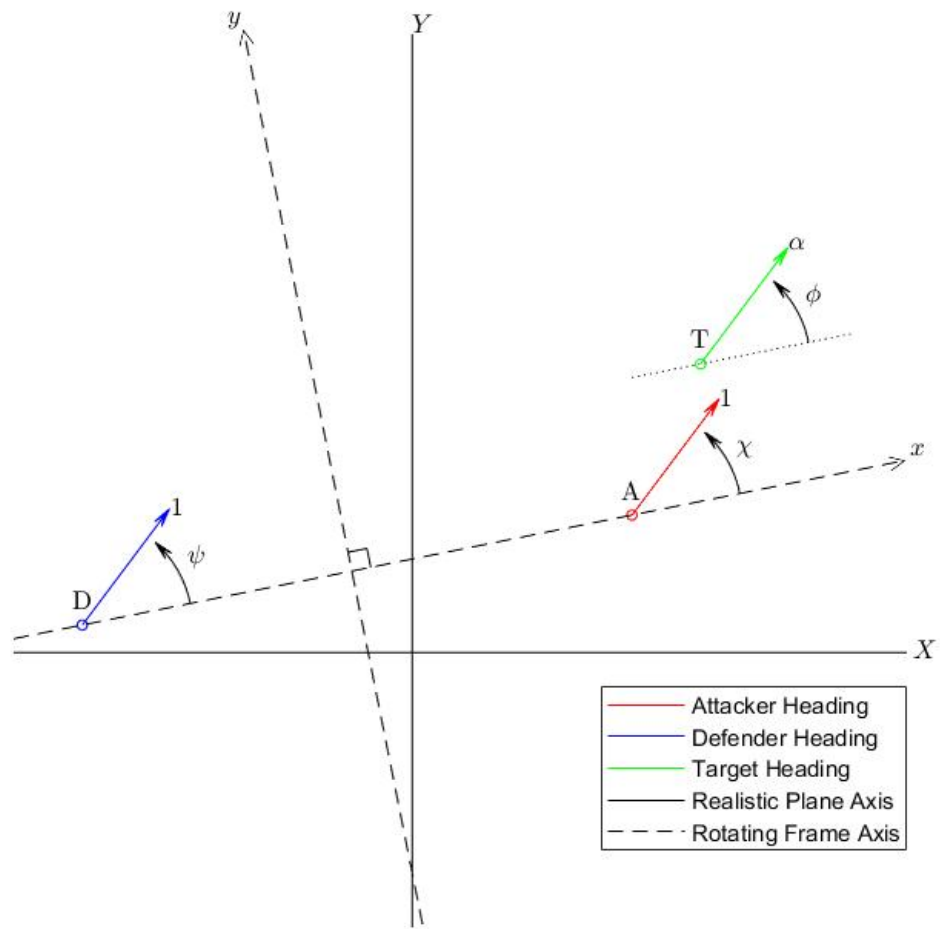
Figure 10. Rotating Reference Frame

Geometry.

The Apollonius circle is the locus of all points whose ratio of distances from two fixed points, say **A** and **T**, is constant. The ratio of the line segments from **T** and **A** to a point on the circumference of the Apollonius circle is the **A**-**T** speed ratio α. The Apollonius circle is critical to understanding the 2 regions of play: (1) R_c where **T** is captured by **A** under optimal play by **A**; (2) R_e where **D** allows **T** to escape. Should one of the player's err, the dynamic Apollonius circle also helps with understanding when play shifts from **A**'s winning region R_c to the **T** & **D** team's winning region R_e, and vice versa.

Given the state of the game, that is the instantaneous positions of players **A** and **T** and the speed ratio parameter α, the center of the dynamic Apollonius circle (x_O, y_O) is

$$x_O = \frac{1}{1 - \alpha^2}(x_T - \alpha^2 x_A), \quad y_O = \frac{1}{1 - \alpha^2} y_T$$

with a radius of

$$\rho = \frac{\alpha}{1 - \alpha^2} d$$

where $d = \sqrt{(x_T - x_A)^2 + y_T^2}$ is the current distance from A to **T**.

State-Space Partition.

The state-space region where under optimal play **A** wins, in which **T** is captured, is denoted by R_c and the state-space region where under optimal play the **T** & **D** team wins, in which **T** escapes, is denoted by R_e. As shown in [15], when $x_T > 0$, there is a minimum speed ratio $\bar{\alpha}$ which guarantees escape for **T** assuming **T** and **D** play optimally. This is attended by the Apollonius circle intersecting the y-axis.

Given x_A, x_T, and y_T this critical speed ratio is

$$\bar{\alpha} = \frac{\sqrt{(x_A + x_T)^2 + y_T^2} - \sqrt{(x_A - x_T)^2 + y_T^2}}{2x_A} \tag{9}$$

whereupon the Apollonius circle is tangent to the y-axis $\equiv$ the orthogonal bisector of the $\overline{\mathbf{AD}}$ segment.

Thus, when x_T is positive, the speed ratio parameter α defines the state-space region R_c, which is $\mathbf{A}$'s region of win in the reduced state-space,

$$R_c = \{(x_A, x_T, y_T) | x_A > 0, \ x_T > 0, \ y_T \geq 0, \ x_A^2 + \frac{y_T^2}{1 - \alpha^2} - \frac{x_T^2}{\alpha^2} < 0\}$$

where under optimal play of $\mathbf{A}$, the capture of $\mathbf{T}$ is guaranteed.

The $\mathbf{T}$ & $\mathbf{D}$ team region of win complements the state space and thus is

$$R_e = \{(x_A, x_T, y_T) | x_A \geq 0, \ x_T > 0, \ y_T \geq 0, \ x_A^2 + \frac{y_T^2}{1 - \alpha^2} - \frac{x_T^2}{\alpha^2} \geq 0\}$$

$$\cup \{(x_A, x_T, y_T) | x_A \geq 0, \ x_T \leq 0, \ y_T \geq 0\}$$

$$\cup \{(x_A, x_T, y_T) | x_A = 0, \ x_T \geq 0, \ y_T \geq 0\}$$

where under optimal play of $\mathbf{T}$ and $\mathbf{D}$, $\mathbf{T}$'s escape is guaranteed.

The Barrier Surface.

By treating the three-player differential game as a game of kind, we analyze the possible discrete outcomes of the game. In contrast, a game of degree focuses on maximizing or minimizing a cost functional. The possible outcomes for the game of kind are

1. $\mathbf{T}$ is captured by $\mathbf{A}$

2. $\mathbf{A}$ is intercepted by $\mathbf{D}$ and $\mathbf{T}$ escapes

32

3. **A**, **T**, and **D** all meet at the same moment, resulting in a draw

The barrier B is the surface which separates the regions R_c and R_e and therefore is

$$B = \{(x_A, x_T, y_T) | x_A \geq 0, \ x_T \geq 0, \ y_T \geq 0, \ x_A^2 + \frac{y_T^2}{1 - \alpha^2} - \frac{x_T^2}{\alpha^2} = 0\}$$

Although the argument may be made that the barrier surface should not include the origin, treating it as such would also exclude the plane $x_A = 0$ from the region R_e and the line $\{x_a = x_T, \ y_t = 0\}$ from the region R_c. Therefore the origin is considered part of the barrier surface.

Should all players play optimally within the state space, the winner can be determined by the side of the surface B of which the initial state lies. Nevertheless, if any of the players fails to play optimally when the initial state lies in his winning region, then the opposing player(s) can take advantage of this by pulling the state across B into their winning region. For example, should **A** fail to play optimally in R_c, the **T** & **D** team could pull the state across the surface B into R_c or to the plane $x_A = 0$ which is conducive to **T**'s escape. The game of kind thus becomes each player pulling the state in the direction of his respective winning region. Should the initial state lie in his winning region, then he would pull deeper into his region, but should the initial state not be in his winning region, then he would pull towards his winning region. The deeper any player can pull the state into his winning region the more likely he will win, for if at some future point in time he does err, then he has established a buffer within his region. From here, the differential game transitions from a game of kind to a game of degree as each player tries to maximize/minimize the state's depth within the current winning region. The overarching goal for each player, however, is still to have the final state located in his winning region. The game of degree in R_e has been solved in [15]. The player's push and pull forces are in equilibrium when the state is and remains on B, the boundary separating R_e and R_c. Should the ini-

33

tial state be on B, players will want to align their controls to pull in the direction normal to B. As is always the case on a barrier surface, the **T** & **D** team will pull in the direction $\vec{n}$ which is normal to the surface B pointing into the region R_e and **A** will pull in the direction of $-\vec{n}$. This results in each player pulling directly into his winning region. Employing these strategies will prevent the state from leaving the surface B and eventually the game will end in a draw. Should a player err he will lose his advantage and the state will penetrate the barrier surface B and enter the opposing team's winning region.

Indeed, the normal to the surface B, $\vec{n}$, is

$$\vec{n} = (x_A, -\frac{x_T}{\alpha^2}, \frac{y_T}{1-\alpha^2})$$

With both teams pulling normal to the surface, albeit in opposite directions, and the state remaining on B, the minimax equation is

$$\max_{\phi,\psi} \min_{\chi} \left. \left(\vec{n} \cdot \vec{f} \right) \right|_B = 0 \tag{10}$$

where

$$\vec{f} = \begin{pmatrix} \dot{x}_A \\ \dot{x}_T \\ \dot{y}_T \end{pmatrix}$$

34

is the state's velocity vector. Performing the minimax operation we obtain

$$\sin\phi = \frac{\frac{\alpha}{1-\alpha^2}y_T}{\sqrt{\frac{1}{\alpha^2}x_T^2 + \frac{\alpha^2}{(1-\alpha^2)^2}y_T^2}}, \qquad \cos\phi = -\frac{\frac{1}{\alpha}x_T}{\sqrt{\frac{1}{\alpha^2}x_T^2 + \frac{\alpha^2}{(1-\alpha^2)^2}y_T^2}}$$

$$\sin\psi = \frac{sign(x_T - \alpha^2 x_A)\left(\frac{1}{1-\alpha^2}\frac{y_T}{x_A}\right)}{\sqrt{1 + \frac{1}{(1-\alpha^2)^2}\frac{y_T^2}{x_A^2}}}, \qquad \cos\psi = \frac{sign(x_T - \alpha^2 x_A)}{\sqrt{1 + \frac{1}{(1-\alpha^2)^2}\frac{y_T^2}{x_A^2}}}$$

$$\sin\chi = \frac{\frac{1}{1-\alpha^2}\frac{y_T}{x_A}}{\sqrt{1 + \frac{1}{(1-\alpha^2)^2}\frac{y_T^2}{x_A^2}}}, \qquad \cos\chi = -\frac{1}{\sqrt{1 + \frac{1}{(1-\alpha^2)^2}\frac{y_T^2}{x_A^2}}}$$

By focusing on surfaces $\{(x_A, x_T, y_T)|x_A \geq 0,\ x_T > 0,\ y_T \geq 0,\ x_A^2 + \frac{y_T^2}{1-\alpha^2} - \frac{x_T^2}{\alpha^2} = c\} \subset R_c$ where $c \leq 0$, we see that the expression $(x_T - \alpha^2 x_A)$ is always non-negative and we therefore obtain the state feedback strategies

$$\left.\begin{aligned}
\sin\widetilde{\phi} &= \frac{\frac{\alpha}{1-\alpha^2}y_T}{\sqrt{\frac{1}{\alpha^2}x_T^2 + \frac{\alpha^2}{(1-\alpha^2)^2}y_T^2}}, \quad \cos\widetilde{\phi} = -\frac{\frac{1}{\alpha}x_T}{\sqrt{\frac{1}{\alpha^2}x_T^2 + \frac{\alpha^2}{(1-\alpha^2)^2}y_T^2}} \\
\sin\widetilde{\psi} &= \frac{\frac{1}{1-\alpha^2}\frac{y_T}{x_A}}{\sqrt{1 + \frac{1}{(1-\alpha^2)^2}\frac{y_T^2}{x_A^2}}}, \quad \cos\widetilde{\psi} = \frac{1}{\sqrt{1 + \frac{1}{(1-\alpha^2)^2}\frac{y_T^2}{x_A^2}}} \\
\sin\widetilde{\chi} &= \frac{\frac{1}{1-\alpha^2}\frac{y_T}{x_A}}{\sqrt{1 + \frac{1}{(1-\alpha^2)^2}\frac{y_T^2}{x_A^2}}}, \quad \cos\widetilde{\chi} = -\frac{1}{\sqrt{1 + \frac{1}{(1-\alpha^2)^2}\frac{y_T^2}{x_A^2}}}
\end{aligned}\right\} \qquad (11)$$

which we refer to as barrier strategies $\sim$. Because on the surface B (where $c = 0$) these $\sim$ strategies allow both the **T** & **D** team to prevent **A** from entering R_c and **A** to prevent the **T** & **D** team from entering R_e, B is a semipermeable surface. By employing these strategies along B both sides will pull equally along the respective surface normals and the straight-line trajectory will stay on B, eventually terminating at the origin and the game resulting in a draw without the state ever leaving B. Should a player not execute his $\sim$ strategy, the state will leave B to his disadvantage.

Figure 11 illustrates paths which the state will take in the reduced state space when the $\sim$ strategies are employed on B and on the plane $y_T = 0$. All paths on B

show the differential game ending in a draw as $x_A = x_T = y_T = 0$ at termination time t_f. Also included are the PP paths that will be taken should the state initially lie on the $y_T = 0$ plane. This plane becomes more important as we consider the family of nested surfaces in R_c where **A** can pull the state to the plane $y_T = 0$ and capture **T** using PP.
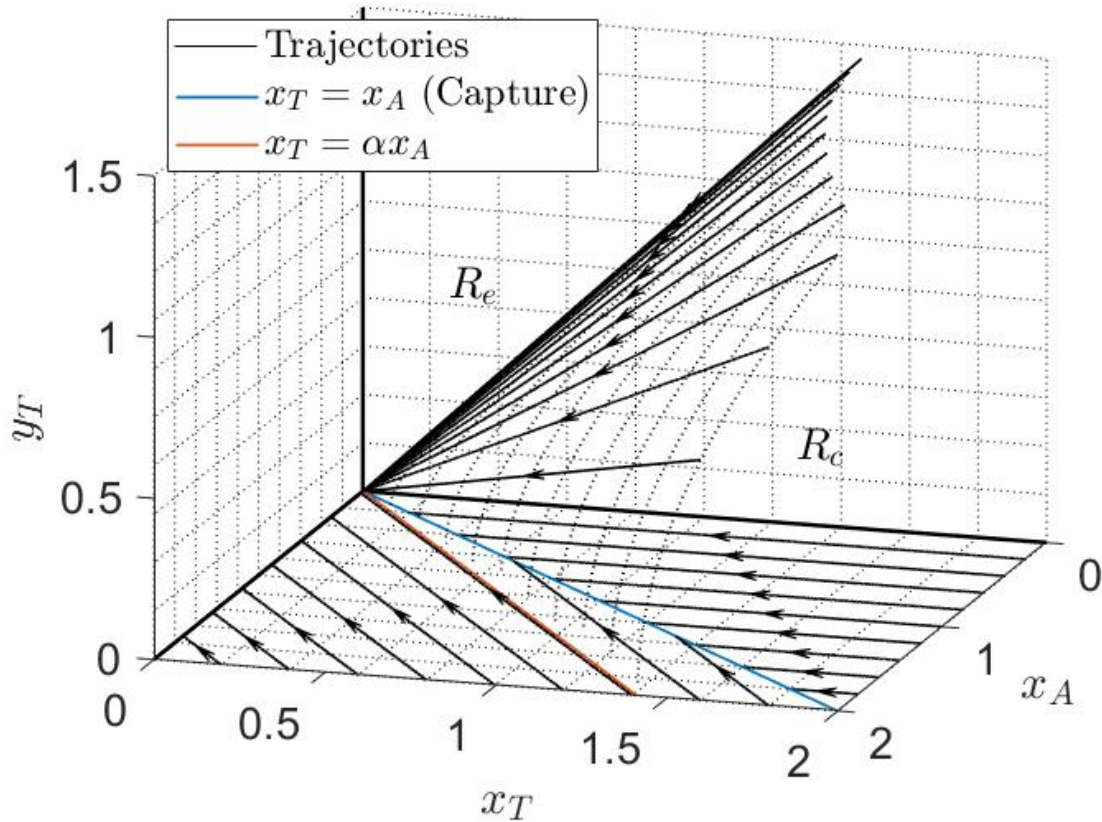
Figure 11. Flow Field on the Barrier Surface and the Plane $y_T = 0$

Figure 12 illustrates the trajectories of the players on B in the realistic plane when employing the $\sim$ strategies. Note how the dynamic Apollonius circle is tangent to the orthogonal bisector of the $\overline{\mathbf{AD}}$ segment, and that all three players head for the point of tangency resulting in a draw.
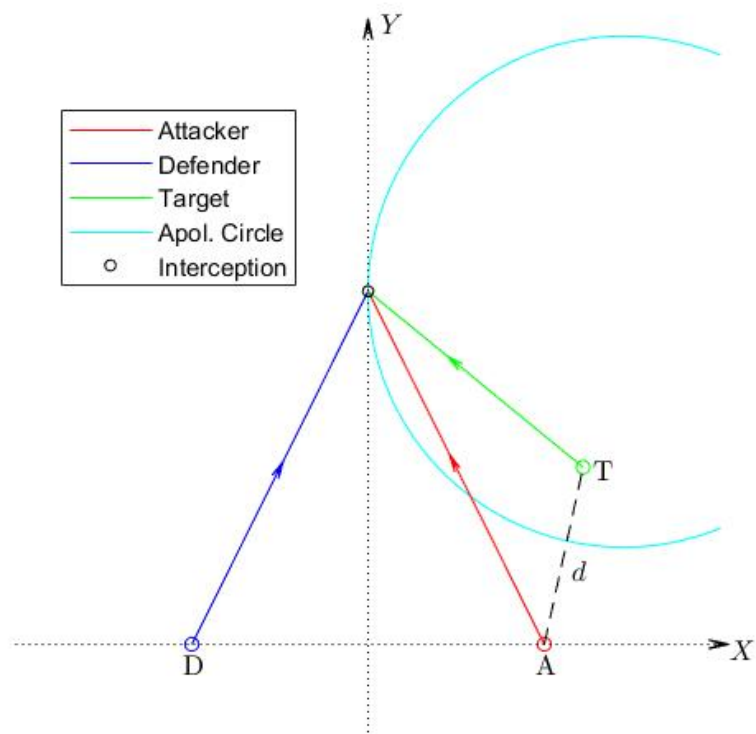
Figure 12. Barrier Surface Action in the Realistic Plane

Nested Surfaces in R_c.

Should the initial state not lie on B, a nested surface can be constructed in R_c on which the state lies. Nested surfaces in R_c, parameterized by $c < 0$, are of the form

$$S_c = \{(x_A, x_T, y_T) | x_A > 0,\ x_T > 0,\ y_T \geq 0,\ x_A^2 + \frac{y_T^2}{1 - \alpha^2} - \frac{x_T^2}{\alpha^2} = c\}$$

where the parameter $c < 0$ yields surfaces in the region R_c, and $c = 0$ is the barrier surface boundary B. Following the same process used to find the $\sim$ strategies, where opposing players are in equilibrium on B, yields the exact same strategies for the surfaces S_c. Because the R.H.S of equation (10) for B is equal to zero, the state will adhere to the barrier surface B when both sides pull in opposite directions, exerting maximal effort. We likewise need to investigate the dynamics on the surface S_c where $c \neq 0$ as both sides pull in opposite directions normal to the surface S_c, $c < 0$. Thus, by inserting strategies (11) into the L.H.S. of equation (10), that is the state is on a surface S_c and the $\sim$ strategies are used, we get

$$\sqrt{\frac{\alpha^2}{(1 - \alpha^2)^2} y_T^2 + \frac{1}{\alpha^2} x_T^2} - \sqrt{\frac{y_T^2}{(1 - \alpha^2)^2} + x_A^2} \tag{12}$$

Now if the state is on a surface S_c,

$$\frac{x_T^2}{\alpha^2} = x_A^2 + \frac{y_T^2}{1 - \alpha^2} - c$$

and by inserting this into eq. (12) we get

$$\sqrt{\frac{y_T^2}{(1 - \alpha^2)^2} + x_A^2 - c} - \sqrt{\frac{y_T^2}{(1 - \alpha^2)^2} + x_A^2} \tag{13}$$

When $c = 0$, the expression in eq. (13) is 0. Because $c = 0$ means the state is

on B, this implies the state will stay on B for $c = 0$. Clearly this does not hold true on the surfaces S_c where $c < 0$. When $c < 0$ the expression (13) will be positive and since the **T** & **D** team is maximizing while **A** is minimizing, the positive result infers the pull towards R_e is larger than the pull into R_c. This occurs despite **A**'s best effort when playing the barrier strategy $\sim$ to not let the states slip any closer to the region R_e. Therefore if play is within the region R_c and the **T** & **D** team plays the $\sim$ strategy, that is, their respective strategies as shown in (11), then there is nothing **A** can do to prevent the state from rising off a surface S_c and approaching the barrier surface B from below. The exact opposite of this is seen in R_e where $c > 0$, in which case there is nothing the **T** & **D** team can do to stop the state from approaching B from above if **A** is playing the $\sim$ strategy.

The family of nested surfaces S_c in R_c and the barrier surface B are illustrated in Figure 13.

3.4 Analysis

Barrier Surface .

Because B is a semipermeable surface, applying the $\sim$ strategies (11) from any initial state on B will result in the state remaining on B. All trajectories are straight lines and converge at the origin, ultimately resulting in the cost/payoff in the ATDDG being zero. Figure 14 illustrates this behavior as the trajectory is seen moving down the barrier surface B until **T** is captured by **A** and **A** is met simultaneously by **D** at the origin: $x_A = 0$, $x_T = 0$, $y_T = 0$. This result is further illustrated in Figure 15 where the dynamic Apollonius circle is seen sliding down the y-axis in the reduced state space. This demonstrates that by having both **A** and the **T** & **D** team play their barrier strategies on B neither side is able to gain the advantage. Note that the (x, y) frame of the reduced state space is not rotating.
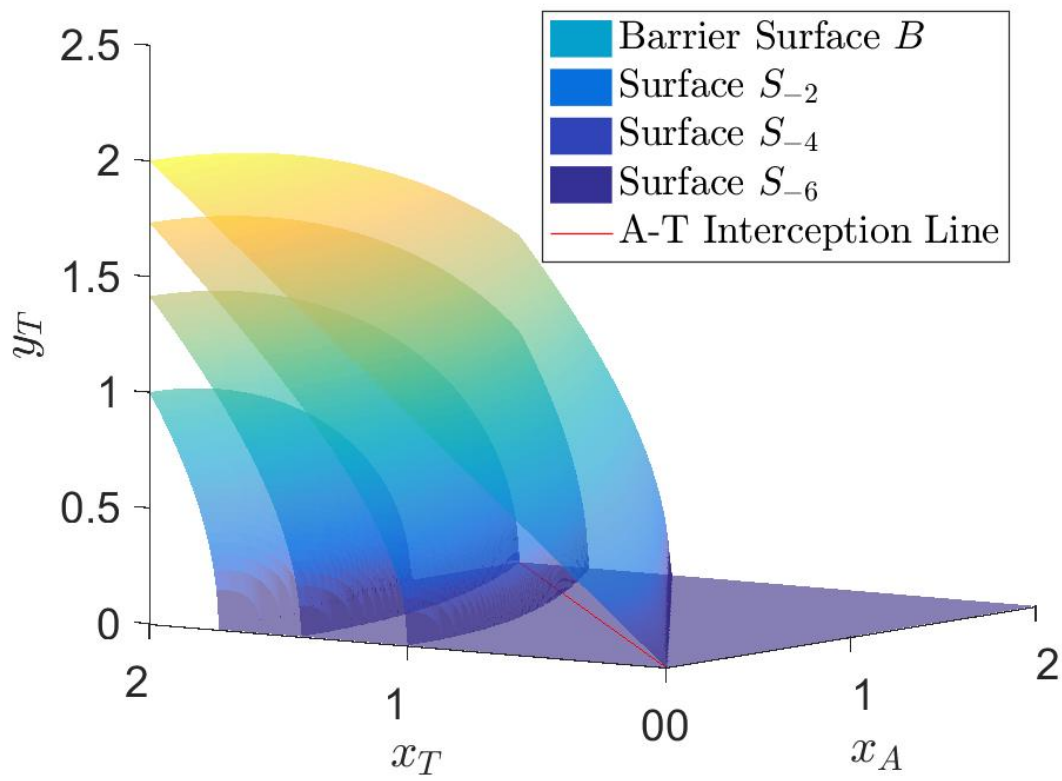
Figure 13. Nested Surfaces $S_c \subset R_c$ in the Reduced State Space
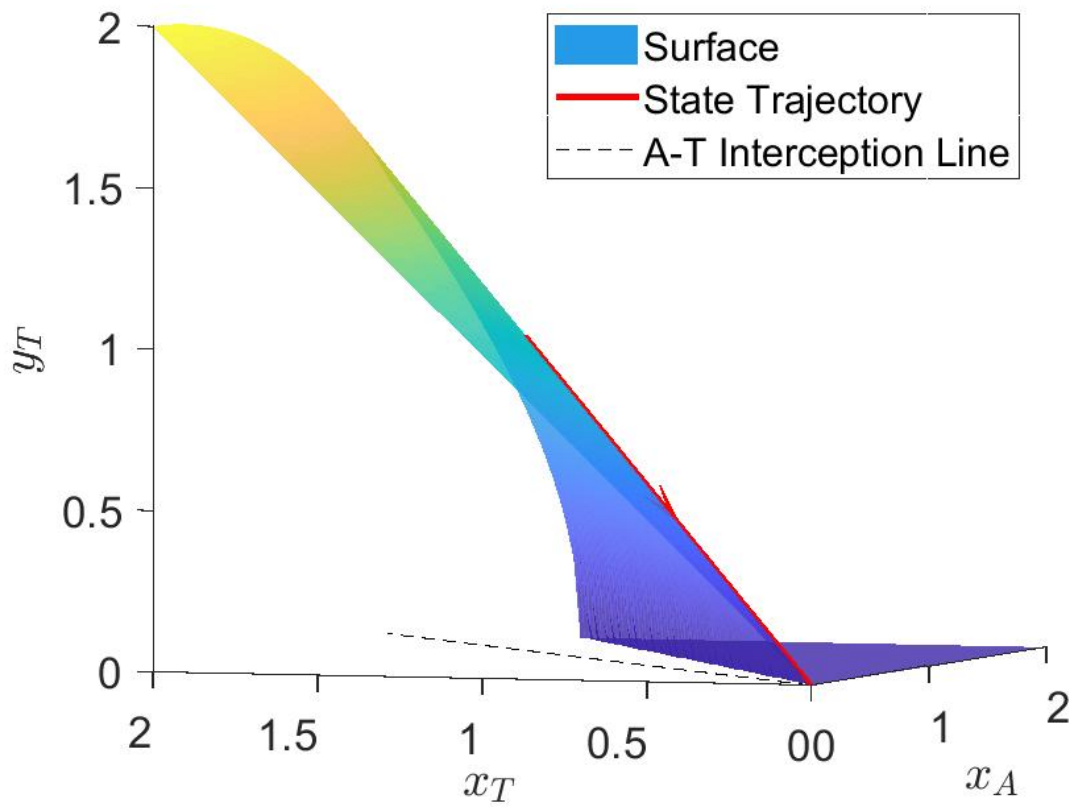
Figure 14. Barrier Surface and a Typical Trajectory
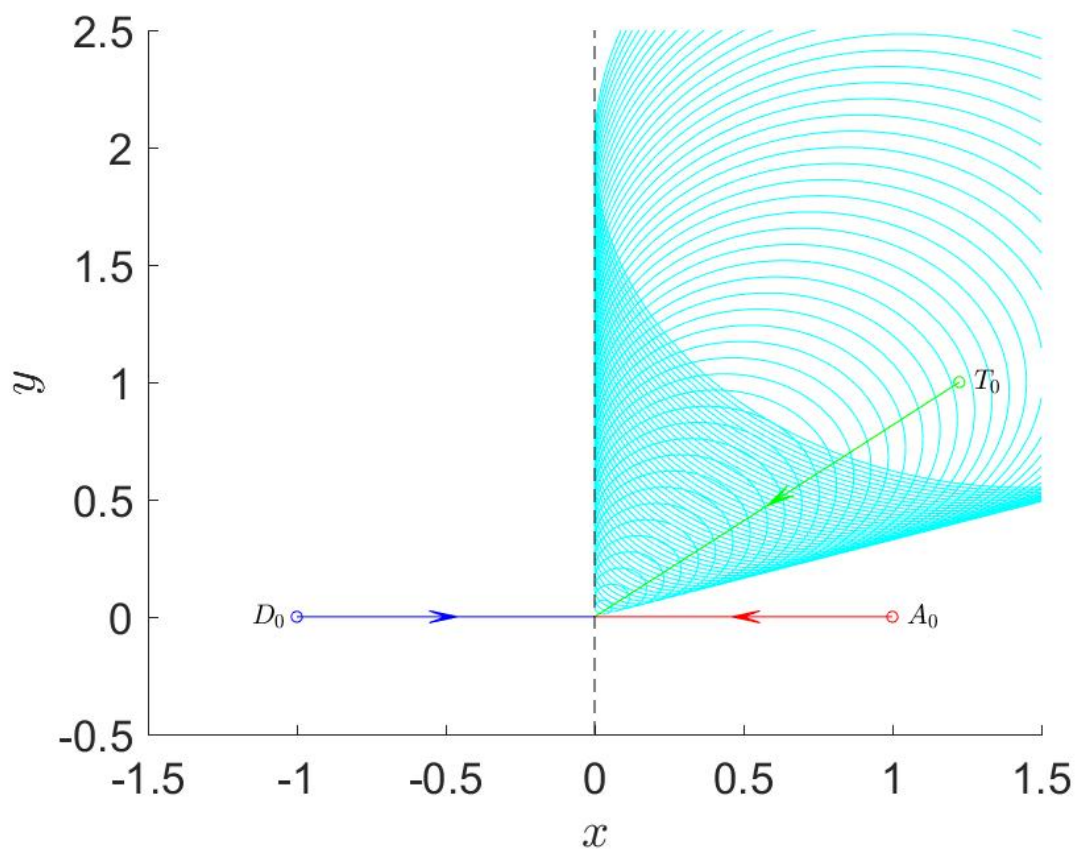
Figure 15. The Players' Barrier Surface Trajectories in the Reduced State Space
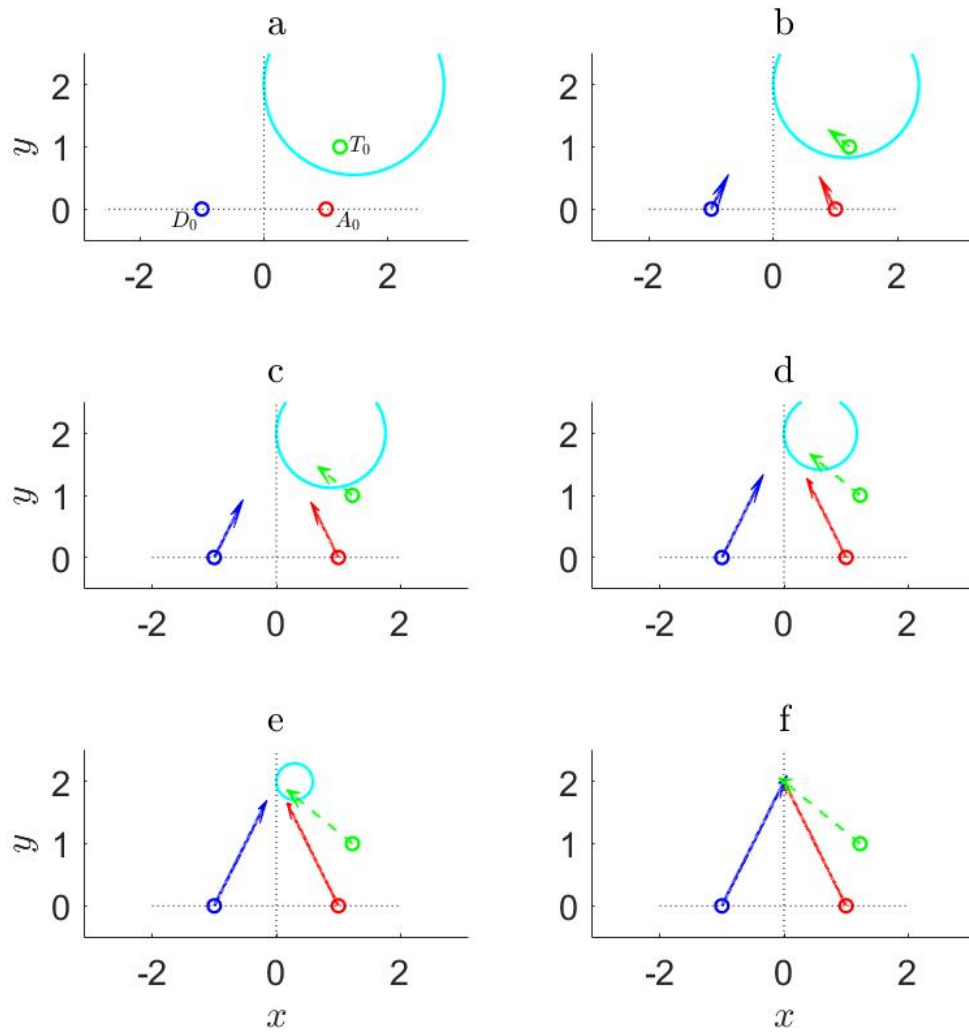
Figure 16. Players' Trajectories in the Realistic Plane when Employing $\sim$ Strategies

To better visualize the dynamics in the realistic plane, Figure 16 is included. This shows each player pursuing a fixed aim point in a straight line which is co-located with the leftmost point of the Apollonius circle and which is the point of tangency of the circle with the y-axis. This point is the farthest left **T** can go before being captured by **A**, should **A** play optimally. The paths shown are the optimal paths in the ATDDG and the minimal cost/maximal payoff is zero.

Nested Surfaces in R_c.

Consider the surfaces S_c where $c < 0$, for example $S_{-0.38} \subset R_c$. It was previously shown that when $c < 0$, the $\sim$ strategies (11), cause the state to rise off of S_c and approach B. Figure 17 shows that despite **A**'s best effort to pull the state
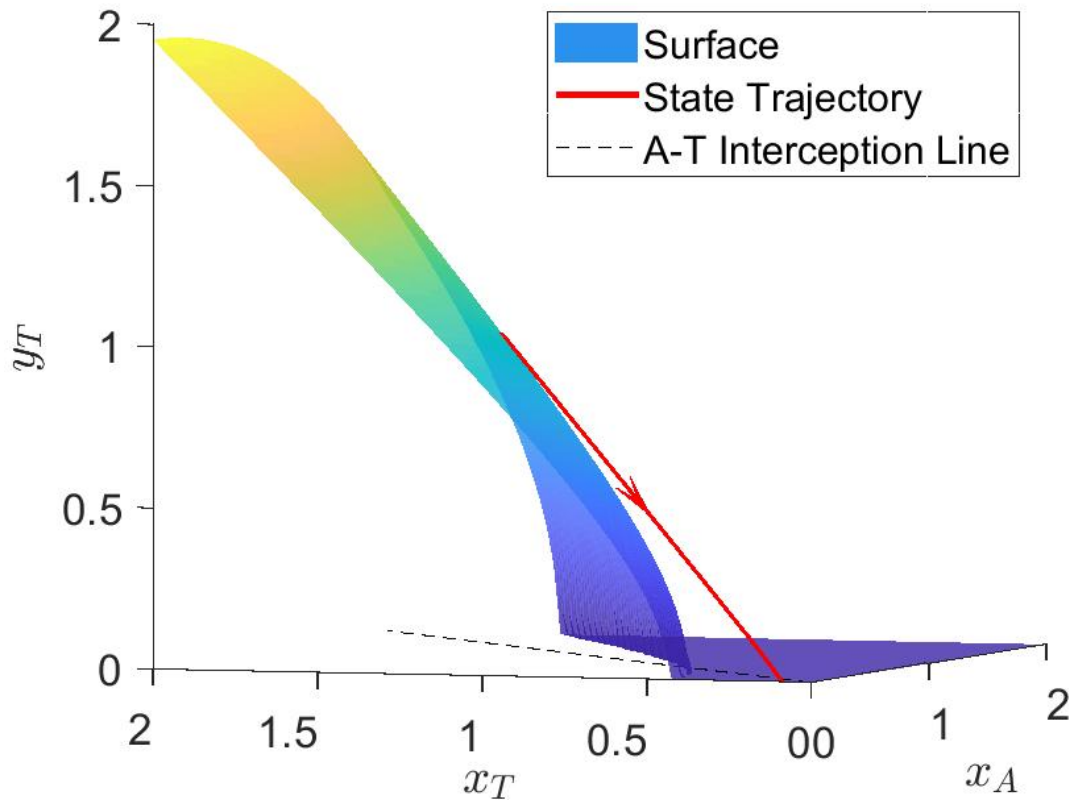
Figure 17. State's Trajectory when Employing $\sim$ Strategies. Initial State is on the Surface $S_{-0.38} \subset R_c$.

44

under the surface S_c (**A** plays the $\sim$ strategy), the state lifts off the surface $S_{-0.38}$ towards the barrier surface B, and **T** ultimately escapes by virtue of the fact that the x_A component of the state reaches 0 before $y_T = 0$; had the state reached the surface $y_T = 0$ while $x_A > 0$, the $\sim$ strategy would have automatically turned into PP and **T** would be captured. Thus the state never reaches the interception line $x_A = x_T$, $y_T = 0$. **T** escapes because as $\lim_{x_A \to 0}$, **A** actually comes under the control of **D**: Because **A** and **D** have equal velocity and simple motion, **A** will not truly be captured by **D**. Instead, **A** will be forced by **D** to flee directly away from **D** as any deviation would cause **A** to immediately be captured by **D**. When **A** is taken over by **D** in this manner, the **T** & **D** team has won because **T** can simply sidestep **A** and forever afterwards be free from the threat of **A**, as the latter is controlled by **D**. In other words, **A** has been eliminated from the game.

Figure 18 and Figure 19 illustrate the player's trajectories in the rotating and realistic planes respectively and provide further insight into **T**'s escape. As shown, this scenario is terminated when **D** meets **A**, even though the state never enters the region R_e above the surface B; but then, recall that the plane $x_A = 0$ is in R_c. By having **A** employ the $\sim$ strategy on surfaces where $c < 0$, **A** becomes suicidal by ultimately passing by **T** only to collide with **D** on the plane $x_A = 0$, whereupon **A** comes under **D**'s control, and **T** can escape. An exception in R_c where **A** is able to capture **T** by playing the $\sim$ strategy is when $y_T(0) = 0$ and $x_T(0) < x_A(0)$. Here, **A** only captures **T** by playing the $\sim$ strategy because he collides with **T** while pursuing the point $(0,0)$, which is the collision point of **A**'s and **D**'s trajectories.

In summary, when all players employ the $\sim$ strategy on surfaces $S_c \subset R_c$ where $c < 0$, y_T does not reach zero until t_f at which time $x_A = 0$. Should y_T reach zero before t_f, then **A** could guarantee its capture of **T** by employing PP in an end game. Had **A**'s position been shifted ever so slightly rightward then y_T would have reached

Figure 18. Players' Trajectories and Dynamic Apollonius Circle when Employing $\sim$ Strategies in the Reduced State Space. Initial State is on the Surface $S_{-0.38}$.

Figure 19. Players' Trajectories when Employing $\sim$ Strategies in the Realistic State Space. Initial State is on the Surface $S_{-0.38}$.

zero and **T**'s capture would be guaranteed by **A** employing PP in the end game after $y_T = 0$ is reached. But when **A** plays the $\sim$ strategy, $y_T = 0$ is not reached before $x_A = 0$ is reached.

In conclusion, the barrier strategy $\sim$ is not a capture strategy in R_c; by **A** playing the barrier strategy $\sim$ in R_c, **A** cannot bring about the capture of **T**.

Nested Surfaces in R_e.

Consider the surfaces S_c where $c > 0$, for example the surface $S_1 \subset R_e$. Here we also see the state departs from the surface S_1. However, the difference here is that now the minimax in eq. (10) is negative and thus the state falls off the surface S_1 and approaches the region R_c. We see this happen in Figure 20 where, despite the **T** & **D** team's best efforts, the state sinks towards the surface S_0 thus approaching the R_c region. Unlike the $S_{-0.38}$ analysis, **T** does not appear to be suicidal, but foolish, since the $\sim$ strategy makes him approach the orthogonal bisector when he could easily cross over where x_T is negative, thus guaranteeing his survival. This foolish trajectory is shown in Figures 21 and 22. Obviously **T** and **D** should not employ the barrier strategy $\sim$ in R_e, but should play their optimal * strategies provided by the solution to the ATDDG in R_e – see [15]. **T**

The barrier strategies are not good strategies in either R_c or R_e, except for on the barrier surface B.

Barrier Strategies against Optimal Strategies.

The players' optimal strategies * for the region R_e have been derived in [15] where the ATDDG was solved: The **T** & **D** team strives to maximize the **A**-**T** separation at the time instant when **A** is met by **D** while **A** strives to minimize said distance. In light of the discovered $\sim$ strategies, the question arises of what will happen should

Figure 20. State's Trajectory when Employing ∼ Strategies. Initial State is on the Surface $S_1 \subset R_c$.
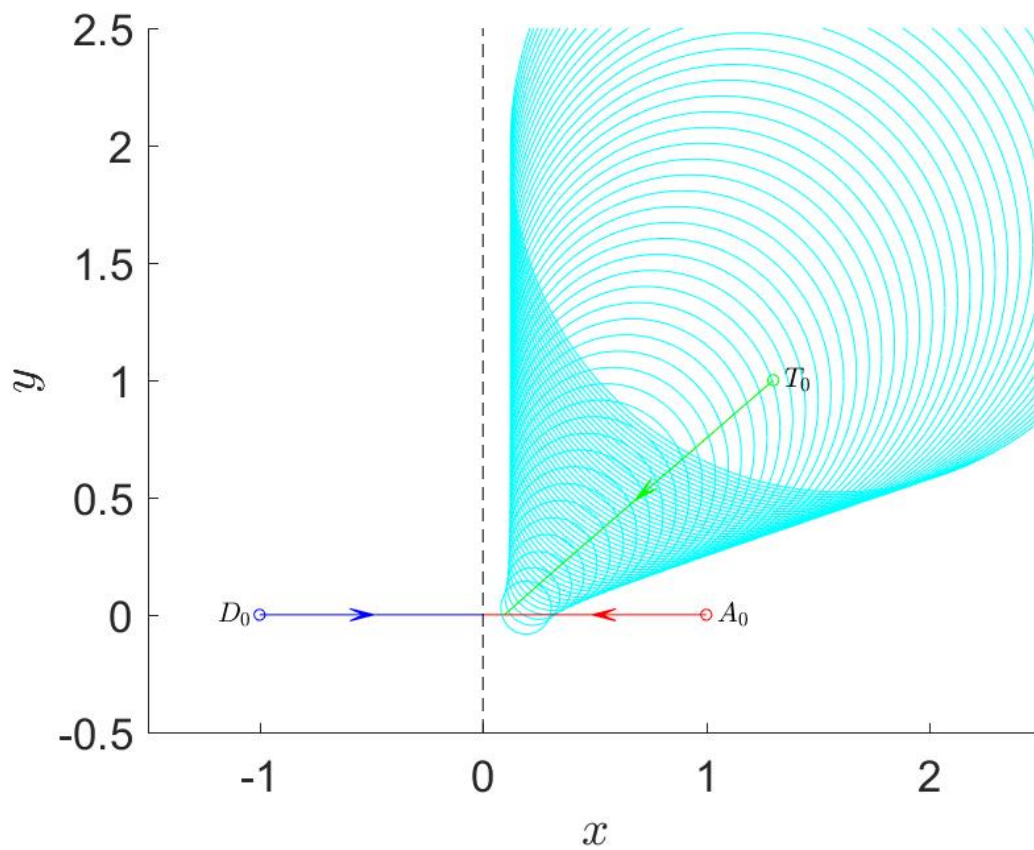
Figure 21. Players' Trajectories and Dynamic Apollonius Circle when Employing $\sim$ Strategies in the Reduced State Space. Initial State is on the Surface S_1.
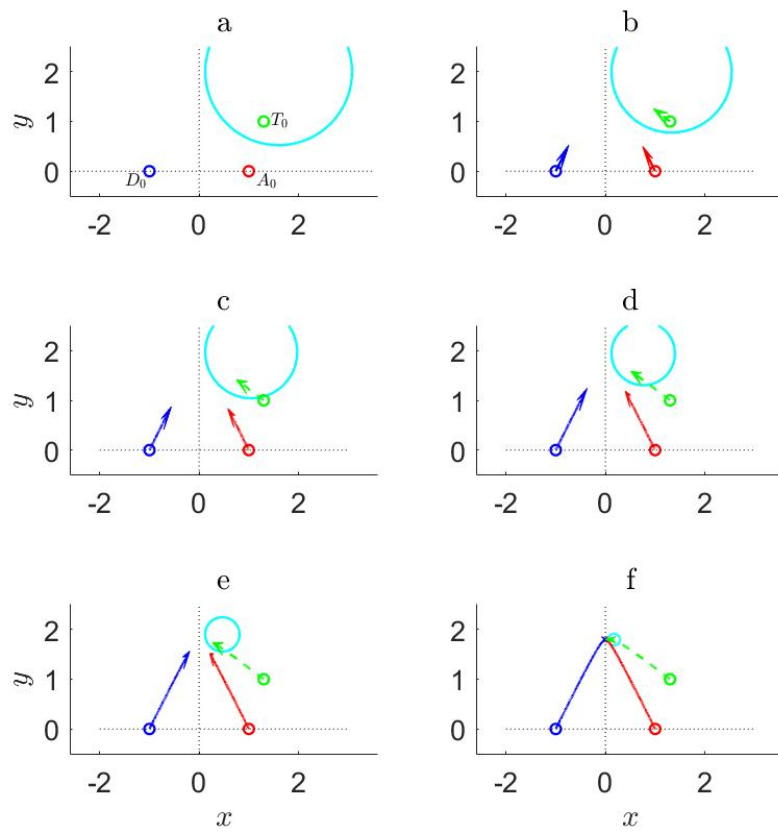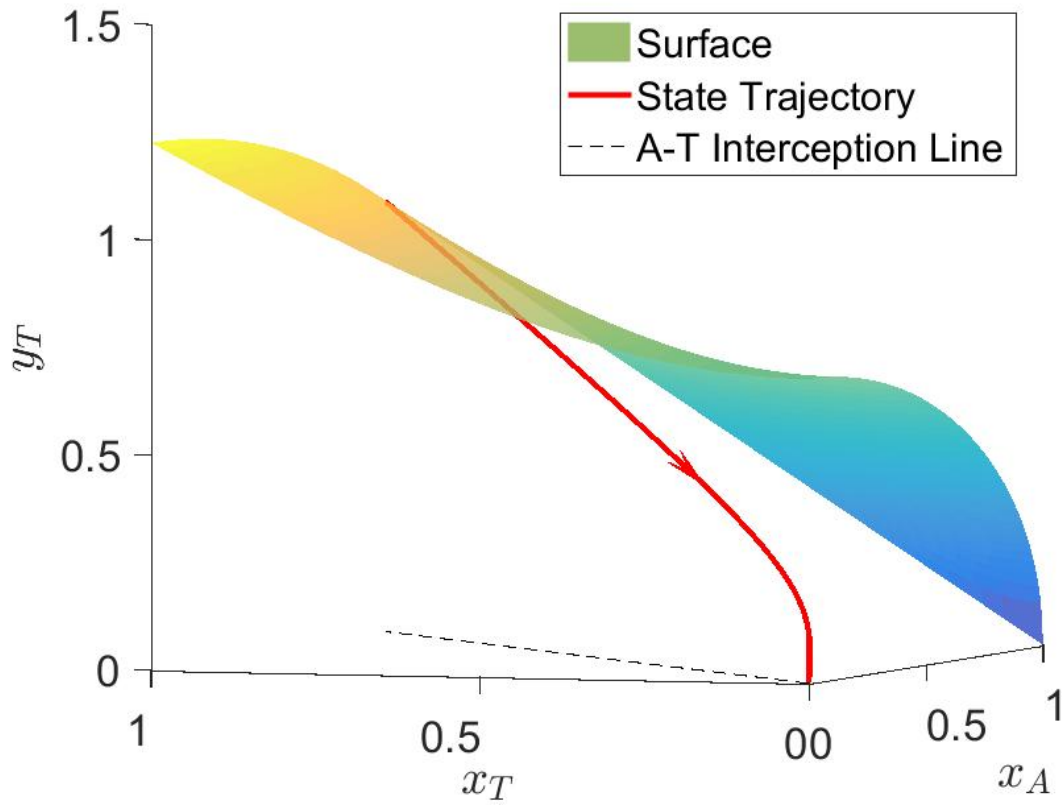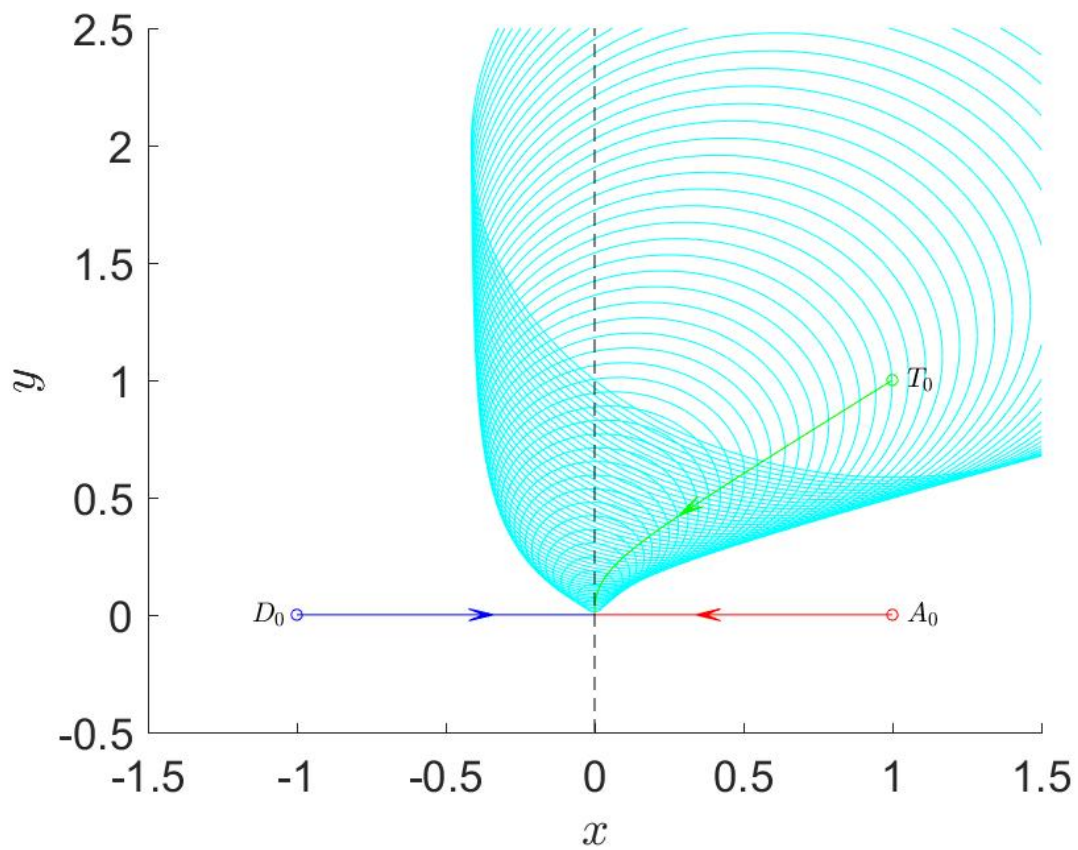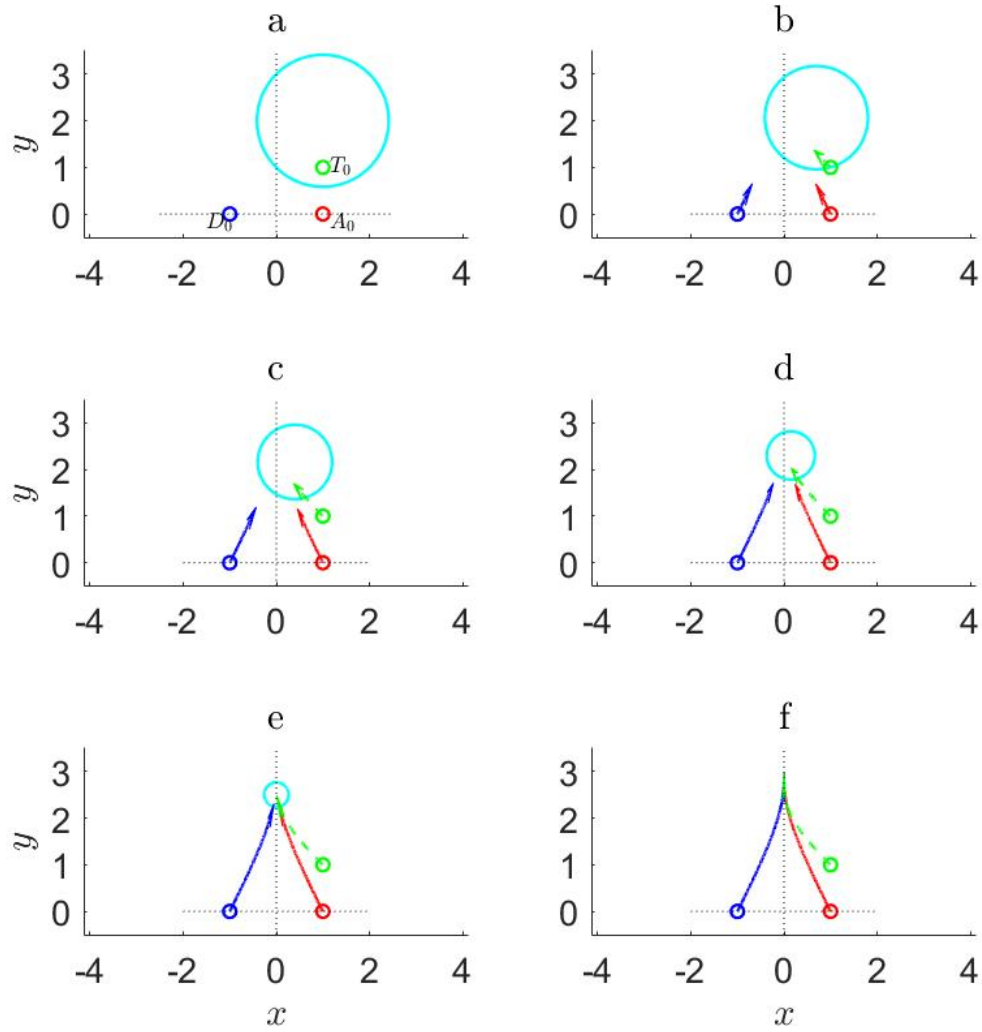
Figure 22. Players' Trajectories when Employing $\sim$ Strategies in the Realistic State Space. Initial State is on the Surface S_1.

a $\sim$ strategy be used against a * strategy. As [15] uses the distance between **T** and the point where **D** intercepts **A** as the performance functional **A**, the * strategy is a guaranteed escape strategy within the region R_e. If **A** plays the $\sim$ strategy while **T** and **D** play * strategies, then **A** should be unable to pull the state from R_e into R_c. If this is not always the case, then the * strategies are not guaranteed escape strategies in the region R_e.

With initial conditions $\{x_a(0) = 1, \ x_t(0) = 1, \ y_t(0) = 1 \}$ and speed ratio $\alpha = \frac{1}{\sqrt{2}}$, the state is in the region R_e. Figure 23 shows the comparison of **A** using the * strategy vs the $\sim$ strategy while the **T** & **D** team employs their * strategies. This figure illustrates the separation that occurs from the initial surface S_1 as time progresses. It was previously shown that should **A** play the $\sim$ strategy within R_e that the state will fall off the initial surface and approach S_0. Therefore the separation seen in Figure 23 is in the direction of S_0, the barrier surface B. For the majority of the calculations, the $\sim$ strategy outperforms the * strategy in terms of pulling the state towards the barrier surface B. However, this advantage is lost in the final moments of play/end game. In fact, there is a correlation of when the seperation distance changes from concave up to concave down and when **T** crosses the orthogonal bisector. From this analysis it appears **A** can pull the states even closer to S_0 by using the $\sim$ strategy while $x_T > 0$, and then switching to the * strategy when $x_T \leq 0$. Unfortunately, this gain will approach zero as $S_c \rightarrow S_0$ as will be shown in Figure 24.

Even though Figure 23 ended with **A**'s * strategy outperforming the $\sim$ strategy in terms of final separation distance from the original surface, the $\sim$ strategy performed better for the majority of the scenarios investigated indicating further analysis is required. Figure 24 shows the separation from S_c when the state is just barely in R_e. Here the two strategies appear to be the same and having **A** play the $\sim$ strategy does not cause the state to enter R_c. This supports the claim that the * strategy obtained

Figure 23. A's * and ∼ Strategies in Region R_e. T and D play their * Strategies with initial conditions $\{x_a(0) = 1, \ x_t(0) = 1, \ y_t(0) = 1\}$.

by solving the game of degree is a guaranteed escape strategy within the region R_e as not even the $\sim$ strategy pulling normal to the surface can bring the state into the R_c region.

This guaranteed escape strategy so should come as no surprise because the value function supplied by the solution of the game of degree, by construction, serves the purpose of a Lyapunov function in the game of kind. In general, embarking on the solution of the game of degree without first due regard to the game of kind might, as a byproduct, yield the solution to the game of kind if one was successful in solving the game of degree. This is a plausible strategy for addressing the game of kind.
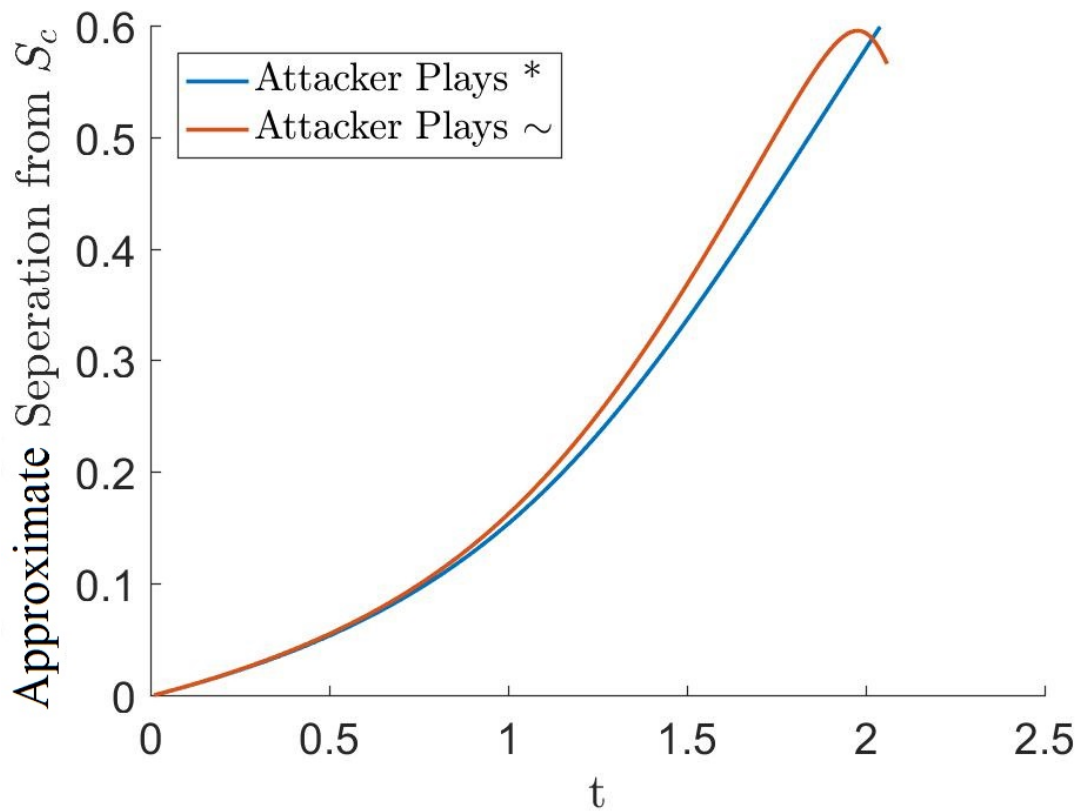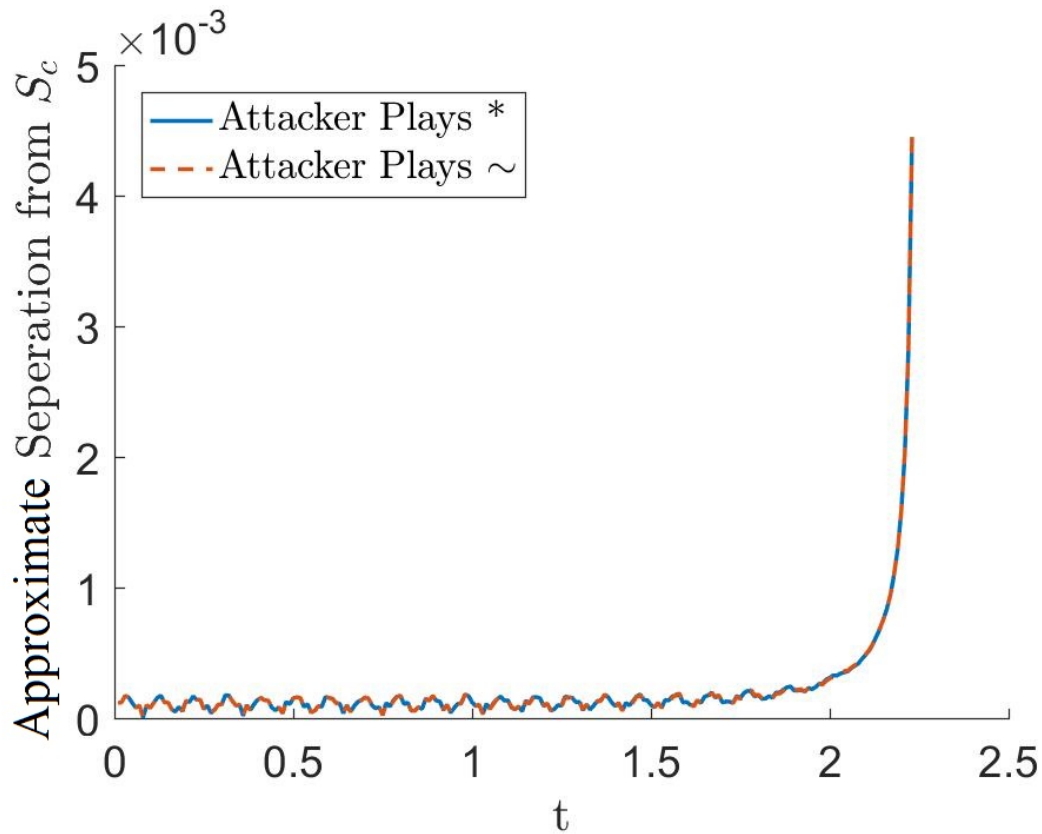

Figure 24. A's * and $\sim$ Strategies in Region R_e. T and D Play * Strategies with initial conditions $\{x_a(0) = 1, \ x_t(0) = 1.2247, \ y_t(0) = 1\}$.

The Game of Kind in R_c: Synthesizing a Capture Strategy for A.

Clearly the players' $\sim$ strategies failed to guarantee either capture of **T** in the R_c region, or escape of **T** in the R_e region. However, analysis of these strategies illustrates that within R_c, **A** was able to interpose himself between **D** and **T**, albeit not until t_f when $x_A(t_f) = 0$. Had the strategy also provided **A** avoidance of **D** s.t. $x_A(t_f) > 0$ when $y_T(t_f) = 0$, then he could guarantee the capture of **T**. Likewise, had **T** been slightly more attracted to **D**, x_T would have turned negative because **T** would cross the orthogonal bisector and guaranteed his escape instead of just approaching the y_T axis as $x_A \to 0$.

Here the first case is addressed, that is, **A**'s capture of **T** in the region R_c.

A can modify his strategy to avoid **D** by establishing a level of avoidance dependent on his distance from **D**. If **D** is far away he will not worry about this threat, but if he is close to **D** then he will strongly avoid **D**. This can be accomplished by using a parameter $\beta = \frac{\epsilon}{x_A}$ where β determines the degree of avoidance of the plane $x_A = 0$ and ϵ determines how close **A** will actually get to **D**. The ϵ value is strongly dependent on the distance of the leftmost point of the Apollonius circle from the orthogonal bisector. If this distance is large, then ϵ can be large and **A** will strongly avoid **D**. If this distance is small, then **A** will need to keep ϵ small enough to allow him to interpose himself between **D** and **T**. As the leftmost point of the Apollonius circle reaches the orthogonal bisector and **T** is nearly able to escape, ϵ will become 0 and there will be no **D** avoidance employed by **A**; in short, the $\sim$ strategies will be used.

Although the inclusion of the parameter β represents a modification to **A**'s $\sim$ strategy in order to avoid **D**, because **D** would expect **A** not to be suicidal, he can assume **A** would employ an avoidance strategy. Therefore β affects how both **A** and **D** behave. This is modeled into our reduced 3-state system as 'leaning' towards x_A

when compared with the normal $\vec{n}$ to a surface S_c, $c < 0$. This new vector is

$$\vec{\bar{n}} = \vec{n} - \beta \left(1,\ 0,\ 0 \right),\ \beta > 0$$

and we can find our new strategies $\bar{\sim}$ using the same process as the $\sim$ strategies, replacing $\vec{n}$ with $\vec{\bar{n}}$ in eq. (10). These modified state feedback $\bar{\sim}$ strategies, parameterized by β, are

$$\sin \bar{\bar{\phi}} = \frac{\frac{\alpha}{1-\alpha^2} y_T}{\sqrt{\frac{1}{\alpha^2} x_T^2 + \frac{\alpha^2}{(1-\alpha^2)^2} y_T^2}}$$

$$\cos \bar{\bar{\phi}} = -\frac{\frac{1}{\alpha} x_T}{\sqrt{\frac{1}{\alpha^2} x_T^2 + \frac{\alpha^2}{(1-\alpha^2)^2} y_T^2}}$$

$$\sin \bar{\bar{\psi}} = \frac{\frac{1}{1-\alpha^2} \left(\frac{1}{\alpha^2} x_T - x_A \right) \frac{y_T}{x_A}}{\sqrt{\frac{1}{(1-\alpha^2)^2} \left(\frac{1}{\alpha^2} x_T - x_A \right)^2 \frac{y_T^2}{x_A^2} + \left(\frac{1}{\alpha^2} x_T - x_A + \beta \right)^2}}$$

$$\cos \bar{\bar{\psi}} = \frac{\frac{1}{\alpha^2} x_T - x_A + \beta}{\sqrt{\frac{1}{(1-\alpha^2)^2} \left(\frac{1}{\alpha^2} x_T - x_A \right)^2 \frac{y_T^2}{x_A^2} + \left(\frac{1}{\alpha^2} x_T - x_A + \beta \right)^2}}$$

$$\sin \bar{\bar{\chi}} = \frac{\frac{1}{1-\alpha^2} \left(\frac{1}{\alpha^2} x_T + x_A \right) \frac{y_T}{x_A}}{\sqrt{\left(\frac{1}{\alpha^2} x_T + x_A - \beta \right)^2 + \frac{1}{(1-\alpha^2)^2} \left(\frac{1}{\alpha^2} x_T + x_A \right)^2 \frac{y_T^2}{x_A^2}}}$$

$$\cos \bar{\bar{\chi}} = -\frac{\frac{1}{\alpha^2} x_T + x_A - \beta}{\sqrt{\left(\frac{1}{\alpha^2} x_T + x_A - \beta \right)^2 + \frac{1}{(1-\alpha^2)^2} \left(\frac{1}{\alpha^2} x_T + x_A \right)^2 \frac{y_T^2}{x_A^2}}}$$

Note that only the **A** and **D** strategies are modified by the ($\bar{\sim}$) strategies; **T**'s strategy is left the same as before, $\sim$, as expected.

In summary, the $\bar{\sim}$ strategy of **A** is designed to initially let him interpose himself between **D** and **T** since $\bar{\sim} \approx \sim$. Then as the **A**-**D** separation decreases the β effect kicks in and since **A** now lies between **T** and **D**, the β effect drives **A** straight for **T**. Indeed, if **A** allows the **A**-**D** separation $2x_A$ to become too small, **D** can rotate the

orthogonal bisector of the $\overline{\mathbf{AD}}$ segment in the direction of **T** by heading in a direction normal to the segment $\overline{\mathbf{AD}}$. This will allow **T** to escape.

Exercising the $\tilde{\sim}$ Strategy of A.

These modified strategies are now implemented for cases where ϵ is set appropriately and where ϵ is set too large. These cases will be $\epsilon = 0.001$ and $\epsilon = 1$.

Figure 25 shows trajectories for the $\epsilon = 0.001$ case. The final window shows a zoomed in plot of how **A** inserts itself between **T** and **D** in the end game, where the Xs represent each player's position at t_f. In fact, for a time **A** runs towards **D**, but once it reaches a certain proximity to **D**, dependent on β, it turns tail and heads to intercept **T**. At this switch point the players are co-linear and **A** simply uses PP to capture **T**. This PP scenario follows the optimal flow diagram of Figure 11 on the $y_T = 0$ plane. It is crucial that ϵ is set to allow these points to become co-linear, otherwise **T** may still be able to escape.

Figure 26 shows trajectories for the $\epsilon = 1$ case. Here we see that **T** is able to escape and termination occurs as the left-hand side of the Apollonius circle reaches the orthogonal bisector as shown in Figure 27. We also see in the final window of Figure 26 that **A** begins avoiding **D** too soon and as a result misses his opportunity to insert himself between **T** and **D**. If the state was deeper in the region R_c then perhaps this ϵ value would guarantee capture of **T**; however, for this initial state it is a poor choice of ϵ.

From this analysis we see that if **A** is able to insert himself between **T** and **D** so that the points **D**, **A**, and **T** become co-linear, then he has guaranteed his capture of **T**. PP of **T** happens automatically when **A** becomes sufficiently close to **D** as set by β. Borderline cases should be further analyzed to ensure that unexpected behavior from the **T** & **D** team won't thwart **A**'s strategy.
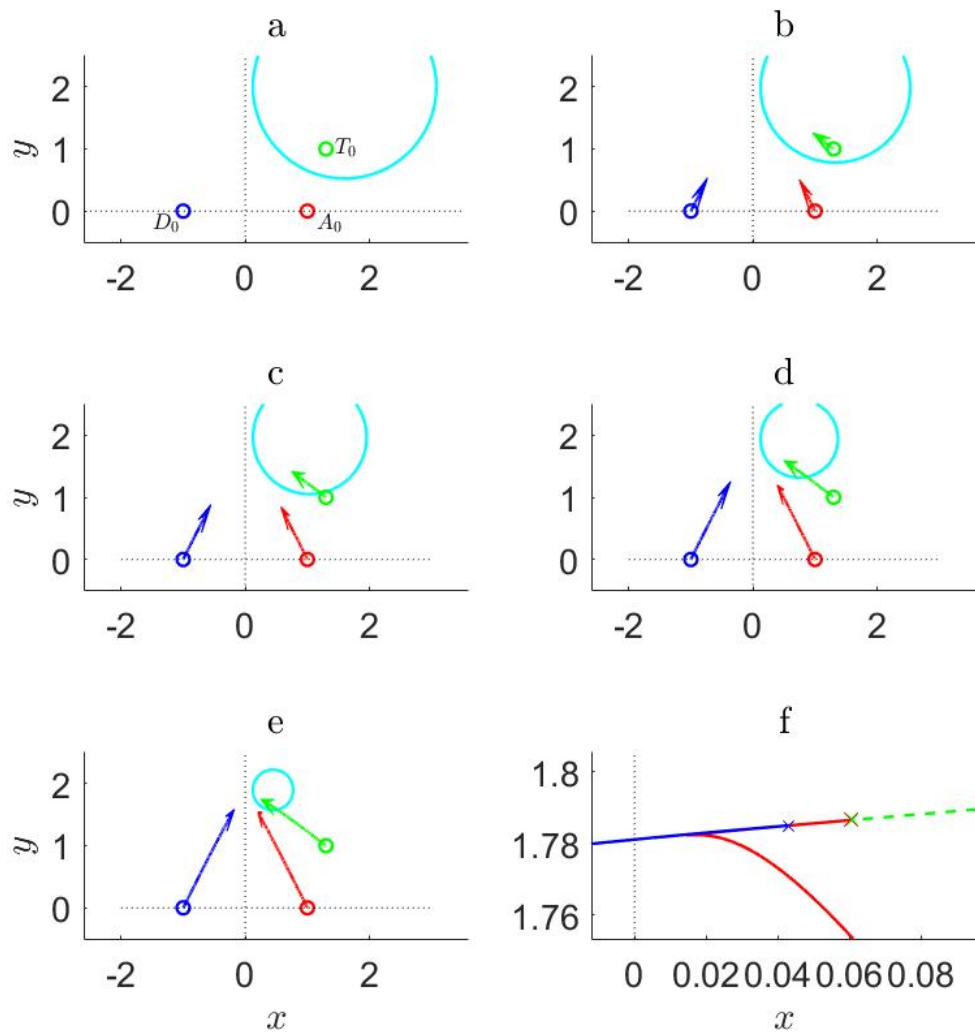
Figure 25. Player's Trajectories Using $\tilde{\sim}$ Strategies with $\epsilon = 0.001$ in the Realistic Plane

58
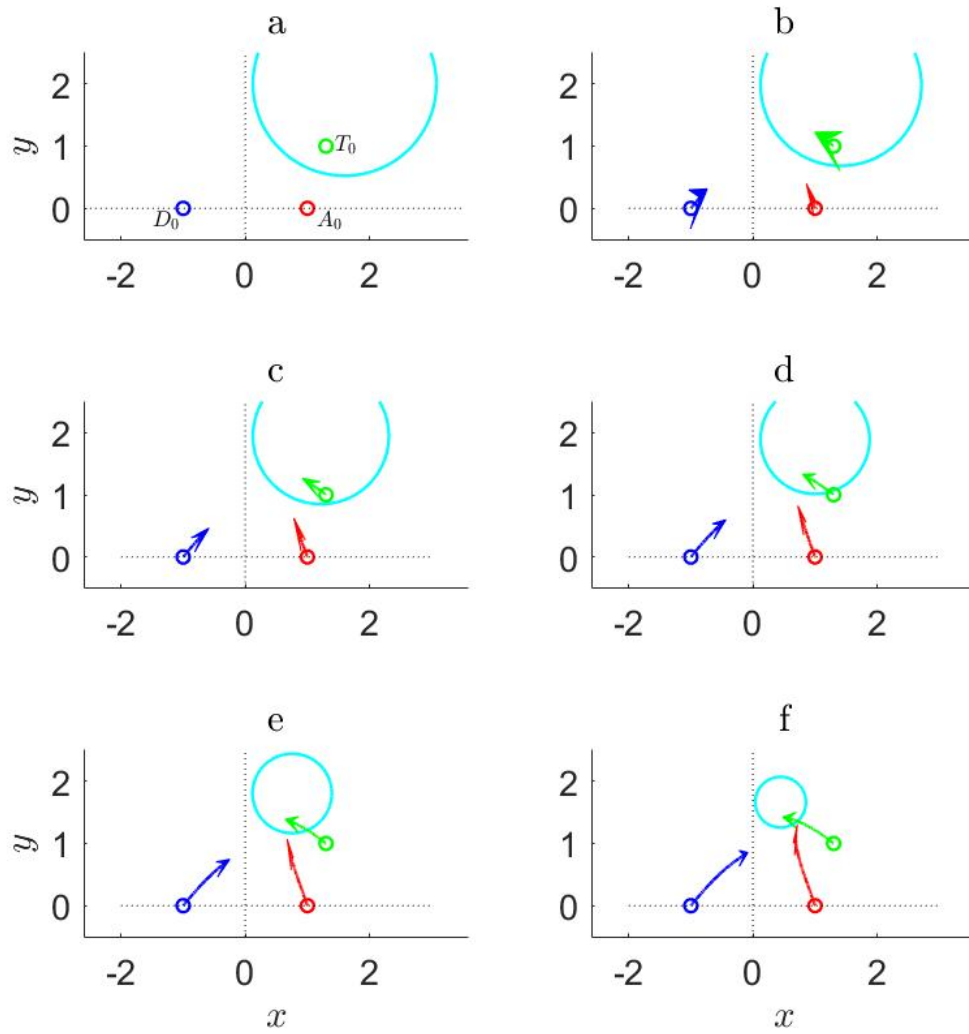
Figure 26. Players' Trajectories in the Realistic Plane when using $\sim$ Strategies with $\epsilon = 1$
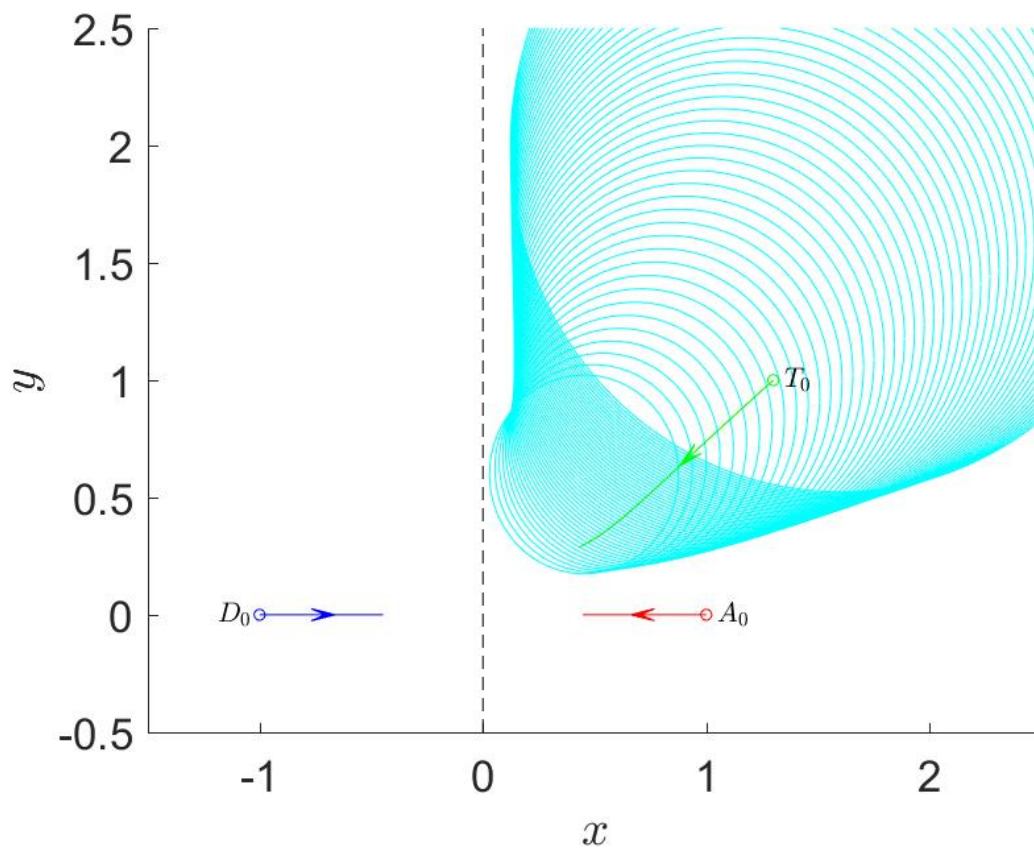
Figure 27. Players' Trajectories in the Reduced State Space when using $\tilde{\sim}$ Strategies with $\epsilon = 1$

In this paper the focus is on **A**'s region of win, R_c. Since optimal strategies for the region R_e have already been presented in [15], guaranteed strategies for this region are not discussed here in detail.

3.5 Conclusion

The capture of a Target by an Attacker in the presence of a Defender in a 3-player pursuit-evasion differential game was investigated. A barrier surface B was constructed which separates the regions of win of the Attacker and the **T** & **D** team. It was seen that for initial states on the barrier surface B when all players employ their respective barrier strategies, the state will follow the barrier surface B down and ultimately result in a draw. As B separates the regions R_c (where **T** will be captured) and R_e (where **T** is able to escape), no player is able to gain an advantage and we see an equilibrium emerge for this unique case. This is the optimal solution along B of the ATDDG.

For states on surfaces S_c where $c \neq 0$ we saw trajectories that certainly are not optimal solutions in a game of degree, but the attendant $\sim$ strategies are of interest as they were derived from the barrier strategies. For both $c < 0$ and $c > 0$ we saw that the barrier strategies positioned the players to have opportunities of win, although continuing with the barrier strategies to t_f, where $x_A = 0$, ultimately led to their demise. By modifying the $\sim$ barrier strategies in R_c where $c < 0$ to derive the $\bar{\sim}$ strategies, we saw that **A** was able to maintain a safe distance from **D** to ensure capture of **T**, provided an appropriate ϵ value was used. Because ϵ being assigned larger values can cause **A** to avoid **D** too early before interposing himself between **T** and **D**, to synthesize **A**'s capture strategy in R_c it is best to set ϵ as small as possible.

IV. Time Optimization Analysis

4.1   Abstract

A pursuit-evasion differential game involving three players, an Attacker/Pursuer, a Target/Evader, and a Defender, is considered. The Defender strives to assist the Target/Evader by intercepting the Attacker/Pursuer before the latter reaches the Target. A barrier surface separates the winning regions of the Attacker and Target-Defender team when employing optimal strategies. The game in the Target-Defender team's region of win has previously been addressed under the header of active target defense. In this paper, the game in the Attacker's region of win where the Defender cannot preclude the Attacker from capturing the Target, given that the Attacker plays optimally, is investigated.

4.2   Introduction

Consider the archetypal pursuit-evasion differential game in the Euclidean plane where the players have simple motion à la Isaacs [10] and the pursuer is faster than the evader. The pursuer's optimal strategy entails Pure Pursuit (PP) while the evader runs for his life. However, what if there was a safe haven region/static sanctuary close by, and the slower evader could avoid being captured by the faster pursuer upon reaching the safe haven before the pursuer reaches him? In this case the evader can run to the safe haven instead of running for his life. Should he arrive at the safe haven before the pursuer reaches him, then the pursuer has lost and the time to capture goes to infinity. Whether or not the evader can reach the safe haven depends on the speed ratio of the pursuer and evader. The state space is therefore partitioned as to whether or not the evader can reach the safe haven – see Figure 28.

This paper considers such a scenario, albeit instead of an evader, a pursuer, and
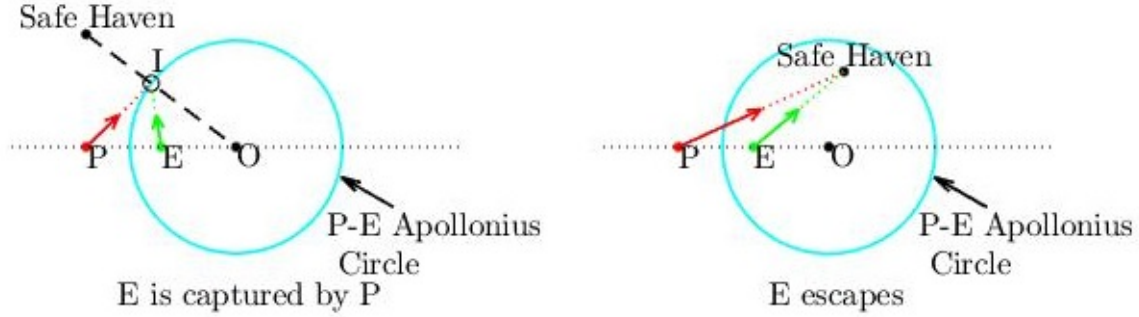
Figure 28. Safe Haven Scenarios

a safe haven/static target set, it deals with an Attacking missile (**A**), a Defending missile (**D**), and a dynamic Target aircraft (**T**). Therefore, this is an Active Target Defense Differential Game (ATDDG) where the sanctuary is the Target and the roles of the Attacker and Defender are assigned to the evader and pursuer respectively. This paper compliments the work in [15], where the game is played in the **T** & **D** team's region of win in which **D** intercepts **A** before the latter captures **T** under optimal play - see also [16]. In contrast, within this paper attention is given to the state-space region where under optimal Attacker play, **T**'s capture by **A** is guaranteed despite the best efforts of the **T** & **D** team. Concurrent work is analyzing this region, using the final Defender-Target separation distance as the performance functional [9]. This paper will instead develop strategies with time as the performance functional. It is shown that **A**'s PP strategy is not globally optimal in his region of win. The subset of **A**'s region of win where PP is the optimal strategy is characterized while escape from PP in the compliment of this region is demonstrated.

4.3 The Active Target Defense Paradigm

The following 3-player pursuit-evasion differential game is considered. A hostile attacking missile **A** seeks to capture a fleeing target **T** which can be thought of as an aircraft. A third player, a defending missile **D**, is introduced who seeks to intercept

A before the latter intercepts **T**.

Assumptions.

1. **A**, **T**, and **D** have simple motion/are holonomic, à la Isaacs – think of a Beyond Visual Range (BVR) engagement.

2. **T**'s speed is less than the **A**'s. If this were not the case then there would be no need for **D**. Thus, the speed ratio $\alpha \triangleq \frac{v_T}{v_A} < 1$ where v_A and v_T are **A**'s and **T**'s velocities respectively.

3. **D**'s speed is the same as **A**'s: $v_D = v_A$; the **A** and **D** missiles have similar capabilities.

4. It is assumed that all players are aware of each other's positions; this is a differential game with complete information where state feedback strategies are sought.

Dynamics.

The state space of the ATDDG encodes each of the players' positions in the realistic plane (X, Y), creating a 6-state system. However the 6-state system can be reduced to 3 states using a non-inertial, rotating reference frame by pegging the x-axis to **A**'s and **D**'s instantaneous positions. The y-axis is the orthogonal bisector of the $\overline{\mathbf{AD}}$ segment. In this rotating reference frame, the states are **T**'s x and y-positions (x_T, y_T) and **A**'s x-position x_A. **A**'s y-coordinate will always be 0 in this state space and **D**'s position will be $(-x_A, 0)$. This rotating reference frame is shown overlaid on the realistic plane in Figure 29 where the **A**, **T**, and **D** players' respective headings χ, ϕ, and ψ are also indicated. Initially the rotating frame (x, y) is aligned with the inertial frame (X, Y).
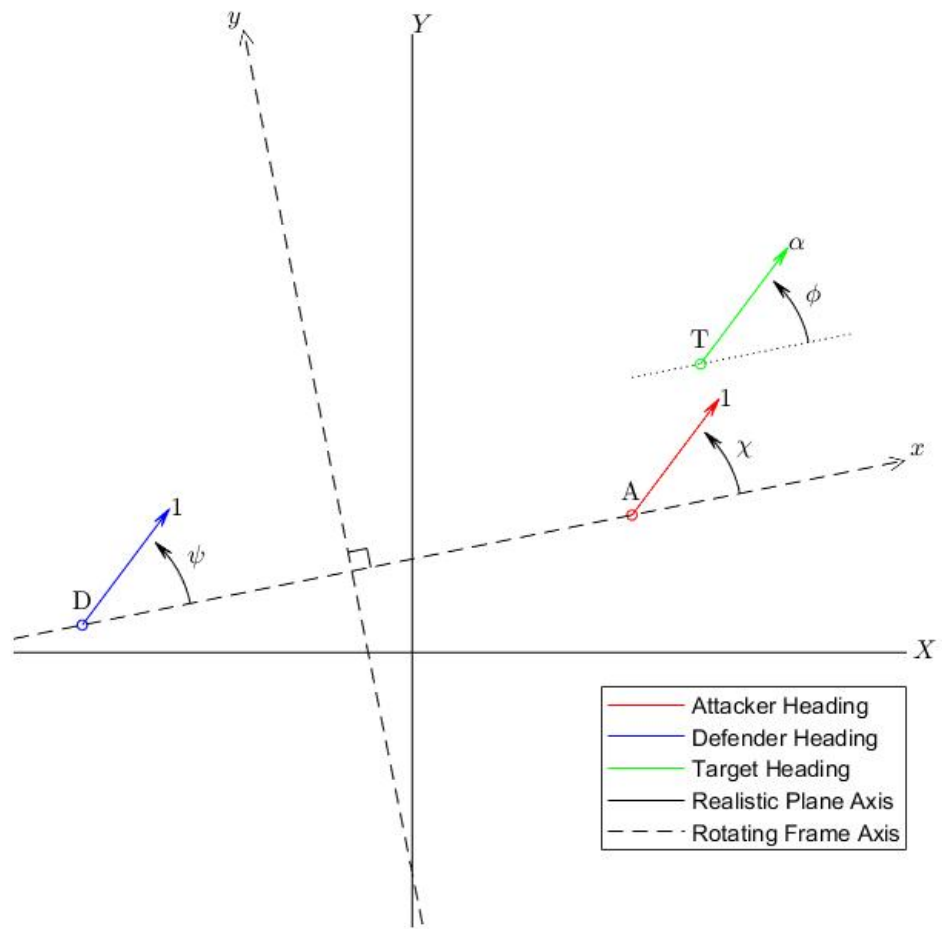
Figure 29. Rotating Reference Frame

Using this rotating reference frame (x, y) the state space is $\{(x_A, x_T, y_T)|x_A \geq 0,\ y_T \geq 0\} \subset \mathbb{R}^3$ and the 3-state system nonlinear dynamics are

$$\dot{x}_A = \frac{1}{2}\left(\cos \chi - \cos \psi\right)$$

$$\dot{x}_T = \alpha \cos \phi - \frac{1}{2}\left(\cos \psi + \cos \chi\right) - \frac{1}{2}\frac{y_T}{x_A}\left(\sin \psi - \sin \chi\right)$$

$$\dot{y}_T = \alpha \sin \phi - \frac{1}{2}\left(\sin \psi + \sin \chi\right) + \frac{1}{2}\frac{x_T}{x_A}\left(\sin \psi - \sin \chi\right)$$

Geometry.

The Apollonius Circle is the locus of all points whose ratio of distances from two fixed points, say $\mathbf{A}$ and $\mathbf{T}$, is constant. The ratio of the line segments from $\mathbf{A}$ and $\mathbf{T}$ to a point on the circumference of the Apollonius circle is the $\mathbf{A}$-$\mathbf{T}$ speed ratio α. The Apollonius circle is critical to understanding the 2 regions of play: (1) R_c where $\mathbf{T}$ is captured by $\mathbf{A}$ under optimal play by $\mathbf{A}$; (2) R_e where $\mathbf{D}$ allows $\mathbf{T}$ to escape. Should one of the player's err, the dynamic Apollonius Circle also helps with understanding when play shifts from $\mathbf{A}$'s winning region R_c to the $\mathbf{T}$ & $\mathbf{D}$ team's winning region R_e, and vice versa.

Given the state of the game, that is the instantaneous positions of players $\mathbf{A}$ and $\mathbf{T}$ and the speed ratio parameter α, the center (x_O, y_O) of the dynamic Apollonius circle is

$$x_O = \frac{1}{1 - \alpha^2}(x_T - \alpha^2 x_A), \quad y_O = \frac{1}{1 - \alpha^2} y_T \tag{14}$$

with a radius of

$$\rho = \frac{\alpha}{1 - \alpha^2} d \tag{15}$$

66

where $d = \sqrt{(x_T - x_A)^2 + y_T^2}$ is the current distance from **A** to **T**.

State-Space Partition.

The state-space region where under optimal play **A** wins is denoted by R_c and the state-space region where under optimal play the **T** & **D** team wins is denoted by R_e. As shown in [15], when $x_T > 0$, there is a minimum speed ratio $\bar{\alpha}$ which guarantees escape for **T** assuming **T** and **D** play optimally. This is attended by the Apollonius Circle intersecting the y-axis, which was previously defined as the orthogonal bisector of the $\overline{\mathbf{AD}}$ segment – see Figure 30. Given x_A, x_T, and y_T, this critical speed ratio is
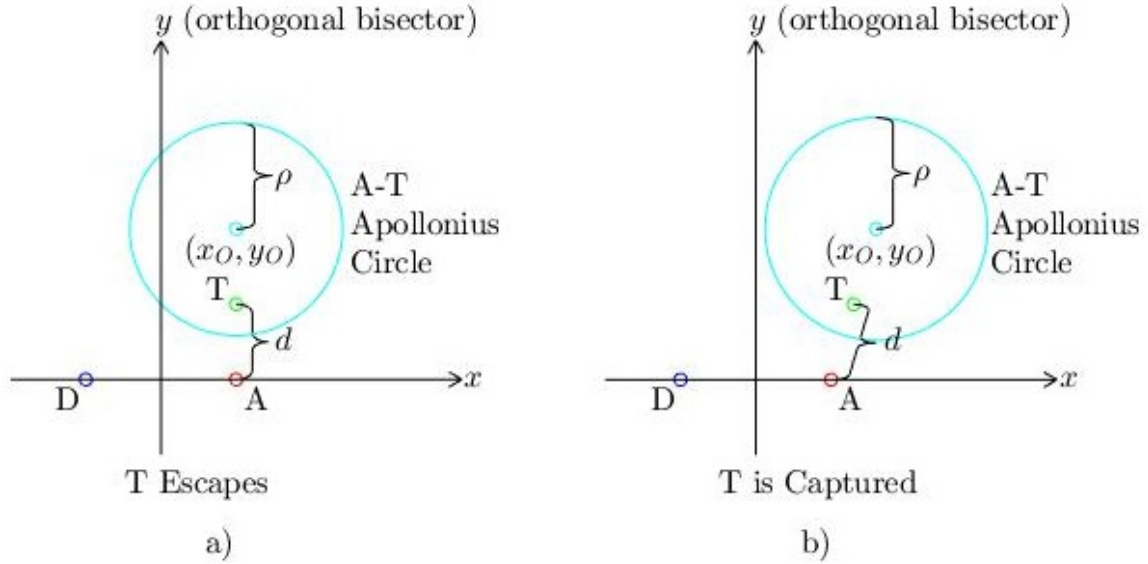

Figure 30. The A-T Apollonius Circle Escape a) and Capture b) Regions

$$\bar{\alpha} = \frac{\sqrt{(x_A + x_T)^2 + y_T^2} - \sqrt{(x_A - x_T)^2 + y_T^2}}{2x_A}$$

whereupon the Apollonius circle is tangent to the y-axis.

Thus, when $x_T(0)$ is positive, $0 \leq \alpha < \bar{\alpha}$ defines the state-space region R_c yielding

67

A's region of win in the reduced state space,

$$R_c = \{(x_A, x_T, y_T) | x_A > 0, \; x_T > 0, \; y_T \geq 0, \; x_A^2 + \frac{y_T^2}{1-\alpha^2} - \frac{x_T^2}{\alpha^2} < 0\}$$

where under optimal play of **A**, the capture of **T** is guaranteed.

The **T** & **D** team region of win

$$
\begin{aligned}
R_e =& \{(x_A, x_T, y_T) | x_A \geq 0, \; x_T > 0, \; y_T \geq 0, \; x_A^2 + \frac{y_T^2}{1-\alpha^2} - \frac{x_T^2}{\alpha^2} \geq 0\}... \\
&... \cup \{(x_A, x_T, y_T) | x_A \geq 0, \; x_T \leq 0, \; y_T \geq 0\}... \\
&... \cup \{(x_A, x_T, y_T) | x_A = 0, \; x_T \geq 0, \; y_T \geq 0\}
\end{aligned}
$$

complements the state space where under optimal play of **T** and **D**, **T**'s escape is guaranteed. This paper focuses the game in on **A**'s winning region, R_c.

State-Space Partition from a Different Angle.

It is typical to only consider the **A** and **T**-based Apollonius circle in the ATDDG. This provides a clear method to visualize which winning region the state is in: Simply put, if the Apollonius circle intersects the orthogonal bisector of the $\overline{\textbf{AD}}$ segment, then **T** is able to escape since **D** intercepts **A** before the latter captures **T**, otherwise **T** will be captured assuming all players play optimally. By instead shifting the perspective to **T** escaping by achieving protection by **D**, an alternative escape mechanism is revealed.

Consider a second Apollonius circle created which determines where **T** and **D** can meet when traveling along straight lines. Should **T** meet **D** before **A** reaches the former, then **T** would be under the protection of **D** and in the winning region of **T**. Figure 31 illustrates this instance. As seen, **T** can reach the T-**D** Apollonius Circle without contacting the **A**-**T** Apollonius Circle. Therefore **T** escapes because he is

now protected by **D** and a safe region develops. This is shown as the shaded region in Figure 31.
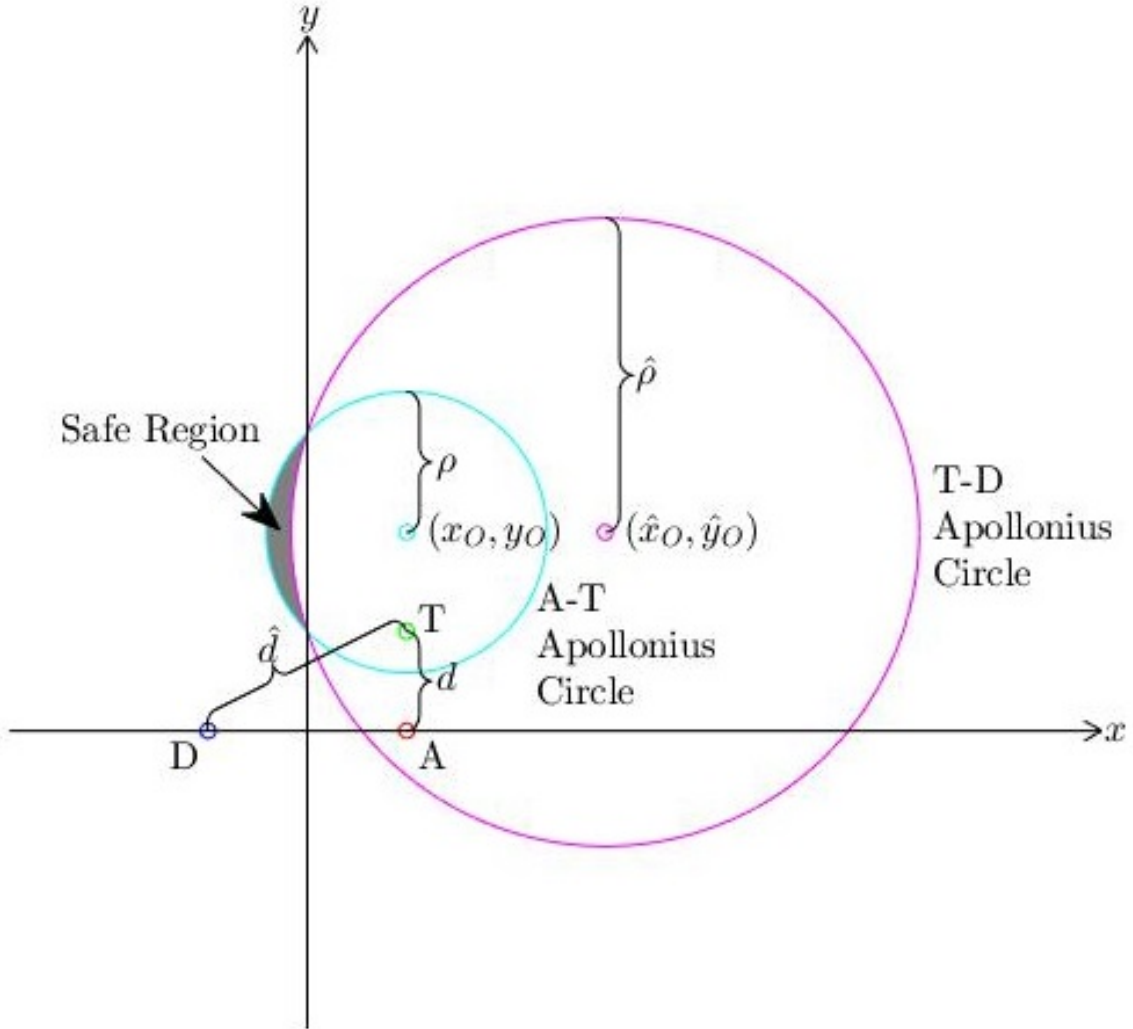
Figure 31. The A-T and T-D Apollonius circles when the state is in R_e

The center of the **A-T** Apollonius circle is given in Eqs. (14). Applying the same logic to the **T-D** Apollonius circle yields the coordinates of its center

$$\hat{x}_O = \frac{1}{1-\alpha^2}\left(x_T + \alpha^2 x_A\right), \quad \hat{y}_O = \frac{1}{1-\alpha^2}y_T$$

As seen $y_O = \hat{y}_O$, which says that these two circles' centers share the same y-

coordinate. Attention thereby shifts to the x_O and $\hat{x}_O$ relationship, and more specifically to the leftmost point of these circles. According to Eq. (15), the circles' radii are

$$\rho = \frac{\alpha}{1 - \alpha^2}d, \quad \hat{\rho} = \frac{\alpha}{1 - \alpha^2}\hat{d}$$

where $\hat{d}$ is the length of the segment $\overline{\mathbf{TD}}$. Since play occurs in the region R_c, the leftmost point of each Apollonius circle will be positive. Because the **T-D** Apollonius circle's leftmost x-coordinate $\hat{x}_{Left} = \hat{x}_O - \hat{\rho}$ must be positive, one can show that the condition

$$x_A^2 - \frac{x_T^2}{\alpha^2} + \frac{y_T^2}{1 - \alpha^2} < 0 \tag{16}$$

must hold. This relationship was previously used to characterize R_c in the ATDDG.

Finally, in order for **T** to be protected by **D** in the region R_c, the relationship $x_{Left} - \hat{x}_{Left} < 0$ must hold; otherwise, **T** will fail to reach the circumference of the **T-D** Apollonius circle as it first must cross the **A-T** Apollonius circle. But this yields

$$x_A^2 - \frac{x_T^2}{\alpha^2} + \frac{y_T^2}{1 - \alpha^2} > 0$$

which contradicts Eq. (16). Therefore escape can only occur within the region R_e characterized in [15] where the ATDDG is analyzed. This alternative escape strategy reinforces the relevance of the previously developed regions R_e and R_c, as well as the barrier surface B which is discussed in the next section.

The Barrier Surface.

Treating the three-player differential game as a Game of Kind allows one to analyze the possible discrete outcomes of the game. In contrast, a Game of Degree focuses on maximizing or minimizing a cost functional. The 3 possible outcomes for the ATDDG Game of Kind are
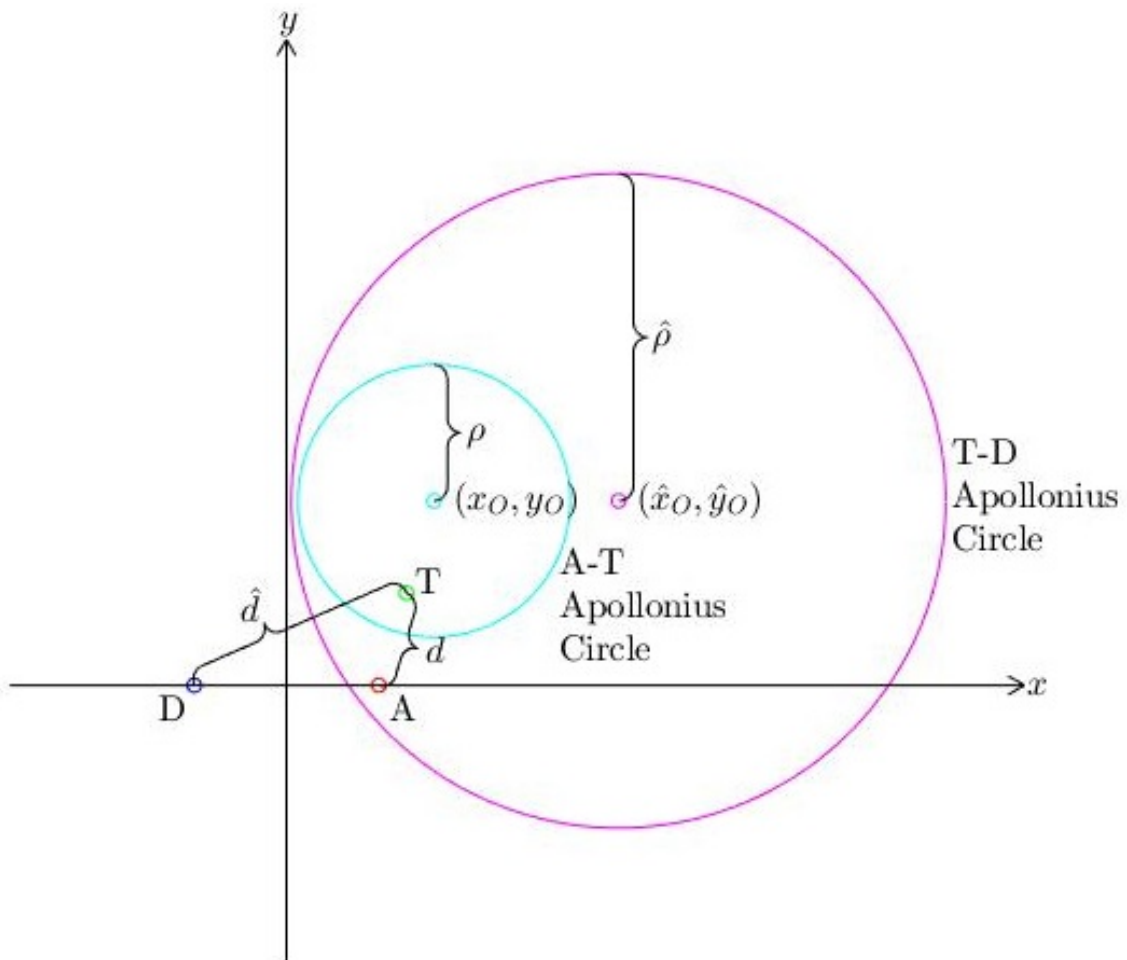
Figure 32. The A-T and T-D Apollonius Circles when the state is in R_c

1. **T** is captured by **A**

2. **A** is intercepted by **D**, and **T** escapes

3. **A**, **T**, and **D** all meet at the same moment, resulting in a draw.

The barrier B is the surface which separates the regions R_c and R_e and is specified in the reduced $\mathbb{R}^3$ state space as

$$B = \{(x_A, x_T, y_T) | x_A \geq 0, \ x_T \geq 0, \ y_T \geq 0, ...$$
$$...x_A^2 + \frac{y_T^2}{1 - \alpha^2} - \frac{x_T^2}{\alpha^2} = 0\}$$

Although the argument may be made that the barrier surface should not include the origin, treating it as such would also exclude the plane $x_A = 0$ from the region R_e and the line $\{x_A = x_T, \ y_T = 0\}$ from the region R_c. Therefore the origin is considered part of the barrier surface. The plane $x_A = 0$ also separates the set R_e and R_c and is included in R_e.

Should all players play optimally, the winner can be determined by the side of the surface B of which the initial state $\{x_A(0), x_T(0), y_T(0)\}$ lies. Nevertheless, if any player fails to play optimally when the initial state lies in his winning region, then the opposing player(s) can take advantage of this by pulling the state across B into their winning region. For example, should **A** fail to play optimally in R_c, the **T** & **D** team could pull the state $\{x_A, x_T, y_T\}$ to the plane $x_A = 0$, which is in R_e. The Game of Kind thus morphs into each player pulling the state in the direction of his respective winning region. If the initial state lies in his winning region, then he would pull deeper into his region, but if the initial state is not be in his winning region, then he would pull towards his winning region. The deeper any player can pull the state into his winning region the more likely he will win, for if at some future point in time he does err, then the buffer he has established within his region will allow him

72

to recover.

Time as the Performance Functional.

Choosing time in this paper as the measure of performance provides several benefits. Most importantly, because **A**'s strategy requires him to capture **T** within his winning region R_c to satisfy the Game of Kind, the solution yields a guaranteed capture strategy. At the same time, by solving the Game of Degree with time as the performance functional, real-world requirements are implicitly taken into consideration. In a real-world engagement, although **A** may behave in a manner that guarantees capture of **T**, there is the risk that **A** runs out of fuel before reaching **T**, as aircraft generally have longer ranges than missiles. By therefore minimizing the flight time required to capture the target, he is also preserving his fuel. In contrast, if the **T** & **D** team maximizes the time to capture, they may cause **A** to run out of fuel and thus prevent **A** from achieving his objective of capturing **T**.

Pure Pursuit.

During PP, **A** heads directly towards **T**'s instantaneous position. **A** relies on his faster speed to catch up to **T**. Because the game dynamics are simple motion, if **A** employs PP in the absence of **D**, then **T**'s best strategy would be to run directly away from **A**, thus maximizing his time to capture. This simple differential game, with t_f as the performance functional, results in both **A** and **T** advancing along straight-line paths until **A** ultimately catches up with and captures **T**. **T** will be captured by **A** at $t_f = \frac{1}{1-\alpha} d_0$ where the initial **A**-**T** separation is d_0. As PP is such a simply understood strategy, it is often found employed in nature. Think of a cheetah chasing its prey or children playing tag. In fact, PP is the pursuer's optimal solution given simple motion dynamics, and the evader's is pure evasion where he flees directly away from

the pursuer.

Now consider **A** using PP against **T** before the launch of **D**. If both players are playing optimally, then it is a PP chase. When **D** is launched, should **A** and/or **T** not react to the presence of the new player **D**, perhaps because they failed to detect **D**'s launch, they will persist with the same strategies already being employed, PP and pure evasion.

Two Sub-Regions within R_c.

When **D** is introduced into the game, **A** will either react by changing his strategy or will persist with PP. Should **A** continue with the PP strategy, two new sub-regions emerge within his purported region of win, R_c: (1) A region R_{cc} where **T**'s capture by **A** who employs PP is guaranteed despite the **T** & **D** team's best efforts; (2) A region R_{ce} where **T** can escape with the help of **D**. An illustration of these regions in Figure 33 shows the regions for **T**, given fixed initial positions of **A** and **D**. The R_e region is also shown. Although this figure was obtained through heuristic arguments, it nonetheless reinforces the fact that such a fragmentation of the state space is possible, which indeed turns out to be the case. This shows that PP is not a global capture strategy for **A** within R_c, courtesy of the presence of **D**.

The Region R_{cc}.

In the region R_{cc}, as long as **A** plays PP, **D** will be unable to protect **T** and the latter will ultimately be captured. **T** will run directly away from **A** and **A** will charge in a straight line for **T** until he is captured. PP guarantees the capture of **T**, and does so in minimum time. Even if **T** attempted other strategies, it would not open up an escape path, but instead only lead to his premature demise. Likewise, no matter what **D** chooses to do, **T** cannot be be protected. Any strategies **D** attempts
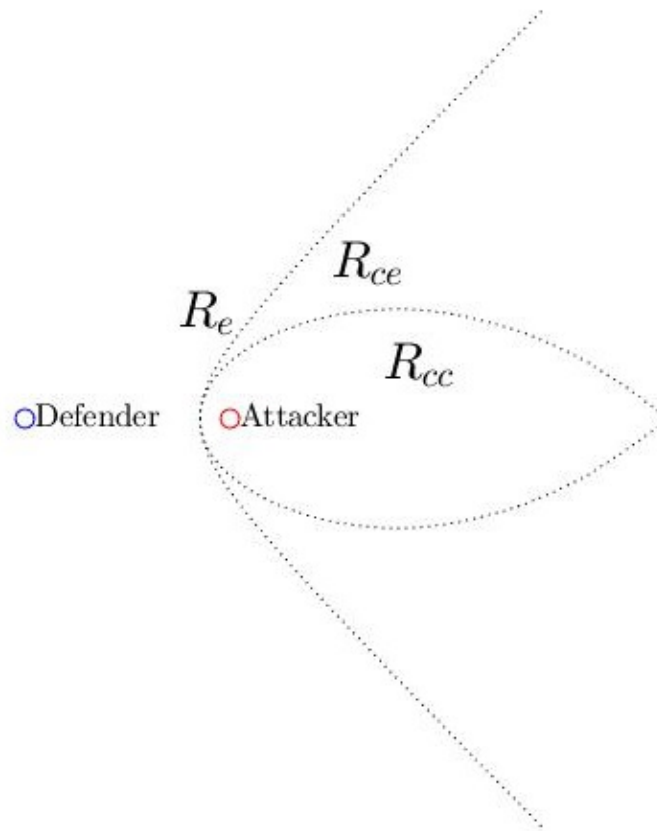
Figure 33. State-Space Partition when A plays PP ($x_a = 1$ cross section)

will ultimately leave the performance functional t_f unchanged, and as such $\mathbf{D}$ is of no consequence when the state is in R_{cc}. The players' optimal control strategies within the region R_{cc} are therefore

$$\chi = \tan^{-1}\left(\frac{y_T}{x_T - x_A}\right), \quad \phi = \tan^{-1}\left(\frac{y_T}{x_T - x_A}\right)$$

where ψ, $\mathbf{D}$'s control, can assume any heading without changing the outcome.

The Region R_{ce}.

In the subregion R_{ce}, if $\mathbf{A}$ chooses to persist with PP, then an opportunity opens up for $\mathbf{T}$ to escape. Here, the $\mathbf{T}$ & $\mathbf{D}$ team will want to find strategies that maximize the extent of the region R_{ce}, as $R_c = R_{ce} \cup R_{cc}$. Whatever these strategies may be, if the state enters the region R_e, then the $\mathbf{T}$ & $\mathbf{D}$ team should switch their strategies to the optimal strategies as developed in [15] for the region R_e.

The $\mathbf{T}$ & $\mathbf{D}$ team will work together to maximize $\mathbf{T}$'s time of capture. Any such region where $\mathbf{T}$ can escape, he will strive to escape, as escape would send the time to capture to infinity. $\mathbf{D}$ will likewise assist $\mathbf{T}$ in escaping. Therefore both $\mathbf{T}$ and $\mathbf{D}$ need strategies that ultimately maximize the temporal performance functional.

Finding T's Heading. Consider an initial state in R_{ce} and the action in the realistic plane (X, Y). Let $\mathbf{T}$ be constrained to travel along a straight line. $\mathbf{T}$ will want this heading to get him as far as possible into the L.H.P. to bring him closer to $\mathbf{D}$. Using pursuit curve analysis, one can find $\mathbf{T}$'s heading, ϕ, that will allow him to maximize his leftward travel before being captured. With θ measured as the angle from the perpendicular of the initial $\mathbf{A}$-$\mathbf{T}$ line segment, one can determine $\mathbf{A}$'s trajectory – see Figure 34. $\mathbf{A}$'s position along the pursuit curve is provided in [4].
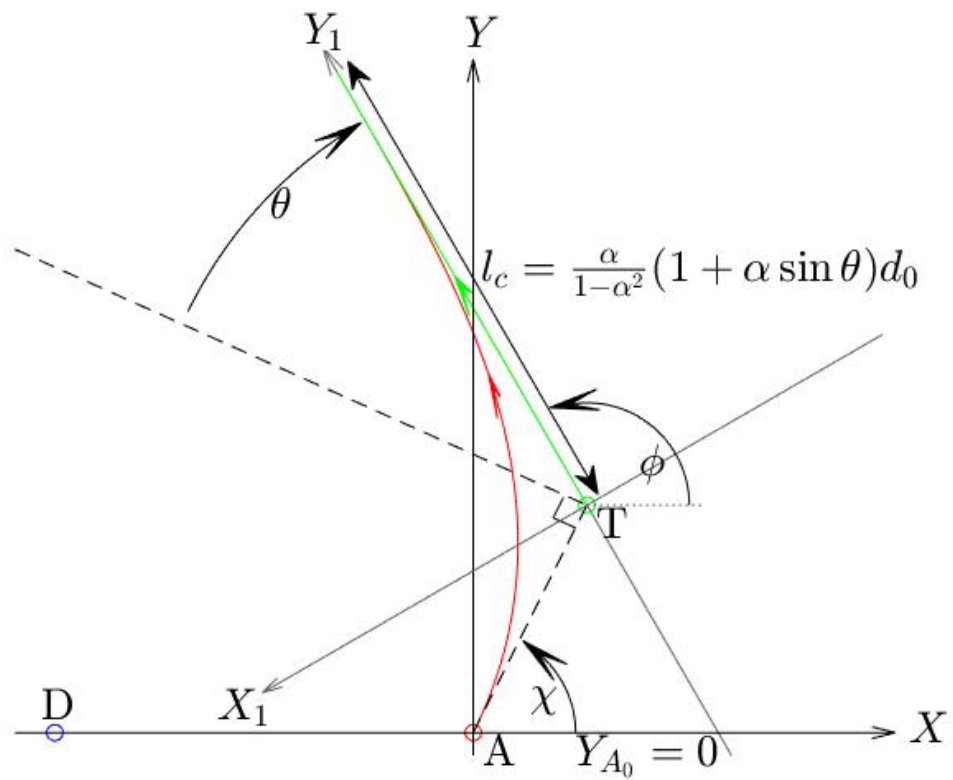
Figure 34. Pursuit Curve with angle $\theta \neq 0$

The pursuit trajectory, seen in Figure 34, is given as

$$\frac{Y_1(X_1)}{d_0 \cos\theta} = \frac{\alpha\left(\sec\theta + \alpha\tan\theta\right)}{1-\alpha^2} + \frac{1}{2}\left\{\frac{1}{1+\alpha}w\left(\frac{X_1}{a\cos\theta}\right)^{1+\alpha} - \frac{1}{1-\alpha}\frac{1}{w}\left(\frac{X_1}{a\cos\theta}\right)^{1-\alpha}\right\}$$

(17)

where

$$w = \sec\theta - \tan\theta$$

Here $\mathbf{T}$ starts at the origin of the (X_1, Y_1) frame and flees along the positive Y_1-axis. Therefore, at $Y_1(0)$, $\mathbf{T}$ will be captured by $\mathbf{A}$ and the distance l_c traveled by $\mathbf{T}$ at the time of capture is

$$l_c = \frac{\alpha}{1-\alpha^2}(1 + \alpha\sin\theta)d_0$$

(18)

With this l_c known, the focus returns to the objective, that is, get $\mathbf{T}$ as far to the left as possible. The x-coordinate of the point of capture

$$X_c = X_T + l_c\cos\phi$$

This describes how far left $\mathbf{T}$ can go on in the realistic plane while both $\mathbf{A}$ and $\mathbf{D}$ start on the X-axis. To translate Eq. (18) to align with the realistic plane, use $\theta = \frac{\pi}{2} - \phi + \chi_0$, which leads to the optimization in ϕ

$$\min_{\phi}\left\{\left[1 + \alpha\cos\left(\phi - \tan^{-1}\frac{Y_{T_0}}{X_{T_0} - X_{A_0}}\right)\right]\cos\phi\right\}$$

(19)

Given $\mathbf{A}$ is playing PP, the optimal course ϕ allows $\mathbf{T}$ to go as far left as possible before being captured. Currently this path is a straight line, but a better path of $\mathbf{T}$ might be a curved trajectory where $\mathbf{T}$ turns into $\mathbf{A}$. This optimal path will be investigated through simulation.

A simple example of the PP curve, where $\phi = \frac{\pi}{2}$, is shown in Figure 35. Here $\mathbf{T}$
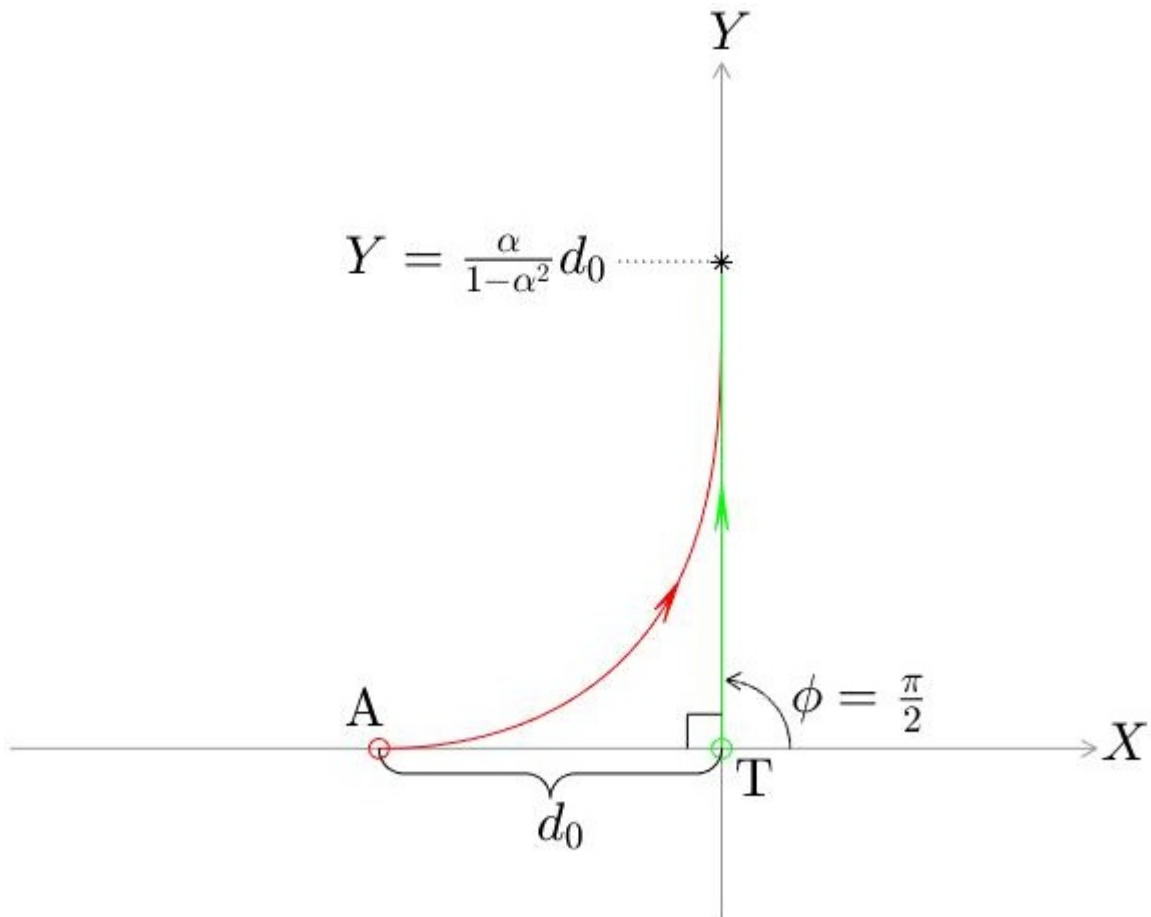
Figure 35. Pursuit Curve when E runs perpendicular to the P-E line segment

travels perpendicular to the initial **A**-**T** Line of Sight (LoS), and **T** is captured at $Y = \frac{\alpha}{1-\alpha^2}d_0$.

D's Strategy. Consider now **D**'s action to intercept **A**. As **T** strives to minimize X_c, **D** will work to bring **A** under his control; in other words make contact with **A**. Once this occurs, **T** has escaped. Using the rotating reference frame (x, y), one strategy **D** may employ would be to mirror **A**'s trajectory across the y-axis. This would keep the (x, y) frame from rotating while the x-axis slides upward. As such, should **T** reach the orthogonal bisector of the original $\overline{\textbf{AD}}$ segment before being captured, then **D** will intercept **A** on the y-axis.

Although this will guarantee **T**'s escape if **T** can reach the orthogonal bisector, **D** can reach **A** sooner if he heads in a straight line to intercept **A**. Indeed, because **D** knows **T**'s heading and responds to **A**'s known PP strategy, **D** can predict where this intercept point will be. **D**'s optimal heading can be computed by analyzing the pursuit curve of **A**. The pursuit curve is given in Eq. (17), but this form is insufficient to directly determine when **D** can intercept **A** using a straight-line trajectory. This can be found by first finding the distance traveled by **A** as a function of his X_1-coordinate in the (X_1, Y_1) frame, and then finding **A**'s position in the realistic plane as a function of X_1. Setting the distance from **D**'s initial position to **A**'s instantaneous position (as a function of X_1) equal to the the distance traveled by **A** will find the interception point. The arc length formula

$$s(X_1) = \int_{d_0 \cos\theta}^{X_1} \sqrt{1 + \left(\frac{dY_1}{dX_1}\right)^2}\, dX_1$$

can be used to find the distance traveled by **A** given X_1.

From eq. 17 calculate

$$\frac{dY_1}{dX_1} = \frac{1}{2}\left[w\left(\frac{X_1}{d_0\cos\theta}\right)^{\alpha} - \frac{1}{w}\left(\frac{X_1}{d_0\cos\theta}\right)^{-\alpha}\right]$$

$$\left(\frac{dY_1}{dX_1}\right)^2 = \frac{1}{4}\left[w^2\left(\frac{X_1}{d_0\cos\theta}\right)^{2\alpha} + \frac{1}{w^2}\left(\frac{X_1}{d_0\cos\theta}\right)^{-2\alpha} - 2\right]$$

Inserting this expression into the arc length formula yields

$$s(X_1) = \frac{1}{2}\int_{d_0\cos\theta}^{X_1}\sqrt{\left[w^2\left(\frac{X_1}{d_0\cos\theta}\right)^{2\alpha} + \frac{1}{w^2}\left(\frac{X_1}{d_0\cos\theta}\right)^{-2\alpha} + 2\right]}\,dX_1$$

and the arc length is found to be

$$s(X_1) = \frac{1}{2}d_0\cos\theta\left\{\frac{1}{1+\alpha}w\left[1 - \left(\frac{X_1}{d_0\cos\theta}\right)^{1+\alpha}\right] + \frac{1}{1-\alpha}\frac{1}{w}\left[1 - \left(\frac{X_1}{d_0\cos\theta}\right)^{1-\alpha}\right]\right\} \tag{20}$$

Now the realistic plane position of **A** must first be expressed as a function of X_1:

$$\left.\begin{aligned}X_A &= X_{T_0} + \sqrt{X_1^2 + Y_1^2}\sin\left(\tan^{-1}\left(\frac{Y_1}{X_1}\right) - \phi\right)\\ Y_A &= Y_{T_0} + \sqrt{X_1^2 + Y_1^2}\cos\left(\tan^{-1}\left(\frac{Y_1}{X_1}\right) - \phi\right)\end{aligned}\right\} \tag{21}$$

where ϕ is the course of **T**.

Using Eqs. (20) and (21), **D** can now calculate a straight-line intercept point by solving for X_1 in

$$[x_{A'}(X_1) + x_{A_0}]^2 + y_{A'}^2(X_1) = s^2(X_1) \tag{22}$$

D could further solve for the critical case $X_1 = 0$ where **D** intercepts **A**, just as the latter is about to intercept **T**, but this would still be constrained by **T**'s straight-line trajectory. If **T**'s straight-line trajectory were optimal than this would produce the surface that separates R_{cc} from R_{ce}. To construct the surface that separates

81

R_{cc} and R_{ce} requires the solution of a quartic equation. However, the constant-course trajectory for **T** is not necessarily the optimal path. **T** can still do better to penetrate deeper towards R_e by not having the straight-line trajectory constraint imposed on him. So the constructed set R_{ce} is only a subset of the true set R_{ce}.

Consider the rotating reference frame when considering the presented **T** & **D** team's strategies. Because it is better for **D** to follow a straight-line path as apposed to mirroring **A**'s path, the (x, y) frame will rotate. A (x, y) frame rotation will cause **T**'s straight-line optimal path to change if recalculated. ϕ thereby becomes dynamic in that **T**'s straight-line trajectory changes at each time step. By dynamically re-calculating the "optimal" ϕ, it is as if the game has reinitialized at each time step. As such, **T**'s straight-line trajectory will not be a straight line in the realistic plane if it is recalculated at each time step with respect to the rotating reference frame (x, y). This will also cause **D**'s trajectory to no longer be a straight line because the predicted path of **A** changes as **T** changes his straight-line trajectory. Because **D**'s path does curve in this case, it is not an optimal trajectory.

PP when A, T and D are Co-linear.

An interesting phenomenon occurs when considering the scenario where the three players are initially collinear with **A** between **T** and **D**. Superficial observation leads one to believe that there is no way for **T** to escape when **A** is playing PP. In fact, if the state is in the region R_{cc} as shown in Figure 33, then this is true and there is nothing the **T** & **D** team can do for **T** to escape. In this case **T** would flee directly away from **A**, thus maximizing the time to capture, and **A** would eventually capture **T** using PP. On the other hand, if there is enough distance between **T** and **A**, such that the state is in the region R_{ce}, that is, **T** is in the R_{ce} designated set in Figure 33, then **T** and **D** can generate trajectories which rotate the (x, y) reference frame's y-axis,

82

the $\overline{\mathbf{AD}}$ orthogonal bisector, towards **T**. By doing so, this bisector will approach the dynamically redrawn **A**-**T** Apollonius circle and **T** will escape when the Apollonius circle contacts the orthogonal bisector. If **T** and **D** are playing optimally, then this will occur unless **A** abandons the PP strategy, which in this region of the state space is suboptimal.

4.4 Analysis

Constant T course when D mirrors A:.

Figure 36 illustrates the game in the realistic plane as **T** holds a constant course ϕ and **D** mirrors **A**'s path across the y-axis. Although initial state is $\{x_A = 1,\ x_T = 1.3,\ y_T = 1\}$, which is well within the region R_c, **D** was able to intercept **A** before the latter captured **T**, thus guaranteeing **T**'s escape. The existence of the subregion R_{ce} is thereby illustrated since **T** was able to escape when **A** played PP. As seen, **D** pulls away from **A** early in the engagement, however **D** would have achieved a much better outcome had he been heading to intercept **A** from the start. Here **T**'s final **A**-**T** separation is 0.064 dimensionless units.

Constant T course when D takes a straight-line path:.

Figure 37 illustrates the player's trajectories in the realistic plane when **T** holds a constant course ϕ and **D** finds the optimal straight-line path to intercept **A**. Here time is not wasted going in the wrong direction as seen when **D** mirrors **A**'s path, but instead **D** is seen taking the optimal path while **T** holds the optimal constant course and **A** employs PP. **D** intercepts **A** at the earliest moment possible and the final **A**-**T** separation is 0.120 dimensionless units, or nearly double as the separation afforded by the previous strategy.

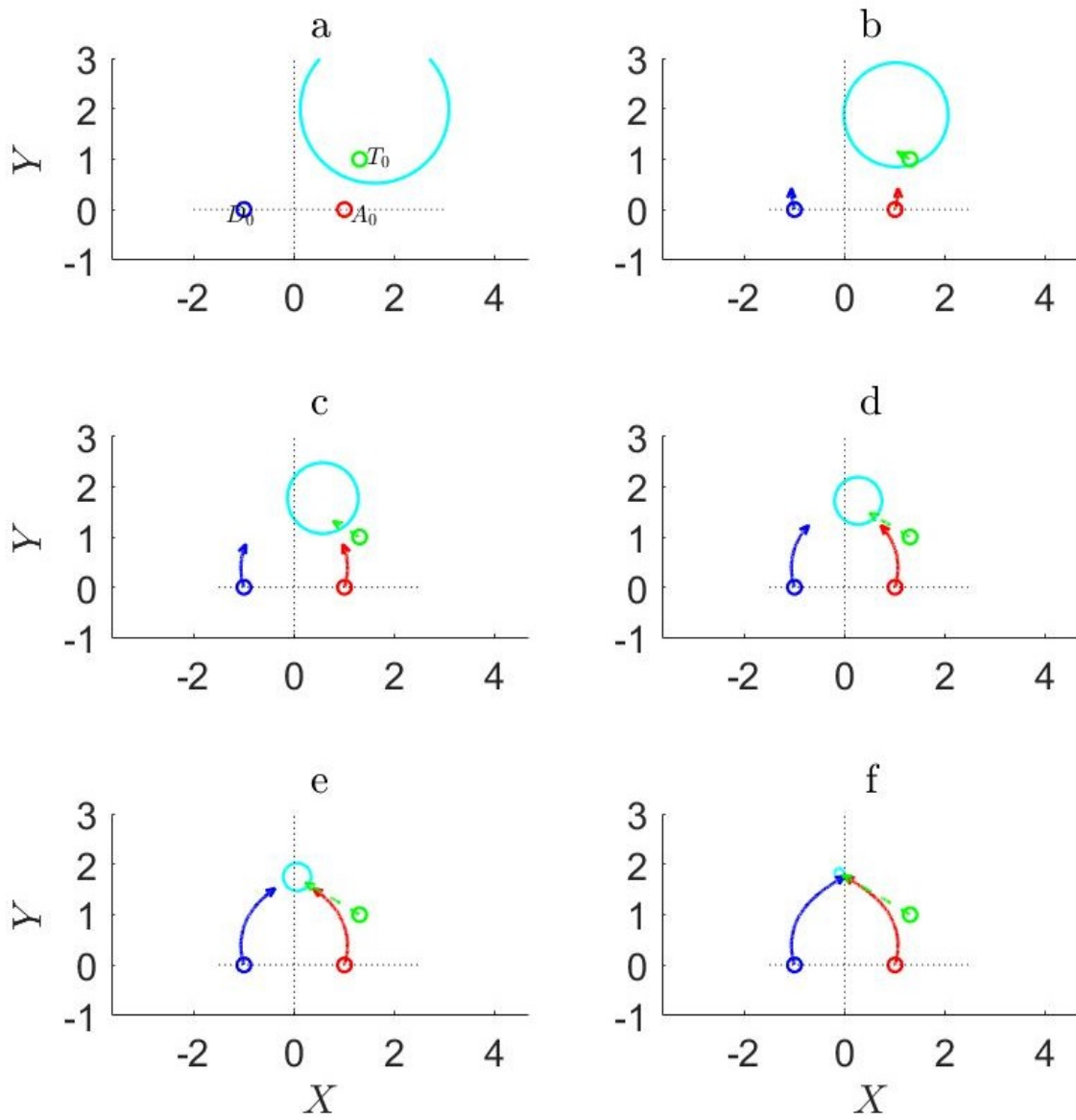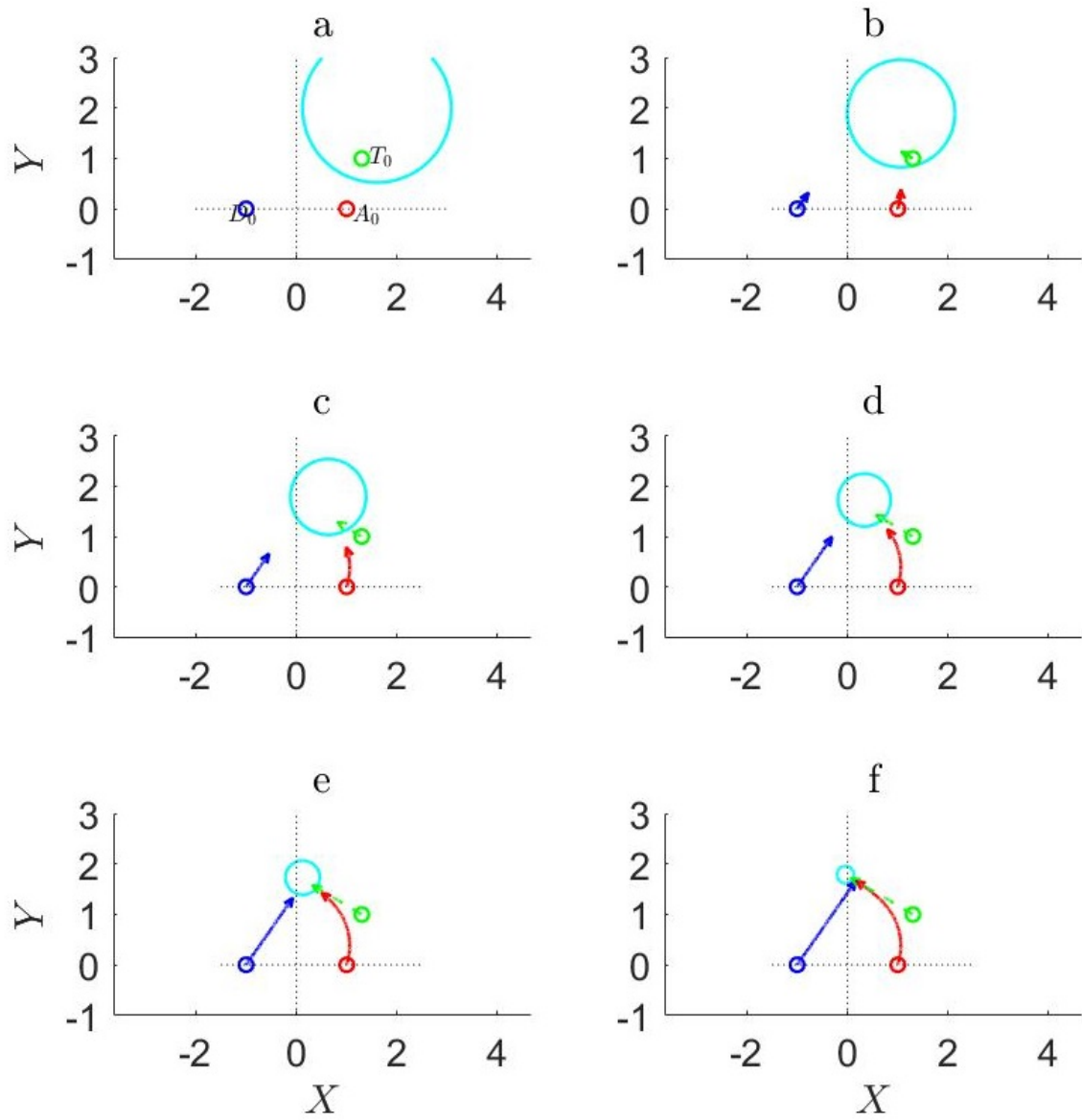**Figure 36. D Mirrors A's PP Strategy in the Realistic Plane** (X, Y)

Figure 37. Constant ϕ Straight-Line Intercept in the Realistic Plane (X, Y)

Dynamic T course when D takes a straight-line path:.

Figure 38 illustrates the players' trajectories in the realistic plane when **T** employs a dynamic ϕ strategy and **D** recalculates the straight-line interception point according to the current ϕ heading. Therefore, both **T**'s and **D**'s trajectories curve slightly as these new paths are dynamically determined. One would expect this dynamic ϕ strategy to produce better results since it is closed-loop, but because this strategy causes **D** to curve, optimality is lost in his strategy and **T** and **D**'s performance deteriorates. Here the final **A**-**T** separation is 0.099 dimensionless units, clearly less than the constant ϕ case. This strengthens the argument that **D**'s optimal strategy is a straight line, as is indeed predicted by the theory of optimal control.

PP when A, T and D are collinear:.

The interesting case where **A**, **T**, and **D** are initially co-linear was also investigated to show how **T** can escape should **A** insist on playing PP. Results are presented in the realistic plane in Figure 39. Here, **T** quickly steps out of the initial co-linear arrangement, and takes a path towards **D**. Because **A** persisted with PP, **T** and **D** were able to rotate the (x, y) reference frame in their favor and open up an escape path. Here **T** employed a constant course strategy and **D** took a straight-line intercept path knowing that **A** employs PP. True optimal strategies would further improve this outcome in the **T** & **D** team's favor.

Fixed T course vs dynamically adjusted T course when A plays PP:.

Previously in this paper, the optimal constant course ϕ of **T** was found which moves the capture point of **T** as far as possible to the right, given **A** plays PP and **T** is committed to a straight-line path. This helps **D** to intercept **A** before **T**'s capture by **A**. However, the optimal escape path for **T** is not necessarily a straight-
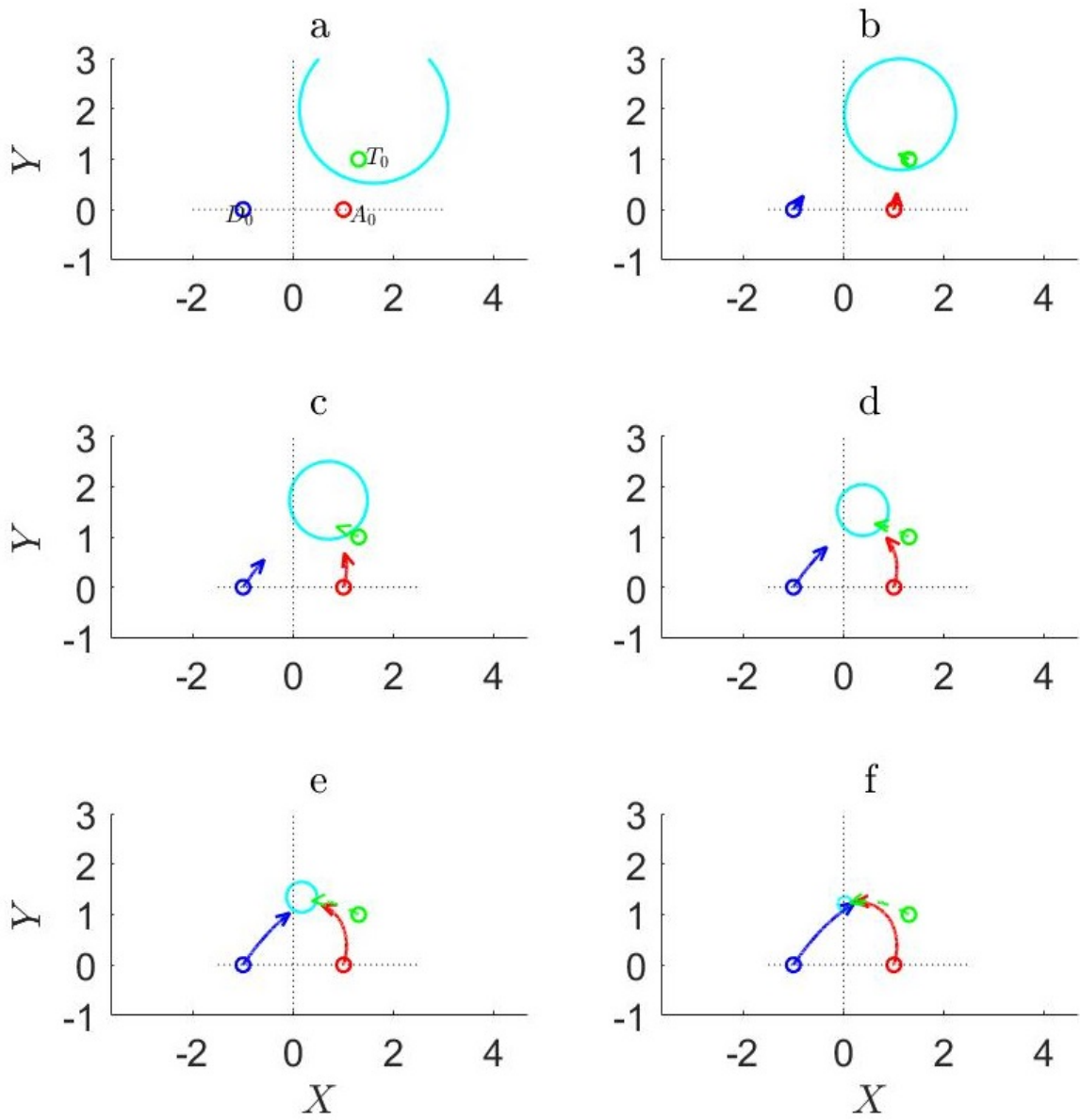
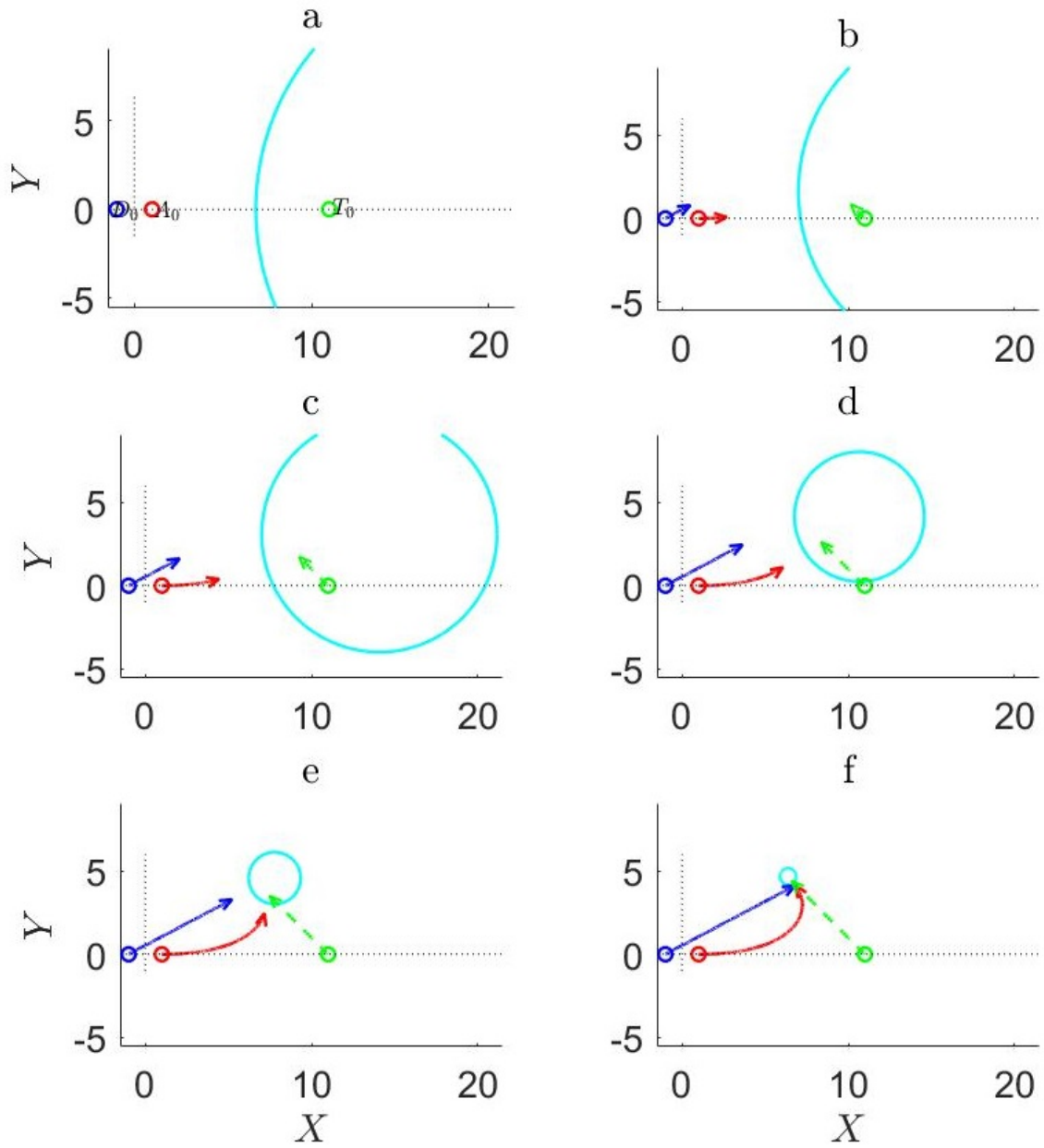**Figure 38. Dynamic ϕ Intercept in the Realistic Plane (X, Y)**

Figure 39. Target Escape Path Example when Player's are Initially Co-linear in the Realistic Plane

line. Figure 40 shows a comparison of an engagement where **T** holds an optimal course ϕ and an engagement where ϕ is dynamically calculated, such that **T** is not constrained to a straight-line trajectory. The straight-line path was determined using MATLAB's `fminbnd` function to perform the static minimization in Eq. (19) and obtain the optimal constant ϕ. MATLAB's `fmincon` was used to find the dynamic ϕ path where at each time-step ϕ can assume a different value. As shown in Figure 40, the two paths are not the same. Thus, it is shown through MATLAB's optimization functions that a constant ϕ is not necessarily optimal.

4.5 Conclusion

The capture of a Target by an Attacker in the presence of a Defender in a 3-player pursuit-evasion differential game was investigated. Because of the presence of the third defending player and **A**'s persistence in employing PP, the original capture region R_c is partitioned into 2 subregions: 1) R_{cc} where **T** will be captured in minimum time if **A** plays PP; 2) R_{ce} where **T** can escape if **A** insists on PP. In the subregion R_{cc}, **A**'s optimal strategy is PP and **T**'s optimal strategy is to flee directly away from **A**. Because **D** is unable to influence the outcome when **A** plays PP in R_{cc}, **D** is irrelevant. In R_{ce}, **A** should abandon PP to prevent **T**'s possible escape. If, however, **A** persists with PP, then the methods presented in this paper can be used by the **T** & **D** team to cause **T**'s escape. **T** could materialize his escape in R_{ce} by finding the straight-line path that would get him as far as possible into the left-half plane. This would place him in a good position to have **D** intercept **A** before the latter can capture **T**. Ultimately this paper showed that in the presence of a defender, PP is not a global capture strategy for **A** in R_c, his winning region.

Constant $\phi*$

Dynamic ϕ

T

A
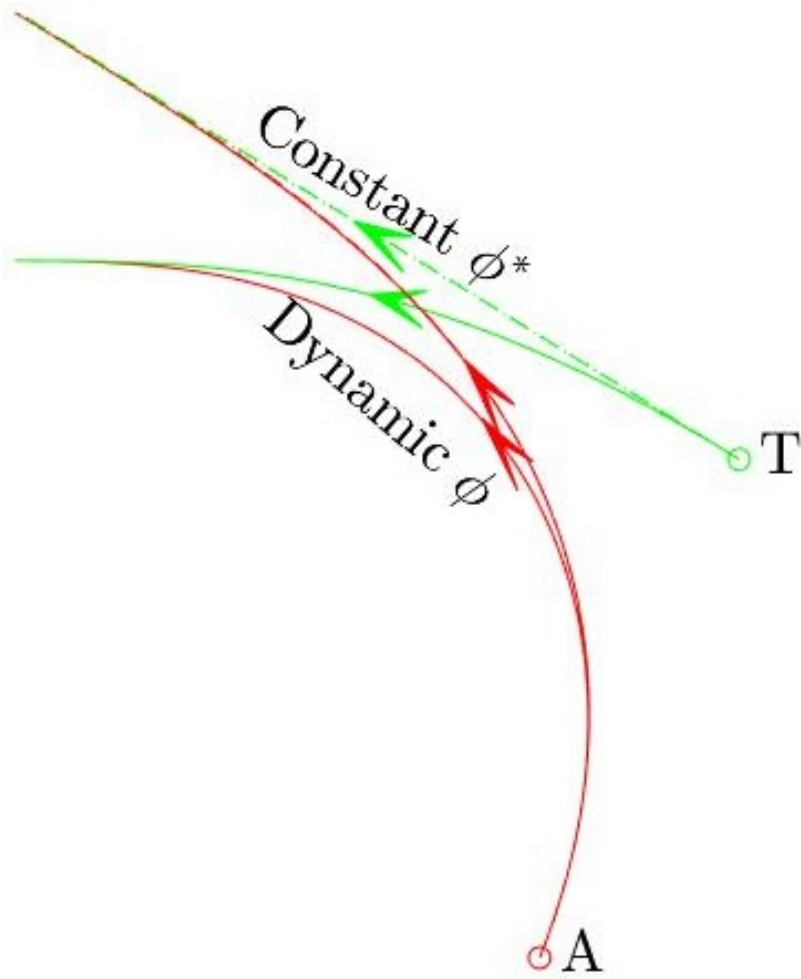
h

Figure 40. Curved and Straight-Line Evasion Strategies

V. Conclusion

The 3-player differential game, referred to as the ATDDG and originally presented by AFRL and AFIT, seems like a simple problem on the surface, but like the Homicidal Chauffeur differential game, the ATDDG quickly develops into a complex problem. The tools to address the game, as developed by Isaacs, help us unravel the complexities with the ultimate goal of obtaining a complete analytic solution. Understanding the discovered strategies helps clear the way to solving more complex problems that have yet to be addressed analytically. They provide insight into how one player can gain an advantage and surprise the adversary by pulling the state into his winning region, and ultimately make us less naive about the intricacies of differential games.

The work presented herein analyzed game play of the ATDDG. Several strategies were presented showing maneuvers that both A and the T & D team can perform to change the system's state in their favor. As summaries are provided within each individual chapter, Chapter V aims to highlight some of the main contributions of the research.

5.1 Optimal Strategies vs Near-Optimal Strategies

Although within this research optimal strategies were found for certain cases, not all strategies optimized the performance functional. For example, the heuristic analysis did not find the minimum/maximum for each player when using the final A-D separation distance as the performance functional. The research did, however, produce what can be considered near-optimal strategies. By having each player chase the left-most point of the A-T Apollonius circle, each player employed a strategy that makes it very difficult for the opposing player to pull the state towards his winning

region. This provides valuable insight into how player's in more complex, but similar, engagements should behave. In such complex scenarios it is beneficial to have an idea as the region where the optimal solution lies. This gives the user a close initial guess to employ an optimizer to find the true global minimum.

This was also shown in Chapter IV, which used time as the performance functional. In the region where T can escape if A employs PP, T and D both now have good initial guesses as to what the true optimal strategy looks like. Clearly a true optimal solution is desired if it can be found, however near optimal solutions still provide valuable insight and aide in research of more complex engagements.

5.2   The Barrier Surface

The analysis of the barrier surface created strategies for each player that prevent the state from leaving the barrier surface, leading to a draw. To our surprise, however, if the state is not on the barrier surface, then the barrier surface strategies caused the players to give up a Game of Kind win, even though the win was clearly possible. Instead the players took rather foolish actions. If the state were in A's region of win, then A became suicidal, even when he had the game in his pocket. If the state was in the T & D team's region of win, then T played foolishly, running along the $\overline{\text{AD}}$ orthogonal bisector, leading to a draw.

Ultimately, analysis of the barrier surface resulted in a Game Of Kind strategy by A, which guarantees his win so long as the state is initially in his winning region. A modified barrier surface strategy accomplished this by including a tuning parameter, β, that prevented A from getting too close to D. This method, however, is not foolproof as an improper selection of the parameter β will cause an over avoidance of D by A, resulting in the latter missing T. Generally it is best to have β as small as possible.

5.3   Pure Pursuit and Time Optimization

In a simple Pure Pursuit differential game where A is chasing T and D is not present, the optimal solution with time as the performance functional is to have A employ PP, and for T to run directly away from A. Introducing D dramatically changed the game, where if A employs PP, T may be able to escape. This research not only showed how this can be done, but presented several strategies the T & D team can use to facilitate T's escape. The results in this work do not present the complete time-optimization solution, but they do provide insight into a partial optimal solution for certain regions.

5.4   Future Work

This research is only a beginning of what can be learned from the ATDDG. Future work should focus on obtaining the complete solution to the ATDDG in A's region of win using time as the performance functional. Such a solution will improve upon current solutions in that it not only solves the Game of Kind, but does so in minimum time. Future work should also look into how the game changes when more hostile attacking missiles engage the target aircraft, or when more defending missiles are available. Doing so will make the game dramatically more complicated, but pulling from the results of this work and related works will be a guide and reference to obtaining the optimal pursuit and evasion strategies.

Although this game was designed to provide insight into a specific aerial engagement, it's applications are by no means limited to this single scenario. This research can be applied to any engagement where a player is trying to protect another from a threat, whether on land, sea, air, or space. Furthermore, the analysis of pursuit curves presented in Chapter IV provide a clear method how to optimally intercept a pursuer.

Appendix A.

A   Solving the Pure Pursuit Case using the Differential Game Method

The non-rotating frame (x, y) is collocated with the Pursuer's (P) instantaneous position. P is chasing an Evader (E) and both players have simple motion/are holonomic, à la Isaacs. Also, both player's have access to E's position relative to P, that is, the state (x, y). P seeks to capture E in minimum time and E strives to maximize the same. χ and ϕ are P's and E's headings respectively, and P has a capture radius of l as shown in Figure 41. Having P employ Pure Pursuit (PP) against E results in
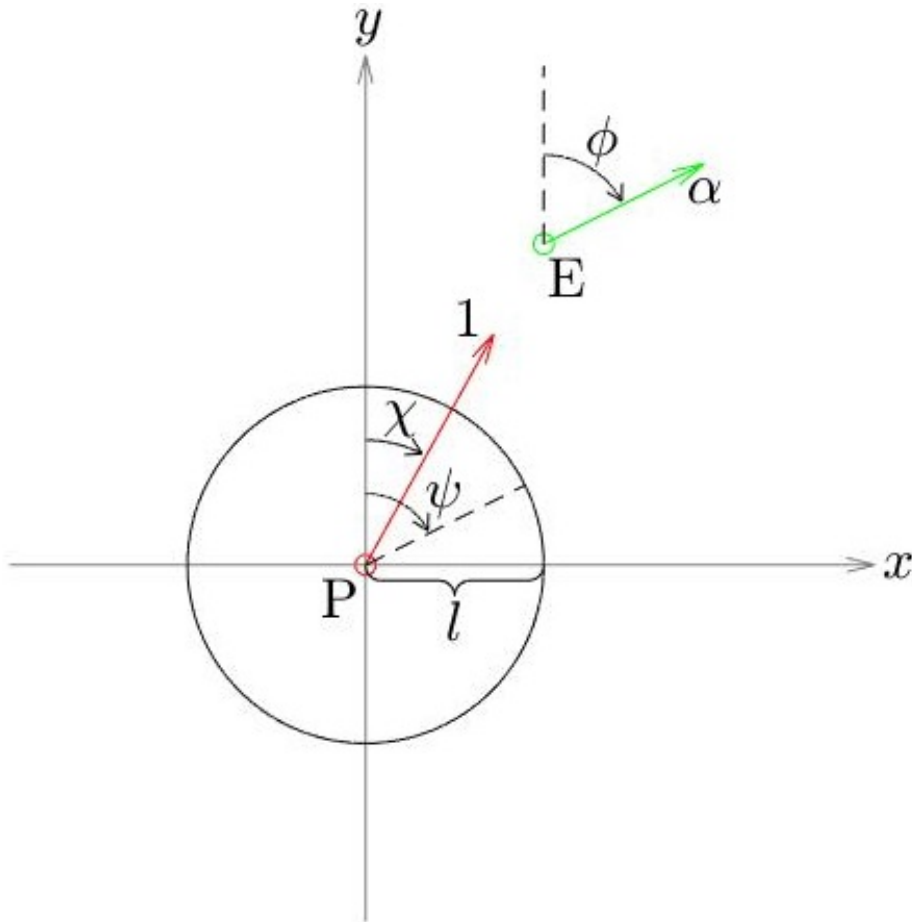

Figure 41. Simple Pursuit/Evasion Differential Game

the linear dynamics

$$\dot{x} = \alpha \sin\phi - \sin\chi, \ x(0) = x_0$$

$$\dot{y} = \alpha \sin\phi - \sin\chi, \ y(0) = y_0, \ 0 \le t \le t_f$$

which in reality are no dynamics. E is captured when it is enveloped by the terminal manifold

$$x^2 + y^2 = l$$

The parameter $0 \le \alpha < 1$ is the speed ratio $\alpha = \frac{v_E}{v_P}$ where v_P and v_E are the respective speeds of P and E. The terminal manifold can be parameterized as

$$x = l \sin\psi, \ y = l \cos\psi, \ 0 \le \psi \le 2\pi$$

As P has simple motion, the whole terminal manifold is usable, and the inward pointing normal to the terminal manifold as P overtakes E is

$$\vec{n} = -a \left(\sin\psi, \ \cos\psi\right)^T, \ a > 0$$

The Hamiltonian

$$\mathcal{H} = -1 + \alpha \left(\lambda_x \sin\phi + \lambda_y \cos\phi\right) - \left(\lambda_x \sin\chi + \lambda_y \cos\chi\right)$$

and $\min_{\phi} \max_{\chi} \mathcal{H}$ is found using Isaacs Lemma on Circular Vectograms [10] such that

$$\sin\phi^* = -\frac{\lambda_x}{\sqrt{\lambda_x^2 + \lambda_y^2}}, \quad \cos\phi^* = -\frac{\lambda_y}{\sqrt{\lambda_x^2 + \lambda_y^2}}$$

$$\sin\chi^* = -\frac{\lambda_x}{\sqrt{\lambda_x^2 + \lambda_y^2}}, \quad \cos\chi^* = -\frac{\lambda_y}{\sqrt{\lambda_x^2 + \lambda_y^2}}$$

The costate equations and the terminal costate (using the transversality condition) are

$$\dot{\lambda}_x = -\frac{\partial \mathscr{H}}{\partial x} = 0, \quad \lambda_x(t_f) = -a \sin \psi$$

$$\dot{\lambda}_y = -\frac{\partial \mathscr{H}}{\partial x} = 0, \quad \lambda_y(t_f) = -a \cos \psi$$

The costate is therefore constant and is

$$\lambda_x(t) = -a \sin \psi, \quad \lambda_y(t) = -a \cos \psi, \quad 0 \le t \le t_f$$

$$\Longrightarrow$$

$$\sin \phi^* = \sin \psi, \quad \sin \chi^* = \sin \psi$$

$$\Longrightarrow$$

$$\phi^*(t) = \psi$$

$$\chi^*(t) = \psi, \quad 0 \le t \le t_f$$

Using the terminal condition

$$\mathscr{H}(t_f) = 0$$

$$\Longrightarrow$$

$$0 = -1 - \alpha a + a$$

$$\Longrightarrow$$

$$a = \frac{1}{1-\alpha} > 0$$

and the constant costate is

$$\lambda_x(t) = -\frac{1}{1-\alpha} \sin \psi, \quad \lambda_y(t) = -\frac{1}{1-\alpha} \cos \psi, \quad 0 \le t \le t_f$$

Lastly, the optimal flow field is found using retrograde integration

$$\mathring{x} = \sin \chi - \alpha \sin \phi = (1 - \alpha) \sin \psi, \ x(\tau = 0) = l \sin \psi$$

$$\mathring{y} = \cos \chi - \alpha \cos \phi = (1 - \alpha) \cos \psi, \ y(\tau = 0) = l \cos \psi, \ 0 \le \tau \le t_f$$

$$\Longrightarrow$$

$$x(\tau) = [l + (1 - \alpha)\tau] \sin \psi$$

$$y(\tau) = [l + (1 - \alpha)\tau] \cos \psi, \ 0 \le \tau \le t_f, \ 0 \le \psi < 2\pi$$

Given x_0 and y_0, P's and E's headings and the time to capture are found as

$$\phi = \chi = \psi = \tan^{-1}\left(\frac{x_0}{y_0}\right)$$

$$t_f = \frac{1}{1-\alpha}\left(\frac{x_0}{\sin \psi} - l\right)$$

Thus, the solution to the differential game à la Isaacs was easily obtained.

B   Solving the Pure Pursuit Case using the Optimal Control Method

Consider P chasing E using a Pure Pursuit strategy. What should E's strategy be? Obviously E must solve the optimal control problem of maximizing the time-to-capture. As before, the whole terminal manifold is usable as P has simple motion. P's strategy is

$$\sin \phi = \frac{x}{\sqrt{x^2 + y^2}}, \quad \cos \phi = \frac{y}{\sqrt{x^2 + y^2}}$$

The nonlinear dynamics are

$$\dot{x} = \alpha \sin \phi - \frac{x}{\sqrt{x^2 + y^2}}, \quad x(0) = x_0$$

$$\dot{y} = \alpha \cos \phi - \frac{y}{\sqrt{x^2 + y^2}}, \quad y(0) = y_0$$

Because the evader is maximizing the time-to-capture, the terminal-manifold normal is pointing outward in the one-sided optimal control problem, such that

$$\vec{n} = a \left(\sin \psi, \ \cos \psi \right)^T$$

The Hamiltonian is now

$$\mathscr{H} = 1 + \alpha \left(\lambda_x \sin \phi + \lambda_y \cos \phi \right) - \lambda_x \frac{x}{\sqrt{x^2 + y^2}} - \lambda_y \frac{y}{\sqrt{x^2 + y^2}} \tag{23}$$

and $\max\limits_{\phi} \mathscr{H}$ is again found using Isaacs Lemma on Circular Vectograms, such that

$$\sin \phi^* = \frac{\lambda_x}{\sqrt{\lambda_x^2 + \lambda_y^2}}, \quad \cos \phi^* = \frac{\lambda_y}{\sqrt{\lambda_x^2 + \lambda_y^2}}$$

The costate equations and the terminal costate (using the transversality condition) are

$$\dot{\lambda}_x = -\frac{\partial \mathscr{H}}{\partial x} = \frac{y}{(x^2 + y^2)^{\frac{3}{2}}} \left(\lambda_x y - \lambda_y x \right), \quad \lambda_x \left(t_f \right) = a \sin \psi$$

$$\dot{\lambda}_y = -\frac{\partial \mathscr{H}}{\partial x} = -\frac{x}{(x^2 + y^2)^{\frac{3}{2}}} \left(\lambda_x y - \lambda_y x \right), \quad \lambda_y \left(t_f \right) = a \cos \psi$$

The state dynamics are updated with the results of the $\max_{\phi} \mathcal{H}$ maximization

$$\dot{x} = \alpha \frac{\lambda_x}{\sqrt{\lambda_x^2 + \lambda_y^2}} - \frac{x}{\sqrt{x^2 + y^2}}, \quad x(0) = x_0$$

$$\dot{y} = \alpha \frac{\lambda_y}{\sqrt{\lambda_x^2 + \lambda_y^2}} - \frac{y}{\sqrt{x^2 + y^2}}, \quad y(0) = y_0, \; 0 \leq t \leq t_f$$

Using the terminal condition

$$\mathcal{H}\left(t_f\right) = 0$$

The Hamiltonian from Eq. 23 can be rewritten at the terminal time as

$$0 = 1 + \alpha \sqrt{\lambda_x^2(t_f) + \lambda_y^2(t_f)} - \frac{1}{l} \left[x(t_f)\lambda_x(t_f) + y(t_f)\lambda_y(t_f) \right]$$

$$\Longrightarrow$$

$$0 = 1 + \alpha a - a$$

$$\Longrightarrow$$

$$a = \frac{1}{1 - \alpha} > 1$$

which leads to the terminal costate

$$\lambda_x(t_f) = \frac{1}{1 - \alpha} \sin \psi, \quad \lambda_y(t_f) = \frac{1}{1 - \alpha} \cos \psi$$

99

Lastly, retrograde integration is performed

$$\mathring{x} = \frac{x}{\sqrt{x^2 + y^2}} - \alpha \frac{\lambda_x}{\sqrt{\lambda_x^2 + \lambda_y^2}}, \quad x(\tau = 0) = l \sin \psi$$

$$\mathring{x} = \frac{y}{\sqrt{x^2 + y^2}} - \alpha \frac{\lambda_y}{\sqrt{\lambda_x^2 + \lambda_y^2}}, \quad y(\tau = 0) = l \cos \psi$$

$$\mathring{\lambda}_x = \frac{y}{\left(x^2 + y^2\right)^{\frac{3}{2}}} \left(x\lambda_y - y\lambda_x\right), \quad \lambda_x(\tau = 0) = \frac{1}{1 - \alpha} \sin \psi$$

$$\mathring{\lambda}_y = -\frac{x}{\left(x^2 + y^2\right)^{\frac{3}{2}}} \left(x\lambda_y - y\lambda_x\right), \quad \lambda_x(\tau = 0) = \frac{1}{1 - \alpha} \cos \psi$$

From here, this set of four nonlinear differential equations must be solved to find the optimal E's heading. It is easier to solve the differential game than it is to solve the one-sided optimal control problem. The solution to the problem was easily obtained using Isaac's differential games method where both P's and E's optimal headings were solved for simultaneously. Paradoxically, solving the optimal control problem for E, given P is employing PP, is much more difficult. However, having already obtained the solution to the differential game yields controls that satisfy the optimal control problem and it can be verified that the solution to the optimal control problem is

$$x(\tau) = [l + (1 - \alpha) \tau] \sin \psi$$

$$y(\tau) = [l + (1 - \alpha) \tau] \cos \psi$$

$$\lambda_x(\tau) = \frac{1}{1 - \alpha} \sin \psi \quad (\equiv \text{const.})$$

$$\lambda_y(\tau) = \frac{1}{1 - \alpha} \cos \psi \sin \psi \quad (\equiv \text{const.}), \quad 0 \le \tau \le t_f, \quad 0 \le \psi < 2\pi$$

Note that for point capture $l \to 0$, it appears that the costate retrograde integration equations $\left\{\mathring{\lambda}_x(\tau = 0), \mathring{\lambda}_y(\tau = 0)\right\}$ have a singularity because of a zero in the

denominator

$$\mathring{\lambda}_x(\tau = 0) = \frac{0}{(0^2 + 0^2)^{\frac{3}{2}}} \left(x\lambda_y - y\lambda_x \right), \quad \lambda_x(\tau = 0) = \frac{0}{(0^2 + 0^2)^{\frac{3}{2}}} \left(x\lambda_y - y\lambda_x \right)$$

However, because

$$x\lambda_y - y\lambda_x = l \sin\psi \frac{1}{1 - \alpha} \cos\psi - l \cos\psi \frac{1}{1 - \alpha} \sin\psi = 0$$

the singularity is eliminated and $\left\{ \mathring{\lambda}_x(\tau = 0) = 0, \ \mathring{\lambda}_y(\tau = 0) = 0 \right\}$

Appendix B.

A   Time-to-Capture in the Region R_{ce}

Bringing back **D** into the game and assuming **A** continues to play **PP** in the region R_{ce}, the question is posed "what should the **T** & **D** team's strategies be?" To find the answer, one must solve the optimal control problem for the **T** & **D** team in the region R_{ce}. As shown in Appendix A for the simple PP/PE game, the optimal control problem is not trivial.
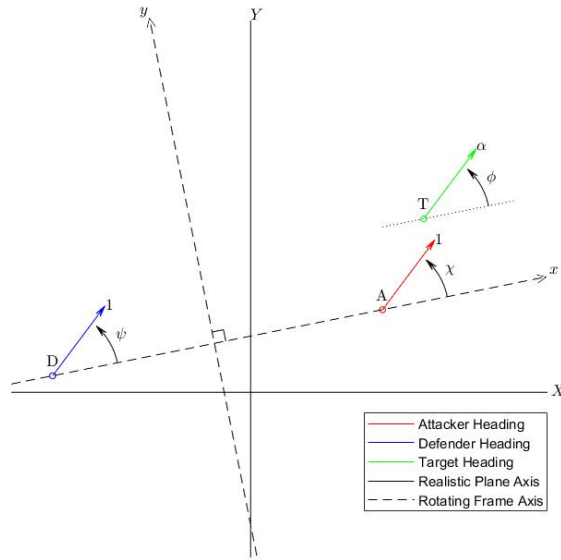

Figure 42. The Rotating Reference Frame overlaid on the Realistic Plane

Referring to the rotating reference frame $\mathbb{R}^3$ as described in [14] – see Figure 42 – where χ, ψ and ϕ are **A**'s, **D**'s, and **T**'s headings respectively when measured from the positive x-axis, the non-linear system dynamics are

$$\dot{x}_A = \frac{1}{2}\left(\cos\chi - \cos\psi\right),\ x_A(0) = x_{A0}$$

$$\dot{x}_T = \alpha \cos \phi - \frac{1}{2} \left(\cos \psi + \cos \chi \right) - \frac{1}{2} \frac{y_T}{x_A} \left(\sin \psi - \sin \chi \right), \ x_T(0) = x_{T0}$$

$$\dot{y}_T = \alpha \sin \phi - \frac{1}{2} \left(\sin \psi + \sin \chi \right) + \frac{1}{2} \frac{x_T}{x_A} \left(\sin \psi - \sin \chi \right), \ y_T(0) = y_{T0}$$

Because **A**'s PP strategy is

$$\sin \chi = \frac{y_T}{\sqrt{\left(x_A - x_T \right)^2 + y_T^2}}, \quad \cos \chi = \frac{x_T - x_A}{\sqrt{\left(x_A - x_T \right)^2 + y_T^2}}$$

the 3-state dynamics become

$$\dot{x}_A = \frac{1}{2} \left(\frac{x_T - x_A}{\sqrt{\left(x_A - x_T \right)^2 + y_T^2}} - \cos \psi \right), \ x_A(0) = x_{A0}$$

$$\dot{x}_T = \alpha \cos \phi + \frac{1}{2} \frac{1}{x_A} \left(\frac{x_A^2 + y_T^2 - x_A y_T}{\sqrt{\left(x_A - x_T \right)^2 + y_T^2}} - y_T \sin \psi - x_A \cos \psi \right), \ x_T(0) = x_{T0}$$

$$\dot{y}_T = \alpha \cos \phi - \frac{1}{2} \frac{1}{x_A} \left[\frac{x_A + x_T}{\sqrt{\left(x_A - x_T \right)^2 + y_T^2}} y_T + \left(x_A - x_T \right) \sin \psi \right], \ y_T(0) = y_{T0}$$

In the region R_{ce} where **D** will intercept **A** if **A** plays PP, consider **D** endowed with a capture radius of $2l$. The terminal manifold is

$$S = \{ (x_A, x_T, y_T) \, | \, x_A = l \}$$

and the inward pointing normal to the terminal manifold S is

$$\vec{n} = (-1, 0, 0)^{\mathrm{T}}$$

$$\Longrightarrow$$

$$\lambda_{x_A} (t_f) = -a, \ \lambda_{x_T} (t_f) = 0, \ \lambda_{y_T} (t_f) = 0, \ a > 0$$

The Hamiltonian is

$$\mathcal{H} = -1 + \alpha\left(\lambda_{x_T}\cos\phi + \lambda_{y_T}\sin\phi\right) - \ldots$$

$$\ldots\frac{1}{2}\frac{1}{x_A}\left\{\left(\lambda_{x_A+\lambda_{x_T}}\right)x_A\cos\psi + \left[\lambda_{x_T}y_T + \lambda_{y_T}(x_A - x_T)\right]\sin\psi\right\}$$

Using Isaacs Lemma on circular vectograms

$$\max_{\phi,\,\psi}\mathcal{H}$$

$$\implies$$

$$\sin\phi = \frac{\lambda_{y_T}}{\lambda_{x_T}^2 + \lambda_{y_T}^2}, \quad \cos\phi = \frac{\lambda_{x_T}}{\lambda_{x_T}^2 + \lambda_{y_T}^2},$$

$$\sin\psi = -\frac{\lambda_{x_T}y_T + \lambda_{y_T}\left(x_A - x_T\right)}{\sqrt{\left[\lambda_{x_T}y_t + \lambda_{y_T}\left(x_A - x_T\right)\right]^2 + x_A^2\left(\lambda_{x_A} + \lambda_{x_T}\right)^2}}$$

$$\cos\psi = -\frac{x_A\left(\lambda_{x_A} + \lambda_{x_T}\right)}{\sqrt{\left[\lambda_{x_T}y_t + \lambda_{y_T}\left(x_A - x_T\right)\right]^2 + x_A^2\left(\lambda_{x_A} + \lambda_{x_T}\right)^2}}$$

and substituting these into the Hamiltonian

$$\mathcal{H} = -1 + \alpha\left(\lambda_{x_T}^2 + \lambda_{y_T}^2\right)^{\frac{1}{2}} + \frac{1}{2}\frac{1}{x_A}\left(f + \frac{g}{h}\right)$$

where

$$f \triangleq \left(\lambda_{y_T}^2 x_A^2 + \lambda_{y_T}^2 x_T^2 + \lambda_{x_T}^2 y_T^2 - 2\lambda_{y_T}^2 x_A x_T - 2\lambda_{x_T}\lambda_{y_T}x_T y_T + 2\lambda_{x_T}\lambda_{y_T}x_A y_T\right)^{\frac{1}{2}}$$

$$g \triangleq (\lambda_{x_T} - \lambda_{x_A})(x_A^2 - x_A x_T) + \lambda_{x_T}y_T^2 - \lambda_{y_T}x_A y_T - \lambda_{y_T}x_T y_T$$

$$h \triangleq (x_A^2 + x_T^2 + y_T^2 - 2x_A x_T)^{\frac{1}{2}}$$

This leads to the Euler-Lagrange equations

$$
\dot{\lambda}_{x_A} = \frac{1}{2}\frac{1}{x_A}\left\{ \frac{a}{x_A}\frac{fh+g}{h} - \frac{\lambda_{y_T}^2(x_A - x_T) + \lambda_{x_T}\lambda_{y_T}y_T}{f} - \ldots \right.
$$
$$
\left. \ldots\frac{\left[(\lambda_{x_T} - \lambda_{x_A})(2x_A - x_T) - \lambda_{y_T}y_T\right]h^2}{h^3} - \frac{g(x_A - x_T)}{h^3} \right\}
$$

$$
\dot{\lambda}_{x_T} = -\frac{1}{2}\frac{1}{x_A}\left\{ \frac{\lambda_{y_T}^2(x_T - x_A) - \lambda_{x_T}\lambda_{y_T}y_T}{f} + \frac{\left[(\lambda_{x_A} - \lambda_{x_T})x_A - \lambda_{y_T}y_T\right]h^2}{h^3} + \frac{g(x_A - x_T)}{h^3} \right\}
$$

$$
\dot{\lambda}_{y_T} = -\frac{1}{2}\frac{1}{x_A}\left\{ \frac{\lambda_{x_T}\lambda_{y_T}(x_A - x_T) + \lambda_{x_T}^2 y_T}{f} + \frac{\left[2\lambda_{x_T}y_T - \lambda_{y_T}(x_A + x_T)\right]h^2}{h^3} - \frac{gy_T}{h^3} \right\}
$$

$$
\dot{x}_A = \frac{1}{2}\left\{ \frac{x_T - x_A}{\sqrt{(x_A - x_T)^2 + y_T^2}} + \frac{(\lambda_{x_A} + \lambda_{x_T})x_A}{\sqrt{\left[\lambda_{x_T}y_T + \lambda_{y_T}(x_A - x_T)\right]^2 + x_A^2(\lambda_{x_A} + \lambda_{x_T})}} \right\}
$$

$$
\dot{x}_T = \frac{1}{2}\left\{ \frac{y_T}{x_A}\left[\frac{y_T}{\sqrt{(x_A - x_T)^2 + y_T^2}} + \frac{\lambda_{x_T}y_T + \lambda_{y_T}(x_A - x_T)}{\sqrt{\left[\lambda_{x_T}y_T + \lambda_{y_T}(x_A - x_T)\right]^2 + x_A^2(\lambda_{x_A} + \lambda_{x_T})}} \right] + \ldots \right.
$$
$$
\left. \ldots 2\alpha\frac{\lambda_{x_T}}{\sqrt{\lambda_{x_T}^2 + \lambda_{y_T}^2}} \right\}
$$

$$
\dot{y}_T = \frac{1}{2}\left\{ 2\alpha\frac{y_T}{\sqrt{\lambda_{x_T}^2 + \lambda_{y_T}^2}} - \frac{1}{x_A}\left[\frac{\lambda_{x_T}(x_A - x_T)y_T + \lambda_{y_T}(x_A - x_T)^2}{\sqrt{\left[\lambda_{x_T}y_T + \lambda_{y_T}(x_A - x_T)\right]^2 + (\lambda_{x_A} + \lambda_{x_T})x_A^2}} - \ldots \right.\right.
$$
$$
\left.\left. \ldots\frac{(x_A + x_T)y_T}{\sqrt{(x_A - x_T)^2 + y_T^2}} \right]\right\}
$$

with

$$
\lambda_{x_A}(t_f) = -\frac{2}{1 - \frac{x_{T_f} - l}{\sqrt{(x_{T_f} - l)^2 + y_{T_f}^2}}} \qquad\qquad x_A(t_f) = l
$$

$$
\lambda_{x_T}(t_f) = 0 \qquad\qquad x_T(t_f) = x_{T_f}
$$

$$
\lambda_{y_T}(t_f) = 0 \qquad\qquad y_A(t_f) = y_{T_f}
$$

From here one integrates in retrograde fashion to obtain the family of optimal trajectories parameterized by x_{T_f} and y_{T_f} which fill the state-space region $R_{ce} \subset \mathbb{R}^3$

Bibliography

1. R. Anderson, M. Pachter, and R. Murphey, "A 3-Player Zero-Sum Differential Game," To appear in *IEEE Aerospace Conference* , 2018.

2. R. Anderson, M. Pachter, and R. Murphey, "Barrier Analysis of a 3-Player Pursuit-Evasion Differential Game," To appear in *Israel Annual Conference on Aerospace Studies* , 2018.

3. R. Anderson, M. Pachter, and R. Murphey, "Defender-Assisted Evasion Maneuvers," Submitted to the *IEEE Conference on Control Technology and Applications* , 2018.

4. J. C. Barton and C. J. Eliezer, "On Pursuit Curves," *J. Austral. Math. Soc. Ser. B* (41), pp. 358–371, 2000.

5. P. Bernhard, "Differential Games: Lecture Notes on the Isaacs-Breakwell Theory," in *Summer School on Differential Games*, (Cagliari, Italy), 1992.

6. J. V. Breakwell and A. W. Merz, "Toward a Complete Solution to the Homicidal Chauffeur Game," in *1st International Conference on the Theory and Application of Differential Games*, pp. 3/1–3/9, (Amherst), 1969.

7. S. Coates, *An Inveestigation of the Homicidal Chauffeur Differential Game.* PhD dissertation, Air Force Institute of Technology, 2017.

8. L. E. Dubins, "On Curves of Minimal Length with a Constraint on Average Curvature, and with Prescribed Initial and Terminal Positions and Tangents," *American Journal of Mathematics* **79**(3), pp. 497–516, 1957.

9. E. Garcia, D. Casbeer, and M. Pachter, "Optimal Target Capture Strategies in the Target-Attacker-Defender Differential Game," *Accepted for presentation at the 2018 ACC* .

10. R. Isaacs, *Differential Games: A Mathematical Theory with Applications to Warfare and Pursuit, Control and Optimization*, John Wiley and Sons, 1965.

11. D. E. Kirk, *Optimal Control Theory: An Introduction*, Prentice-Hall, 1970.

12. A. W. Merz, "The Homicidal Chauffeur," Tech. Rep. 3, 1974.

13. R. B. Myerson, *Game Theory: Analysis of Conflict*, Harvard University Press, 1991.

14. M. Pachter, E. Garcia, and D. Casbeer, "Toward a Solution of the Active Target Defense Differential Game," *to appear in Dynamic Games and Applications* , 2018.

15. M. Pachter, E. Garcia, and D. W. Casbeer, "Active Target Defense Differential Game," *2014 52nd Annual Allerton Conference on Communication, Control, and Computing, Allerton 2014* , pp. 46–53, 2014.

16. M. Pachter, E. Garcia, and D. W. Casbeer, "The Differential Game of Guarding a Target," *AIAA J. of Guidance, Control, and Dynamics* , to appear.

17. E. R. Pinch, *Optimal Control and the Calculus of Variations*, Oxford University Press, 1993.

18. L. Pontryagin, "ON THE THEORY OF DIFFERENTIAL GAMES," *Uspekhi Mat. Nauk* **21**(4), pp. 219–274, 1966.

REPORT DOCUMENTATION PAGE

1. REPORT DATE *(DD–MM–YYYY)*	2. REPORT TYPE	3. DATES COVERED *(From — To)*
22–03–2018	Master's Thesis	Sept 2016 — Mar 2018

4. TITLE AND SUBTITLE

Defender-Assisted Evasion and Pursuit Maneuvers

5a. CONTRACT NUMBER

5b. GRANT NUMBER

5c. PROGRAM ELEMENT NUMBER

6. AUTHOR(S)

Anderson, Roger S, Capt, USAF

5d. PROJECT NUMBER

17G130

5e. TASK NUMBER

5f. WORK UNIT NUMBER

7. PERFORMING ORGANIZATION NAME(S) AND ADDRESS(ES)

Air Force Institute of Technology
Graduate School of Engineering and Management (AFIT/EN)
2950 Hobson Way
WPAFB OH 45433-7765

8. PERFORMING ORGANIZATION REPORT NUMBER

AFIT-ENG-MS-18-M-007

9. SPONSORING / MONITORING AGENCY NAME(S) AND ADDRESS(ES)

Air Force Office of Scientific Research
Dr. Frederick Leve, Program Officer
875 North Randolph Street, Suite 325, Room 3112
Arlington, VA. 22203-1768
dycontrol@afosr.af.mil
DSN 696-7309

10. SPONSOR/MONITOR'S ACRONYM(S)

AFOSR/RT

11. SPONSOR/MONITOR'S REPORT NUMBER(S)

12. DISTRIBUTION / AVAILABILITY STATEMENT

DISTRIBUTION STATEMENT A:
APPROVED FOR PUBLIC RELEASE; DISTRIBUTION UNLIMITED.

13. SUPPLEMENTARY NOTES

This work is declared a work of the U.S. Government and is not subject to copyright protection in the United States.

14. ABSTRACT

Motivated by the possibilities afforded by active target defense, a 3-agent pursuit-evasion differential game involving an Attacker/Pursuer, a Target/Evader, and a Defender is considered. The Defender strives to assist the Target by intercepting the Attacker before the latter reaches the Target. A barrier surface in a reduced state space separates the winning regions of the Attacker and Target-Defender team. In this thesis, attention focuses primarily on the Attacker's region of win where, under optimal Attacker play, the Defender cannot preclude the Attacker from capturing the Target. Both optimal and suboptimal strategies are investigated. This thesis uses several methods to breakdown and analyze the 3-player differential game.

15. SUBJECT TERMS

Differential Games, Controls, Optimization, Pursuit Curves

16. SECURITY CLASSIFICATION OF:			17. LIMITATION OF ABSTRACT	18. NUMBER OF PAGES	19a. NAME OF RESPONSIBLE PERSON
a. REPORT	b. ABSTRACT	c. THIS PAGE			Dr. Meir Pachter, AFIT/ENG
U	U	U	UU	122	19b. TELEPHONE NUMBER *(include area code)* (937) 255-3636, x7247; meir.pachter@afit.edu